

# **INFLUENCE OF HEAT-TREATMENT ON STRUCTURE AND PROPERTIES OF NICKEL - TITANIUM ALLOY**

Thesis

Submitted in partial fulfillment of the requirements for the degree of

**DOCTOR OF PHILOSOPHY**

by

**SRIRAM MUKUNDA**

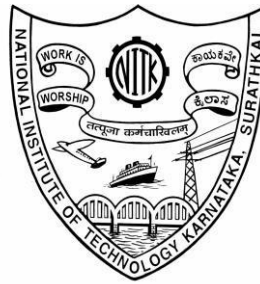
Under the guidance of

**Dr. NARENDRA NATH. S**

**Dr. MERVIN A. HERBERT**

Professor

Associate Professor



DEPARTMENT OF MECHANICAL ENGINEERING

NATIONAL INSTITUTE OF TECHNOLOGY KARNATAKA,

SURATHKAL, MANGALORE – 575025

April - 2021

## DECLARATION

I hereby declare that the Research Thesis entitled “**Influence of Heat-Treatment on Structure and Properties of Nickel - Titanium Alloy**” which is being submitted to the **National Institute of Technology Karnataka, Surathkal** in partial fulfillment of the requirements for the award of the Degree of **Doctor of Philosophy in Mechanical Engineering** is a *bonafide report of the research work carried out by me*. The material contained in this Research Thesis has not been submitted to any other Universities or Institutes for the award of any degree.

Register Number: **110662ME11P05**

Name of the Research Scholar: **SRIRAM MUKUNDA**

Signature of the Research Scholar: 

Department of Mechanical Engineering

Place: NITK-Surathkal

Date: 7/4/2021

## CERTIFICATE

This is to certify that the Research Thesis entitled “**Influence of Heat-Treatment on Structure and Properties of Nickel - Titanium Alloy**” submitted by **Mr. SRIRAM MUKUNDA (Register Number: 110662ME11P05)** as the record of the research work carried out by him, *is accepted as the Research Thesis submission* in partial fulfillment of the requirements for the award of the Degree of **Doctor of Philosophy**.

  
**Dr. NARENDRA NATH. S**

Professor  
Dept. of Mechanical Engg  
NITK Surathkal

  
**Dr. MERVIN A. HERBERT**

Associate Professor  
Dept. of Mechanical Engg  
NITK Surathkal

  
**Chairman-DRPC**



## ACKNOWLEDGMENT

With a deep sense of gratitude, I wish to express my sincere gratitude towards my supervisors **Dr. Narendra Nath. S**, Professor, Department of Mechanical Engineering, National Institute of Technology Karnataka, Surathkal and **Dr. Mervin A. Herbert**, Associate Professor, Department of Mechanical Engineering, National Institute of Technology Karnataka, Surathkal for their excellent guidance and unconditional support throughout my work. I received excellent academic feedback from them, which has stood in good stead while writing the thesis. I whole heartedly thank them for their invaluable support and encouragement offered during the course of the investigation.

I take the opportunity to thank **Dr. Srikanth Rao**, Professor and Head, Department of Mechanical Engineering, for his continued support offered in the completion of the work.

I profusely thank **Dr. S M Murigendrappa**, Professor, Department of Mechanical Engineering, **Dr K Rajendra Udupa**, Professor, Department of Metallurgical and Materials Engineering and **Dr. M N Satyanarayana**, Professor, Department of Physics for their continuous and timely suggestions as members of Research Program Assessment Committee.

I take the opportunity to thank **Dr. K Uma Maheshwar Rao**, Director, NITK Surathkal and **Prof. A. Nityananda Shetty**, Dean (Academics), NITK Surathkal for extending their valuable support in completion of my research work

I wish to express my sincere gratitude to all the faculty members of the Department of Mechanical Engineering, NITK Surathkal for their continuous appreciation and support all through the research work.

I express my sincere most gratitude to **Dr B S Murty**, Director, Indian Institute of Technology, Hyderabad and (Former) Professor, Department of Metallurgical and Materials Engineering, Indian Institute of Technology, Chennai for having given the

opportunity to carry out major part of the experimental work at Research & Development Lab, Department of Metallurgical and Materials Engineering, IIT Chennai.

I express my deepest gratitude to **Prof. N R Shetty**, Director, NMIT for providing me the inspiration and making available of his support in a good number of ways. I would like to thank **Dr. H C Nagaraj**, Principal, NMIT Bangalore, for his timely support and encouragement in the completion of research work. I would like to take the opportunity to thank **Dr. Sudheer Reddy J**, Professor and Head, Department of Mechanical Engineering, NMIT Bangalore for having offered excellent support in carrying out the research work along with the regular academic work load.

I express my gratitude towards **Dr. K. Venkateshwaralu**, Scientist, Materials Division, National Aerospace Limited (NAL) to have provided me an excellent opportunity in carrying out experiments at the facility in NAL.

I take the opportunity to thank **Dr. Srilatha Rao**, Professor and Head, Department of Chemistry, NMIT Bangalore and **Mrs. Sowmyashree**, Assistant Professor, Department of Chemistry, NMIT Bangalore to have provided me an excellent opportunity to carry out experiments at their Lab to bring about a completion in the research work.

I express my sincere most gratitude to **Dr. B K Muralidhara**, Professor, Department of Mechanical Engineering, NMIT Bangalore, formerly Professor, Department of Mechanical Engineering, UVCE, Bangalore University for having been a pillar of strength and having offered excellent guidance in the completion of my thesis.

I am indebted to my colleagues, **Dr. Vinyas M** and **Dr. Pradeep V Badiger** of Department of Mechanical Engineering, NMIT Bangalore for their extraordinary guidance and encouragement during the entire process of the research work.

I would profusely thank my father, **Dr. P G Mukunda**, Professor, Department of Mechanical Engineering, NMIT Bangalore for having been a pillar of strength in offering the necessary technical guidance and moral support in completing my research work. I would like to share this moment of happiness with my mother, **Mrs. Vasantha Mukunda**, brother, **Mr. Vasudevan Mukunda** and sister-in-law, **Mrs. Anuradha Vasudevan** for their fabulous encouragement.

[*Sriram M*]

## ABSTRACT

In this present investigation, the low temperature annealing heat-treatment was carried out at four different temperatures between 300°C and 450°C. The observation of the microstructure has been carried out using transmission electron microscopy as per ASTM F86. An EDAX analysis has been carried out as per ASTM F1375 - 92(2012) to ascertain the chemical composition. An x-ray diffraction has been carried out as per ASTM F2024 - 10(2016) to ascertain the phases present in the alloy. The DSC has been carried out as per ASTM D3418 on the alloy to analyze the transformation temperatures to confirm the superelastic nature of the material. The material has been subjected to mechanical testing by performing the tensile test as per ASTM E8 and Vickers hardness test as per ASTM E92 – 17. The tribological characteristics of the material has been analyzed as per ASTM G-132a by conducting abrasive wear test at room temperature. The superelasticity test has been performed as per ASTM F2516-18 at room temperature by varying the magnitude of strain. An electrochemical corrosion test has been conducted as per ASTM F-2129 on NiTi alloy with a prepared solution to study the corrosion resistance of the same.

The salient results of the systematic investigation carried out within the scope of the investigation indicate that the chemical composition of the constituents present in the alloy assessed by EDAX analysis indicate that the Ni-Ti alloy used in this investigation is a 50:50 Ti-Ni alloy which is well within the tolerance limit for 50:50 TiNi alloy as per ASTM F1375 - 92(2012). The alloy is seen to be slightly on the Titanium-rich side.

The TEM of the as-received NiTi alloy indicates the presence of martensite which appears as a needle-like region and also a shaded region indicating presence of dislocation network. Whereas the 50% Nickel - 50% Titanium alloy subjected to optimum low temperature annealing heat-treatment at 350°C for one-hour duration indicates the presence of martensite, dislocation network and formation of NiTi alloy grains. The extent of dislocation network has relatively reduced and the grain size of NiTi alloy has relatively increased.

The XRD of as-received NiTi alloy indicates that the presence of martensitic and austenitic phase. Whereas, the X-ray diffractogram of the 50% Nickel – 50% Titanium alloy subjected to optimum low temperature heat-treatment at 350°C for one-hour duration indicates that the presence of martensitic phase, austenitic phase and an additional Rhombohedral phase.

The DSC thermogram of the as-received NiTi alloy indicates that there are no significant peaks seen in the heating as well as the cooling curves meaning that there are no distinct phase transformations of either Austenite-Martensite or Martensite-Austenite present in the material. Whereas, the DSC thermogram of 50% Nickel - 50% Titanium alloy subjected to optimum low temperature heat-treatment at 350°C for one-hour duration indicates that the material shows a single-stage transformation from austenite-martensite phase in the cooling cycle and a two-stage transformation from martensite-rhombohedral phase and rhombohedral-austenite phase in the heating cycle.

The tensile test carried out for the as-received material in this investigation indicates that the material is super-elastic by nature. The comparison of the ultimate tensile strength of as-received 50% Nickel - 50% Titanium alloy and the alloy sample subjected to an optimum low temperature annealing heat-treatment of 350°C for a duration of 1 hour indicates that there is an improvement in ultimate tensile strength of 350°C heat-treated sample by 44.40% as compared to that of as-received 50% Nickel - 50% Titanium alloy. The Vickers Pyramid Number of as-received material is 421 VPN. The comparison of hardness of 50% Nickel - 50% Titanium alloy subjected to optimum low temperature annealing heat-treatment at 350°C for one-hour duration with the hardness of as-received material indicates that the hardness has increased by 14.5% as compared to hardness of as-received 50% Nickel - 50% Titanium alloy.

The abrasive wear test indicates that when the load is increased, the wear mass loss rate is relatively at a higher rate upto 15N and with further increase in the load, the mass loss rate is relatively at a slower rate. The comparison of the abrasive wear between the as-received 50% Nickel - 50% Titanium alloy and 50% Nickel - 50% Titanium alloy subjected to optimum low temperature annealing treatment at 350°C for one-hour duration indicates that the mass loss of low temperature annealed 50% Nickel - 50% Titanium alloy is lesser by 37.17% to 47.58% than the mass loss of as -received 50%

Nickel - 50% Titanium alloy. This trend of reduction in the mass loss or in other words the improvement in wear resistance has been found true at all the axial loads investigated within the scope of this investigation.

The variation of strain for different levels of stress during loading and after release of load at different pre-determined strain values indicate that the material even after loading upto stress level of 700 MPa does not break but returns back to the original stress value after release of the load indicating that the unloading curve had followed a hysteresis path compared to loading curve by returning back to the same point which means that the material is exhibiting superelastic behavior. The extent of improvement in Superelasticity of 50% Nickel - 50% Titanium alloy subjected to optimum low temperature annealing heat-treatment of 450°C for one-hour duration is in the range of 54.5% to 95.2 % as compared to superelasticity of as-received material.

The electrochemical corrosion study carried out for as-received NiTi alloy indicates that the electrochemical corrosion rate for the material was found to be 0.0613 mm/year. The corrosion rate of 50% Nickel - 50% Titanium alloy subjected to low temperature annealing heat-treatment at different temperatures is less than the corrosion rate of as-received 50% Nickel - 50% Titanium alloy. The extent of improvement in the corrosion resistance of 50% Nickel - 50% Titanium alloy subjected to optimum low temperature annealing heat-treatment at 350°C for one-hour duration is 35.72% as compared to corrosion resistance of as-received 50% Nickel - 50% Titanium alloy.

*Keywords: Shape Memory Effect, Superelasticity, Vickers Hardness, Ultimate Tensile Strength, Abrasive Wear, Corrosion Behavior*



# TABLE OF CONTENTS

DECLARATION	i
CERTIFICATE	ii
ACKNOWLEDGEMENT	iii
ABSTRACT	v
TABLE OF CONTENTS	viii
LIST OF TABLES	xiv
LIST OF FIGURES	xviii
NOMENCLATURE	xxv
SYMBOLS	xxvi
<b>1 INTRODUCTION</b>	<b>1</b>
1.1 Smart Materials	1
1.2 Types of Smart Materials	1
1.3 Shape Memory Alloys	2
1.4 Selection of alloy for the present investigation	2
1.5 Manufacture of NiTi alloy and parameters affecting the properties	4
1.6 Outline of the Thesis	6
<b>2 LITERATURE REVIEW</b>	<b>9</b>
2.1 Introduction	9
2.2 Basics of Nickel-Titanium Alloy	9
2.3 Annealing of Nickel-Titanium Shape Memory Alloy	14
2.4 Transmission Electron Microscopic Studies of Nickel-Titanium Alloy	23
2.5 X-Ray Diffraction Studies of Nickel-Titanium Alloy	26
2.6 Differential Scanning Calorimetric Studies of Nickel-Titanium Alloy	27
2.7 Mechanical Properties of Nickel-Titanium Alloy	33

2.8	Tribological Characteristics of Nickel-Titanium Alloy	35
2.9	Superelastic Behavior of Nickel-Titanium Alloy	41
2.10	Electrochemical Corrosion Characteristics of Nickel-Titanium Alloy	44
2.11	Scope of the Present Investigation	48
<b>3</b>	<b>EXPERIMENTAL WORK</b>	<b>51</b>
3.1	Introduction	51
3.2	Nickel-Titanium Alloys	51
3.3	Conduction of Low Temperature Annealing Heat-Treatment	52
3.4	To Observe the Samples Under Transmission Electron Microscopy	53
3.5	EDS Analysis	55
3.6	X-Ray Diffraction Studies	56
3.7	Differential Scanning Calorimetric Studies	57
3.8	Evaluation of Mechanical Properties	58
3.8.1	Evaluation of UTS	58
3.8.2	Evaluation of hardness	59
3.9	Evaluation of Tribological Characteristics	61
3.10	Study of Superelastic Behavior	63
3.11	Evaluation of Corrosion Characteristics	64
3.12	Conclusion	67
<b>4</b>	<b>RESULTS AND DISCUSSION</b>	<b>69</b>
4.1	Introduction	69
4.2	Studies on Nickel-Titanium Alloy Without any Heat-Treatment	69
4.2.1	Microstructure observation under TEM	69
4.2.2	EDS analysis	70
4.2.3	X-Ray diffraction studies	71
4.2.4	Differential scanning calorimetry	72
4.3	Mechanical Properties	74
4.3.1	Ultimate tensile strength	74
4.3.2	Hardness	77

4.3.3	Tribological characteristics	78
4.3.4	Superelastic behavior	80
4.3.5	Corrosion characteristics	83
4.4	Studies on Nickel-Titanium Alloy Subjected to Low Temperature Annealing Heat-Treatment	84
4.4.1	Microstructure observation under TEM	84
4.4.2	EDS analysis	87
4.4.3	X-Ray diffraction studies	87
4.4.4	Differential scanning calorimetry	91
4.5	Mechanical Properties	98
4.5.1	Ultimate tensile strength	98
4.5.2	Hardness	104
4.5.3	Tribological characteristics	106
4.6	Superelastic Behavior	113
4.7	Corrosion Characteristics	123
4.8	Comparison of As-Received and Low Temperature Annealing Heat-Treated 50% Nickel - 50% Titanium Alloys	129
4.8.1	Comparison of transmission electron micrographs of as-received and low temperature annealing heat-treated 50% Nickel - 50% Titanium alloys	130
4.8.2	Comparison of EDS of as-received and low temperature annealing heat-treated 50% Nickel - 50% Titanium alloys	130
4.8.3	Comparison of X-Ray diffractogram of as-received and low temperature annealing heat-treated 50% nickel - 50% titanium alloys	130
4.8.4	Comparison of differential scanning calorimetry results of as-received and low temperature annealing heat-treated 50% nickel - 50% titanium alloys	132

4.8.5	Comparison of ultimate tensile strength of as-received and low temperature annealing heat-treated 50% Nickel - 50% Titanium alloys	134
4.8.6	Comparison of hardness of as-received and low temperature annealing heat-treated 50% Nickel - 50% Titanium alloys	136
4.8.7	Comparison of abrasive wear characteristics of as-received and low temperature annealing heat-treated 50% nickel - 50% titanium alloys	136
4.8.8	Comparison of superelasticity behavior of as-received and low temperature annealing heat-treated 50% nickel - 50% titanium alloys	138
4.8.9	Comparison of corrosion rate of as-received and low temperature annealing heat-treated 50% nickel - 50% titanium alloys	140
4.9	Summary	142
<b>5</b>	<b>CONCLUSIONS AND SCOPE FOR FUTURE WORK</b>	143
5.1	Introduction	143
5.2	Studies on As-received and Low temperature Heat-treated Nickel-Titanium Alloy	143
5.2.1	Microstructure observation under TEM	143
5.2.2	EDS analysis	144
5.2.3	X-Ray diffraction studies	144
5.2.4	Differential scanning calorimetry	144
5.2.5	Mechanical properties	145
5.2.6	Tribological characteristics	147
5.2.7	Superelastic behavior	147
5.2.8	Corrosion characteristics	148

5.3	Comparative Study of Nickel-Titanium Alloy Without Any Heat-Treatment and Nickel-Titanium Alloy Subjected to Different Low Temperature Annealing Heat-Treatments	149
5.3.1	Comparison of transmission electron micrographs of as-received and low temperature annealing heat-treated 50% nickel - 50% titanium alloys	149
5.3.2	Comparison of EDAX of as-received and low temperature annealing heat-treated 50% nickel - 50% titanium alloys	149
5.3.3	Comparison of X-Ray diffractogram of as-received and low temperature annealing heat-treated 50% nickel - 50% titanium alloys	149
5.3.4	Comparison of differential scanning calorimetry results of as-received and low temperature annealing heat-treated 50% nickel - 50% titanium alloys	150
5.3.5	Comparison of ultimate tensile strength of as-received and low temperature annealing heat-treated 50% nickel - 50% titanium alloys	150
5.3.6	Comparison of hardness of as-received and low temperature annealing heat-treated 50% nickel - 50% titanium alloys	150
5.3.7	Comparison of abrasive wear characteristics of as-received and low temperature annealing heat-treated 50% nickel - 50% titanium alloys	151
5.3.8	Comparison of superelasticity behavior of as-received and low temperature annealing heat-treated 50% nickel - 50% titanium alloys	151
5.3.9	Comparison of corrosion characteristics of as-received and low temperature annealing heat-treated 50% nickel - 50% titanium alloys	151

5.4	Scope for Future Work	152
	<b>REFERENCES</b>	153
	<b>LIST OF PUBLICATIONS AND CONFERENCES</b>	166
	<b>BIODATA</b>	168

## LIST OF TABLES

<b>Table No.</b>	<b>Description</b>	<b>Page No.</b>
Table 1.1	Different properties of CuZnAl, CuAlNi and NiTi shape memory alloys	3
Table 3.1	Low Temperature Heat-treatment Temperature and Time Duration for 50% Nickel - 50% Titanium alloy for subjecting to Tensile Test	53
Table 4.1	Atomic Distribution of different elements obtained through EDAX analysis for the Ni-Ti alloy used in this investigation	71
Table 4.2	Stress and strain values of as-received NiTi alloy during the assessment	75
Table 4.3	Hardness Values of 50% Nickel - 50% Titanium alloy	77
Table 4.4	Abrasive Wear characteristics of as-received 50% Nickel - 50% Titanium alloy	78
Table 4.5	Area enclosed within loading and unloading curves of stress vs strain diagram for as-received 50% Nickel - 50% Titanium alloy for different pre-determined strain rates	82
Table 4.6	Electrochemical corrosion rate for as-Received 50% Ni - 50% Ti alloy	84
Table 4.7	Transformation temperatures of different phases in 50% Nickel - 50% Titanium alloy when subjected to low temperature annealing heat-treatment at different temperatures	94
Table 4.8	Phase Transformation temperature range for 50% Nickel - 50% Titanium alloy when subjected to low temperature annealing heat-treatment at different temperatures	96
Table 4.9	Stress and strain values of heat-treated NiTi alloy during the assessment	98

Table 4.10	Hardness of heat-treated 50% Nickel - 50% Titanium when subjected to low temperature annealing heat-treatment at different temperatures	105
Table 4.11	Abrasive Wear characteristics of 50% Nickel - 50% Titanium alloy subjected to low temperature annealing heat-treatment at 300°C for one hour	106
Table 4.12	Abrasive Wear characteristics of 50% Nickel - 50% Titanium alloy subjected to low temperature annealing heat-treatment at 350°C for one hour	107
Table 4.13	Abrasive Wear characteristics of 50% Nickel - 50% Titanium alloy subjected to low temperature annealing heat-treatment at 400°C for one hour	108
Table 4.14	Abrasive Wear characteristics of 50% Nickel - 50% Titanium alloy subjected to low temperature annealing heat-treatment at 450°C for one hour	109
Table 4.15	Area enclosed within loading and unloading curves of stress vs strain diagram for 50% Nickel - 50% Titanium alloy subjected to low temperature annealing heat-treatment at 300°C for different pre-determined strain rates	120
Table 4.16	Area enclosed within loading and unloading curves of stress vs strain diagram for 50% Nickel - 50% Titanium alloy subjected to low temperature annealing heat-treatment at 350°C for different pre-determined strain rates	120
Table 4.17	Area enclosed within loading and unloading curves of stress vs strain diagram for 50% Nickel - 50% Titanium alloy subjected to low temperature annealing heat-treatment at 400°C for different pre-determined strain rates	121



Table 4.18	Area enclosed within loading and unloading curves of stress vs strain diagram for 50% Nickel - 50% Titanium alloy subjected to low temperature annealing heat-treatment at 450°C for different pre-determined strain rates	121
Table 4.19	Corrosion Current and Electrochemical corrosion rate for 50% Nickel - 50% Titanium alloy subjected to low temperature annealing heat-treatment at 300°C	124
Table 4.20	Corrosion Current and Electrochemical corrosion rate for 50% Nickel - 50% Titanium alloy subjected to low temperature annealing heat-treatment at 350°C	125
Table 4.21	Corrosion Current and Electrochemical corrosion rate for 50% Nickel - 50% Titanium alloy subjected to low temperature annealing heat-treatment at 400°C	126
Table 4.22	Corrosion Current and Electrochemical corrosion rate for 50% Nickel - 50% Titanium alloy subjected to low temperature annealing heat-treatment at 450°C	127
Table 4.23	Electrochemical corrosion rate for 50% Nickel - 50% Titanium alloy subjected to low temperature annealing heat-treatment at different temperatures	128
Table 4.24	Hardness and Electrochemical corrosion rate for 50% Nickel - 50% Titanium alloy subjected to low temperature annealing heat-treatment at different temperatures	129
Table 4.25	Comparison of Ultimate tensile Strength (UTS) of as-received and low temperature annealing heat-treated 50% Nickel - 50% Titanium alloy	135
Table 4.26	Comparison of Vickers Hardness of as-received and low temperature annealing heat-treated 50% Nickel - 50% Titanium alloy	136

Table 4.27	Comparison of Abrasive Wear characteristics of as-received and low temperature annealing heat-treated 50% Nickel - 50% Titanium alloy	137
Table 4.28	Comparison of Superelasticity of as-received and low temperature annealing heat-treated 50% Nickel - 50% Titanium alloy	139
Table 4.29	Comparison of Corrosion Rate of as-received and low temperature annealing heat-treated 50% Nickel - 50% Titanium alloy	141

## LIST OF FIGURES

<b>Figure No.</b>	<b>Description</b>	<b>Page No.</b>
Figure 1.1	Relationship between $M_s$ and Nickel atomic % (Pelton et al. 2001)	5
Figure 2.1	Austenitic (left) and martensitic (right) structures of NiTi compound (Alan R. Pelton et al. 2003)	10
Figure 2.2	NiTi phase diagram (Velmurugan et al. 2018)	12
Figure 3.1	SIGMA box furnace	52
Figure 3.2	TECHNAI Transmission Electron Microscopy set-up	54
Figure 3.3	Carl Zeiss Scanning Electron Microscopy set-up	55
Figure 3.4	D8 Advance X-Ray Diffraction set-up	56
Figure 3.5	Perkin Elmer Differential Scanning Calorimetry set-up	57
Figure 3.6	PC-2000 Electronic Tensometer	59
Figure 3.7	Vickers Hardness Tester	60
Figure 3.8	DUCOM Wear Testing Machine	61
Figure 3.9	5582 INSTRON Machine	63
Figure 3.10	600E Electrochemical Analyzer	65
Figure 4.1	Microscopic image of as-received 50% Nickel - 50% Titanium alloy when observed under Transmission Electron Microscope	69
Figure 4.2	Diffraction Pattern of as-received 50% Nickel - 50% Titanium alloy used in this investigation when observed under Transmission Electron Microscope	70
Figure 4.3	EDAX analysis spectrum of as-received 50% Nickel - 50% Titanium alloy used in this investigation	71
Figure 4.4	X-Ray Diffraction of as-received 50% Nickel - 50% Titanium alloy	72

Figure 4.5	Differential Scanning Calorimetry curve of as-received 50% Nickel - 50% Titanium alloy	73
Figure 4.6	Tensile curve of as-received 50% Nickel - 50% Titanium alloy	75
Figure 4.7	Fractograph of the as-received NiTi alloy when observed under SEM at a magnification of 5000X	76
Figure 4.8	Wear Mass Loss of as-received 50% Nickel - 50% Titanium alloy	78
Figure 4.9	Worn surface of as-received 50% Nickel - 50% Titanium at 2000 and 5000 when observed under Scanning Electron Microscope	79
Figure 4.10	Stress versus strain graph for as-received 50% Nickel - 50% Titanium alloy at 2% pre-determined strain level during loading and release of load	80
Figure 4.11	Stress versus strain graph for as-received 50% Nickel - 50% Titanium alloy at 6% pre-determined strain level during loading and release of load	80
Figure 4.12	Stress versus strain graph for as-received 50% Nickel - 50% Titanium alloy at 8% pre-determined strain level during loading and release of load	81
Figure 4.13	TAEFL plot for as received 50% Nickel - 50% Titanium alloy subjected to the corrosive medium of Hank's solution	83
Figure 4.14	Microscopic image of 50% Nickel - 50% Titanium alloy subjected to low temperature annealing heat treatment at 300°C when observed under Transmission Electron Microscope	84
Figure 4.15	Microscopic image of 50% Nickel - 50% Titanium alloy subjected to low temperature annealing heat treatment at 350°C when observed under Transmission Electron Microscope	85

Figure 4.16	Microscopic image of 50% Nickel - 50% Titanium alloy subjected to low temperature annealing heat treatment at 400°C when observed under Transmission Electron Microscope	85
Figure 4.17	Microscopic image of 50% Nickel - 50% Titanium alloy subjected to low temperature annealing heat treatment at 450°C when observed under Transmission Electron Microscope	86
Figure 4.18	X-Ray Diffractogram of 50% Nickel - 50% Titanium alloy subjected to low temperature annealing heat treatment at 300°C	88
Figure 4.19	X-Ray Diffractogram of 50% Nickel - 50% Titanium alloy subjected to low temperature annealing heat treatment at 350°C	88
Figure 4.20	X-Ray Diffractogram of 50% Nickel - 50% Titanium alloy subjected to low temperature annealing heat treatment at 400°C	89
Figure 4.21	X-Ray Diffractogram of 50% Nickel - 50% Titanium alloy subjected to low temperature annealing heat treatment at 450°C	90
Figure 4.22	DSC Thermogram of 50% Nickel - 50% Titanium alloy subjected to low temperature annealing heat treatment at 300°C	92
Figure 4.23	DSC Thermogram of 50% Nickel - 50% Titanium alloy subjected to low temperature annealing heat treatment at 350°C	92
Figure 4.24	DSC Thermogram of 50% Nickel - 50% Titanium alloy subjected to low temperature annealing heat treatment at 400°C	93

Figure 4.25	DSC Thermogram of 50% Nickel - 50% Titanium alloy subjected to low temperature annealing heat treatment at 450°C	93
Figure 4.26	Tensile Curve of 50% Nickel - 50% Titanium alloy subjected to low temperature annealing heat treatment at 300°C	99
Figure 4.27	Tensile Curve of 50% Nickel - 50% Titanium alloy subjected to low temperature annealing heat treatment at 350°C	100
Figure 4.28	Tensile Curve of 50% Nickel - 50% Titanium alloy subjected to low temperature annealing heat treatment at 400°C	100
Figure 4.29	Tensile Curve of 50% Nickel - 50% Titanium alloy subjected to low temperature annealing heat treatment at 450°C	101
Figure 4.30	Fractograph of 300°C heat-treated NiTi alloy when observed under SEM at a magnification of 5000X	101
Figure 4.31	Fractograph of 350°C heat-treated NiTi alloy when observed under SEM at a magnification of 5000X	102
Figure 4.32	Fractograph of 400°C heat-treated NiTi alloy when observed under SEM at a magnification of 5000X	103
Figure 4.33	Fractograph of 450°C heat-treated NiTi alloy when observed under SEM at a magnification of 5000X	103
Figure 4.34	Abrasive Wear characteristics of 50% Nickel - 50% Titanium alloy subjected to low temperature annealing heat-treatment at 300°C for one hour	107
Figure 4.35	Abrasive Wear characteristics of 50% Nickel - 50% Titanium alloy subjected to low temperature annealing heat-treatment at 350°C for one hour	108
Figure 4.36	Abrasive Wear characteristics of 50% Nickel - 50% Titanium alloy subjected to low temperature annealing heat-treatment at 400°C for one hour	109
Figure 4.37	Abrasive Wear characteristics of 50% Nickel - 50% Titanium alloy subjected to low temperature annealing heat-treatment at 450°C for one hour	110

Figure 4.38	Worn surface of 50% Nickel - 50% Titanium heat-treated at 300°C at 2000 and 5000 when observed under Scanning Electron Microscope	111
Figure 4.39	Worn surface of 50% Nickel - 50% Titanium heat-treated at 350°C at 2000 and 5000 when observed under Scanning Electron Microscope	112
Figure 4.40	Worn surface of 50% Nickel - 50% Titanium heat-treated at 400°C at 2000 and 5000 when observed under Scanning Electron Microscope	112
Figure 4.41	Worn surface of 50% Nickel - 50% Titanium heat-treated at 450°C at 2000 and 5000 when observed under Scanning Electron Microscope	112
Figure 4.42	Stress verses strain graph for 50% Nickel - 50% Titanium alloy subjected to low temperature annealing heat treatment at 300°C at 2% pre-determined strain level during loading and release of load	114
Figure 4.43	Stress verses strain graph for 50% Nickel - 50% Titanium alloy subjected to low temperature annealing heat treatment at 300°C at 6% pre-determined strain level during loading and release of load	114
Figure 4.44	Stress verses strain graph for 50% Nickel - 50% Titanium alloy subjected to low temperature annealing heat treatment at 300°C at 8% pre-determined strain level during loading and release of load	115
Figure 4.45	Stress verses strain graph for 50% Nickel - 50% Titanium alloy subjected to low temperature annealing heat treatment at 350°C at 2% pre-determined strain level during loading and release of load	115
Figure 4.46	Stress verses strain graph for 50% Nickel - 50% Titanium alloy subjected to low temperature annealing heat treatment at	

	350°C at 6% pre-determined strain level during loading and release of load	116
Figure 4.47	Stress verses strain graph for 50% Nickel - 50% Titanium alloy subjected to low temperature annealing heat treatment at 350°C at 8% pre-determined strain level during loading and release of load	116
Figure 4.48	Stress verses strain graph for 50% Nickel - 50% Titanium alloy subjected to low temperature annealing heat treatment at 400°C at 2% pre-determined strain level during loading and release of load	117
Figure 4.49	Stress verses strain graph for 50% Nickel - 50% Titanium alloy subjected to low temperature annealing heat treatment at 400°C at 6% pre-determined strain level during loading and release of load	117
Figure 4.50	Stress verses strain graph for 50% Nickel - 50% Titanium alloy subjected to low temperature annealing heat treatment at 400°C at 8% pre-determined strain level during loading and release of load	118
Figure 4.51	Stress verses strain graph for 50% Nickel - 50% Titanium alloy subjected to low temperature annealing heat treatment at 450°C at 2% pre-determined strain level during loading and release of load	118
Figure 4.52	Stress verses strain graph for 50% Nickel - 50% Titanium alloy subjected to low temperature annealing heat treatment at 450°C at 6% pre-determined strain level during loading and release of load	119
Figure 4.53	Stress verses strain graph for 50% Nickel - 50% Titanium alloy subjected to low temperature annealing heat treatment at 450°C at 8% pre-determined strain level during loading and release of load	119



Figure 4.54	TAEFL plot i.e. semi log plot of current on log scale vs potential on plain scale for 50% Nickel - 50% Titanium alloy subjected to low temperature annealing temperature of 300°C in a corrosive medium of pH value 7.5	123
Figure 4.55	TAEFL plot for 50% Nickel - 50% Titanium alloy subjected to low temperature annealing temperature of 350°C in a corrosive medium of Hank's solution	125
Figure 4.56	TAEFL plot for 50% Nickel - 50% Titanium alloy subjected to low temperature annealing temperature of 400°C in a corrosive medium of Hank's solution	126
Figure 4.57	TAEFL plot for 50% Nickel - 50% Titanium alloy subjected to low temperature annealing temperature of 450°C in a corrosive medium of Hank's solution	127
Figure 4.58	X Ray Diffraction of as-received 50% Nickel - 50% Titanium alloy	131
Figure 4.59	X-Ray Diffractogram of 50% Nickel - 50% Titanium alloy subjected to low temperature annealing heat treatment at 350°C	131
Figure 4.60	Differential Scanning Calorimetry curve of as-received 50% Nickel - 50% Titanium alloy	133
Figure 4.61	DSC Thermogram of 50% Nickel - 50% Titanium alloy subjected to low temperature annealing heat treatment at 350°C	133
Figure 4.62	Comparison of Abrasive Wear characteristics of as-received and low temperature annealing heat-treated 50% Nickel - 50% Titanium alloy	137

## NOMENCLATURE

TEM	Transmission Electron Microscopy
XRD	X-ray Diffraction
SEM	Scanning Electron Microscope
EDAX	Energy Dispersive Spectroscopy
VIM	Vacuum Induction Melting
VAR	Vacuum Arc Remelting
DSC	Differential Scanning Calorimetry
rpm	Rotations per minute
SME	Shape Memory Effect
SE	Superelasticity
$A_s$	Austenitic Start Temperature
$A_f$	Austenitic Finish Temperature
$M_s$	Martensitic Start Temperature
$M_f$	Martensitic Finish Temperature
UTS	Ultimate Tensile Strength

## SYMBOLS

CR	Corrosion Rate	mm/year
VPN	Vickers Pyramid Number	Kg/mm <sup>2</sup>
P	Load	Kg
D	Diameter	mm
A	Area	mm <sup>2</sup>
L	Wear Loss	cm
I <sub>corr</sub>	Corrosion Current	amps
K	Constant for corrosion rate	mm/(amp-cm-year)
d	Density	gm/cm <sup>3</sup>
EW	Equivalent Weight	gms

# CHAPTER 1

## INTRODUCTION

### 1.1 Smart Materials

Smart materials, also called as intelligent materials, are ones, which are designed to have one or more properties tailored in a controlled manner using external factors such as stress, temperature, pH, light or chemical compounds. The changes in the properties are reversible and are also repeated many times. The smart materials are used in a number of devices such as sensors, actuators and artificial muscles.

### 1.2 Types of Smart Materials

The following are the type of smart materials:

- Piezoelectric materials: Piezoelectric materials are ones that produce voltage upon the application of an external force. Since the effect applies in a reverse manner, a voltage across the sample will produce stress within sample. The structures made from the materials can bend, expand or contract upon voltage application.
- Photovoltaic materials: Photovoltaic materials are the ones that convert light to electric current.
- Shape memory alloys: These materials can be subjected to large deformations, upon temperature as well as stress applications. The shape memory effect occurs because of martensitic phase change and the elasticity induced at higher temperatures.
- Electroactive polymers: These materials undergo volumetric changes when exposed to electric or magnetic fields.
- Magneto strictive materials: These materials demonstrate a change in their shape upon the application of magnetic field and there is also change in the magnetization found during the external application of force.
- Magnetic shape memory alloys: These materials change their shape when the significant magnetic field is changed or altered.

- Temperature responsive polymers: These are the class of smart materials that undergo changes upon temperature.

### **1.3 Shape Memory Alloys**

A shape memory alloy is one that can undergo deformation when cooled below a prescribed temperature but returns to its predetermined shape when heated. The other names given to the shape memory alloy are memory metal, smart metal, and smart alloy or muscle wire. Many parts that are fabricated out of shape memory alloy could be light-weight, solid state alternatives to conventional actuators such as pneumatic and motor-based systems. A large number of shape memory alloys have been discovered since early 1900s. Many of the alloys, even though combinations of two or three different metals exhibit the properties that are of a single crystal which does not make them very useful for many of the applications. However, among the various alloys, a few have emerged as being very useful for a variety of applications such as CuZnAl, CuAlNi, nearly-equiatomic NiTi and to name a few. The two main properties of these alloys are shape memory effect and superelasticity. The shape memory effect describes the ability of the material to memorize its original shape and even after a huge plastic deformation revert back to its original shape after subsequent heating. The Superelastic effect refers to the material undergoing a large plastic deformation upto 8% strain and return back to its original shape after unloading. The stiffness of the material is observed to be non-linear with strain.

### **1.4 Selection of Alloy for the Present Investigation**

The various properties of three classes of shape memory alloys viz CuZnAl alloy, CuAlNi alloy and NiTi alloy has been presented in table 1.1.

Table 1.1 Different properties of CuZnAl, CuAlNi and NiTi shape memory alloys

<b>Alloy Property</b>	<b>NiTi alloy</b>	<b>CuZnAl alloy</b>	<b>CuAlNi alloy</b>
Melting point (°C)	1300	950-1020	1000-1050
Density (g/cc)	6.45	7.64	7.12
Thermal conductivity (W/m °C)	18	120	30-43
Electrical resistivity ( $\mu\text{-}\Omega\text{-cm}$ )	70-100	8.5-9.7	11-13
Young's modulus (GPa)	83 (austenite)	72 (beta-phase)	85 (beta-phase)
	26-48 (martensite)	70 (martensite)	80 (martensite)
Yield Strength (MPa)	195-690 (austenite)	350 (beta-phase)	400 (beta-phase)
	70-140 (martensite)	80 (martensite)	130 (martensite)
Ultimate tensile strength (MPa)	895	600	500-800
Shape memory strain (%)	8.5	4	4
Transformation range (°C)	<110	<120	<200
Transformation hysteresis (°C)	30-50	15-25	15-20

As seen in table 1.1, it is observed that NiTi alloy has the lowest density of 6.45 gm/ccs that gives it an advantage of light-weight in many of the applications. The difference between the Young's modulus of austenitic and martensitic phase makes it very suitable for many mechanical as well as bio-medical applications. Another property highlighted in table 1.1 depicts the highest shape memory strain of 8% making it very suitable for applications such as cardiovascular stents that need to be really squeezed and inserted into the human body. The NiTi alloy among the three alloys is very specific in its behaviour of being able to remember its shape-set state and return back to its original state after being deformed severely upto maximum of 8%. NiTi alloy has special properties such as higher ductility, lower density and higher resistance to corrosion as well as being able to be used in a wide range of applications. In this context, NiTi alloy has been found to be the most suitable material in this investigation as a material for study.

## **1.5 Manufacture of NiTi Alloy and Parameters Affecting the Properties**

The manufacture of NiTi alloy is carried out in two stages: the cast is produced through vacuum induction melting (VIM) followed by vacuum arc remelting (VAR). In VIM, the cast ingot is obtained by heating the Nickel and Titanium raw materials in a carbon crucible by varying magnetic fields. The ingot is cut into suitable shapes to be recast by VAR. In the process of VAR, the cast pieces are placed in a water-cooled Copper crucible and then re melted and cast into suitable wires or rods of needed dimension. Both VIM and VAR are carried out in high vacuum purged with inert gas such as Argon considering the reactivity of Titanium. Further, the manufacture of the NiTi alloy is preceded by carrying out hot and cold working of the cast ingot in order to achieve chemical homogeneity as well as dimensional control. Hot working is carried out followed by cold working. In hot working procedure, the initial dimension is reduced to a much smaller dimension. This is followed by cold working for dimensional accuracy and surface finish. Hot working is usually carried out at temperatures that are above the recrystallization temperature. Cold working is carried out well below the recrystallization temperature to increase the yield stress of the material and better dimensional control. To overcome the problem of cold working, the alloy is heat-treated at subsequent intervals to relieve the internal stresses caused by cold working. The heat-treatment temperature and time, needs to be carefully monitored to adjust the amount of excess Nickel coming out of the matrix. The internal stresses as well as the superelastic property can be controlled by a combination of cold working and heat-treatment processes. However, there are certain challenges associated with the manufacture of NiTi alloy. The tight compositional control needed to manufacture the alloy as a minute variation in the composition would lead to a migration from superelasticity to shape memory and vice-versa. This would pose a threat to the application where the alloy is being used for. The second challenge is the reactivity of Titanium with oxygen and carbon. This would cause a dip in the atomic percentage of Titanium in the alloy leading to a drastic change in the properties of the alloy.

In this investigation, studies have been carried out on certain properties of equi-atomic binary Nickel-Titanium alloy. The Nickel-Titanium alloy used in this investigation is procured from a commercial manufacturer. The cause of the alloy procurement is the tight compositional control needed to manufacture the alloy. As per figure 1.1, a small shift in the composition could bring about a major change in the  $M_s$  temperature of the material. The processing of the as-cast NiTi alloy to its final shape has to be carried out by the same procedure. The properties of the alloy depend on grain size, grain orientation and number of dislocations. Since the facilities available to us were not adequate, the alloy was procured from a manufacturer. The alloy was confirmed to possess shape memory property by the manufacturer.

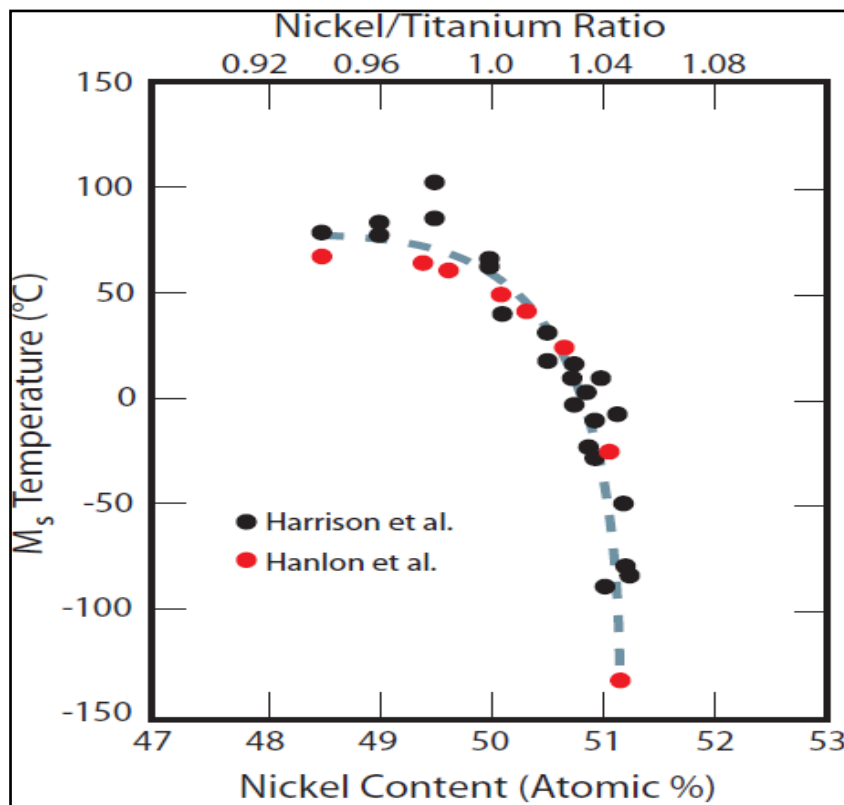


Figure 1.1 Relationship between  $M_s$  and Nickel atomic % (Pelton et al. 2001)

Figure 1.1 indicates that 0.1 atomic % shift in the Nickel content seems to alter the Martensitic start temperature  $M_s$  by 10°C. Also, 1 atomic % shift in the Nickel content alters the  $M_s$  temperature by 100°C. The material is expected to be superelastic when the working temperature lies between Austenitic finish temperature ( $A_f$ ) and martensitic



deformation temperature ( $M_d$ ) (Pelton et al. 2001), hence it was essential to control the smallest change in the Nickel content during manufacture.

## 1.6 Outline of the Thesis

- An EDAX was performed on the procured material to confirm the chemical composition of the nearly equi-atomic NiTi alloy. The chemical composition of the NiTi alloy would give a fair idea about the changes in the property of the alloy when subjected to thermal treatment.
- A low temperature heat-treatment was performed to evaluate its effect on the structure as well as properties of the alloy. Nickel-Titanium alloy has been used in a number of medical applications due to its bio-compatibility. Nickel-rich NiTi alloys show a drastic change in the microstructure as well as mechanical properties when subjected to thermal treatment. Whereas, Titanium-rich NiTi alloys did not exhibit any major change in their microstructure as well as mechanical properties upon subjecting to heat-treatment as per literature (Pelton et al. 2003).
- The microstructure of this alloy was examined using Transmission Electron Microscopy. As per the manufacturer, the cold-working is seen to induce nano-sized grains and also dislocations, and hence, TEM was employed to confirm the nano-sized grain of this material.
- The X-ray diffraction is carried out on the alloy to study the effect of heat-treatment and confirm the phases present in the alloy. The as-received and heat-treated materials are analysed for phases using XRD.
- DSC is performed on the NiTi alloy to investigate the transformation temperatures in order to confirm whether the material is shape memory as suggested by the manufacturer or a superelastic one. The effect of heat-treatment on the transformational temperatures was analysed through DSC. Since the working temperature needs to be between  $A_f$  and  $M_d$  (Pelton et al. 2001).
- The alloy being used in a number of mechanical and bio-medical applications, the mechanical properties are investigated by performing tension test and

Vickers Hardness test. The tension test is conducted to evaluate the UTS of the as-received and study the effect of heat-treatment on the tensile properties. Vickers Hardness test is carried out as the Hardness of this material is very high and would not be feasible with Brinell and Rockwell Hardness test. The effect of heat-treatment on the mechanical properties is analysed to suit particular applications.

- The wear properties of this material are investigated by conducting Abrasive wear test on the as-received and heat-treated NiTi alloy samples. The abrasive wear was performed since the material was found to be very hard and the wear was observed to be of the order of the run-out of the machine.
- Superelastic behaviour test was performed on the NiTi alloy samples to investigate extent of superelasticity of the alloy. This test was conducted to confirm the suitability of the material for a number of mechanical as well as bio-medical applications. The effect of heat-treatment on the superelastic behaviour was investigated for this material.
- The corrosion property of this material is investigated by performing an electrochemical corrosion test to investigate the bio-compatibility property of the alloy. The test is conducted using an artificial solution similar to body fluids. The effect of heat-treatment on the corrosion behaviour is also investigated in this study.

The present thesis has been divided into 5 chapters as follows:

## **CHAPTER 1**

Explains the basics of smart materials, shape memory alloys, reason for choosing NiTi alloy, challenges in manufacture of NiTi alloy and methodology adopted for investigation of various properties of NiTi alloy.

## **CHAPTER 2**

Survey of the research work carried out by researchers and the gaps in literature are presented. Also, explains the scope of the present investigation, objectives of research work.

### **CHAPTER 3**

Experimental procedure involving the methodology of research work, experimental setup and procedure followed for the investigation of each property are presented.

### **CHAPTER 4**

The results are presented and discussions of results are done. The results of as-received NiTi alloy and NiTi alloy heat-treated at different temperatures are presented. Comparison of the results of as-received and heat-treated NiTi alloy and discussions on the same is presented.

### **CHAPTER 5**

The conclusions drawn from the experimental work are presented. Also, scope for future work is listed.

## CHAPTER 2

### LITERATURE SURVEY

#### 2.1 Introduction

In the previous chapter, the different properties of shape memory alloys, superior properties of NiTi alloys and the parameters affecting the properties have been briefly introduced. Further, the outline of the present work has also been presented. In this chapter, a detailed available published literature on various aspects of 50% Nickel - 50% Titanium alloy has been reviewed and presented under the following headings.

#### 2.2 Basics of Nickel-Titanium Alloy

NITINOL, nearly equi-atomic NiTi shape memory alloy is a boon for many bio-medical applications such as cardiovascular stents, orthodontic arch wires and a lot more (Stockel et al. 2000) (Wholey et al. 2002). The main cause of the preference of this wonder material is based on its unique combination of its remarkable properties such as shape memory effect and pseudo elasticity combined with its bio-compatibility (Pelton et al. 2003). This phenomenon of Nitinol has been discovered since the 1960s and it has been a wide source of information in many of the technical journals and also international conferences.

The exceptional properties of NiTi shape memory alloy is from the reversible solid-state Martensitic transformation. At high temperature NITINOL exists in a body-centred-cubic structure known as the parent or B2 phase, wherein this phase resembles the CsCl structure. Upon lowering the temperature by cooling the material, NITINOL transforms into martensite, that is a monoclinic structure known as the B19' or the daughter phase. The temperature range over which the transformation from austenite to martensite takes place upon cooling and the reverse transformation to austenite takes place upon heating is called transformation temperature range. Typically, there are four transition temperatures namely martensitic start temperature ( $M_s$ ), martensitic temperature ( $M_f$ ), Austenitic start temperature ( $A_s$ ) and Austenitic finish temperature

( $A_f$ ). These four transition temperatures show the starting and ending of the phase change upon cooling as well as heating.

The austenitic and martensitic crystal forms are shown in the figure 2.1.

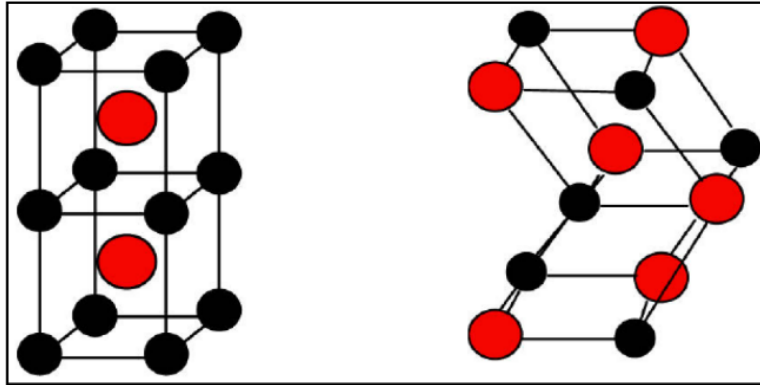


Figure 2.1 Austenitic (left) and martensitic (right) structures of NiTi compound (Alan R. Pelton et al. 2003)

There are two aspects of this phase transformation. First, the transformation is reversible. The martensite, when heated above a specific temperature transforms into the simple austenitic phase. Second, the transformation in both the directions is instantaneous. Martensite's crystal structure (B19') has the unique ability to undergo limited deformation without causing any breakage to the atomic bonds. This process is known as twinning that consists of rearrangement of atomic planes without causing a slip unlike Steel where the transformation to martensite takes place by the slip phenomenon. When the material in the martensitic phase is heated, it is reverted back to austenite irrespective to whether the martensite is deformed or not. The alloy undergoes a 6-8% strain at the martensitic phase. The Austenitic structure undergoes a solid-solid deformation by the phenomenon of Twinning and forms martensite. It is indicated by (K B. 2003) that the Austenitic structure forms martensite in the form of self-accommodating twins. The formed structure is the reduction of the stored strain energy of the sample that undergoes martensitic transformation during the cooling of the alloy sample. This minimization that leads to the twinning is the structure of NiTi gets twinned internally due to being a shear type of a transformation. However, in literature (Pitteri M et al. 2003) it is stated that the cooling of the Austenitic structure below a prescribed temperature makes it to form self-accommodating twins. At the

micron level however, there are changes in the structure that can be identified performing microscopic studies. The structure is seen to have a total change from the so-called cubic to the orthorhombic, which is distorted. According to the literature this particular phase is considered to have 12 variants that are taking the huge strains given by the so-called neighbouring variant such that the resultant strains are zero. It is reported that the 12 variants are correlated with each other and the so-called relationships namely lattice-invariant twin, deformation twin and variant accommodation twin. As per the literature (Pitteri M et al. 2003), apart from deformation twinning, accommodation twin and invariant twin show no specific change in their shapes.

There are a lot of controversies that always the self-accommodating twins do not form in the case of martensitic transformation in all the cases. It is mentioned by (Saburi T et al. 1979) that the self-accommodating twins play a very important role in the formation of daughter phase martensite and renders it as reversible. The self-accommodating twins to take place depends on the symmetry of the atomic arrangement in the parent Austenitic lattice as per (K, B. 1992). It is also observed as per (K, B. 1992) that there is a very minute reduction in the volume of the parent phase that leads to the self-accommodating twins. It has been proposed by (Saburi T et al. 1979) that the self accomodating twins are called as plate groups that are formed by four habit planes of a crystalline lattice about a pole pertaining to the indices (110) of the parent austenitic structure.

According to various literature martensitic transformations are considered as displacive transformations, wherein, there is very small movement of the atoms and they adjust so that it forms a very stable crystal structure. It is considered that when austenite transforms into martensite heat is released during specific experimentations rendering the transformation as exothermic (Adharapurapu et al. 2007).

It has been discovered by (Duerig et al. 1990) that the properties of shape memory and pseudo-elasticity occur due to the diffusionless transformation between the parent Austenitic phase and the daughter Martensitic phase. The main temperature used in many of the bio-medical applications is the Austenitic finish temperature ( $A_f$ ) and this

particular temperature is discovered to govern the transition from one phase to the other i.e. from shape memory to the superelastic phase. This temperature of  $A_f$  can be varied to suit the bio-medical requirements depending upon whether the application is a superelastic or a shape memory one. This variation is brought about by performing various ageing processes on the alloy material. The NiTi alloy is found to have a very narrow compositional range below the melting temperature of about  $600^\circ\text{C}$  as seen in the binary phase diagram (Pelton et al. 1994). The best method according to “ASTM F-2004 standards” (F2004-00, 2002) was to perform the Differential Scanning Calorimetry and confirm the formation of the alloy ingots.

This phase transition of NiTi alloy is illustrated in the binary phase diagram as shown in figure 2.2.

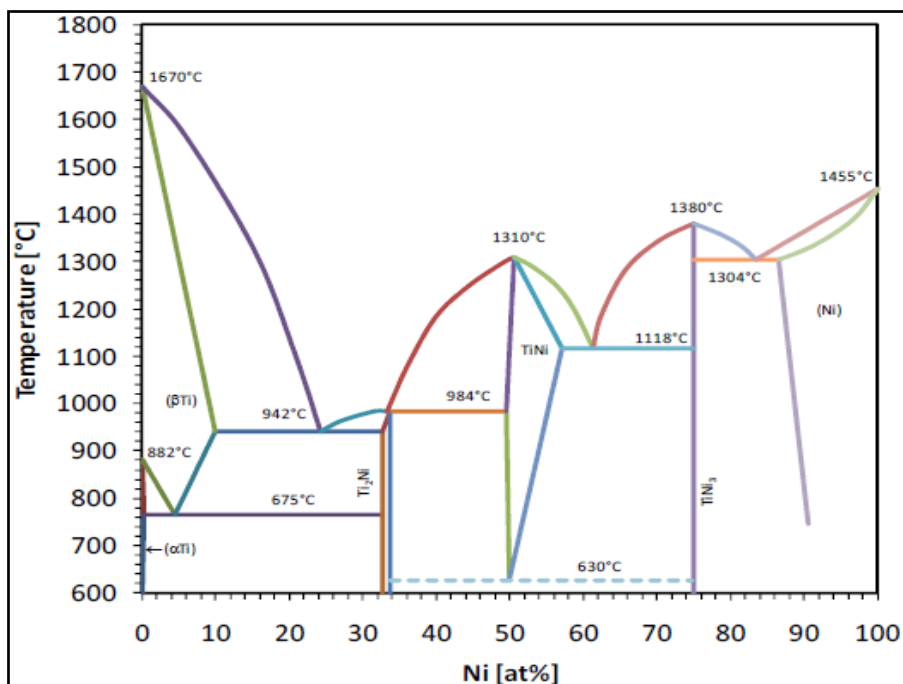


Figure 2.2 NiTi phase diagram (Velmurugan et al. 2018)

As seen from figure 2.2, Nitinol is an ordered intermetallic compound having a very narrow composition range below  $630^\circ\text{C}$ . Nitinol is seen to be composed of approximately 50% Nickel by atomic percent and the rest being Titanium. Below the temperature of  $630^\circ\text{C}$  any small deviations in the stoichiometric 50:50 composition makes the alloy be in a two-phase field. It is clear from figure 2.2 that controlling the

amounts of Nickel and Titanium becomes very important in achieving a correct composition for a specific application.

The transformation temperature is seen to be very much dependent on the contents of Nickel and Titanium. The addition of excess Titanium starts forming  $Ti_2Ni$  incoherent equilibrium precipitates without impacting the NiTi matrix as well as the transformation temperature. These  $Ti_2Ni$  particles are inert and are not at all affected by any aging treatment and are just treated as inclusions in the binary NiTi matrix (Pelton et al. 2001). The Nickel-rich alloy offers some very interesting results. It is also studied that many alloys with more than 50.3 atomic % Nickel are found to be unstable at room temperature and are affected by the aging that leads to the precipitation of  $Ni_3Ti$  equilibrium precipitates leading to a more equi-atomic 50:50 NiTi matrix thereby increasing the transformation temperature. It is also observed from figure 1.1 of previous chapter that a minute 0.1 at% change in the Nickel content changes the transformation temperature by  $10^{\circ}C$  whereas a 1 atomic % change in the Nickel content changes the transformation temperature by  $100^{\circ}C$ . Many applications require the controlling of the transformation temperatures to  $\pm 5^{\circ}C$  which accounts to the controlling of the composition to within  $\pm 0.05\%$ .

The NiTi alloy is used extensively in a number of applications such as orthodontic wires, cardiovascular devices, and orthopaedic applications in a number of surgical instruments.

The Nickel-Titanium shape memory alloys have formed a major part in the minimally invasive surgical procedures. The prime reason for NiTi alloy becoming a major leader in surgical instruments is its capability of recovering a major part of the deformation caused to it under any circumstances (G et al. 1999).

In orthopaedic applications, the NiTi alloy is used as a spacer in the vertebrae of humans. This helps in the prevention of any unwanted motion of the spinal column during the recovery process undergone by a patient during a surgery. This prevents from any unwanted damage taking place (Lagoudas et al. 1999). The spacer inserted in the vertebrae is seen to apply a slow and steady load on the spinal cord so as to prevent any injury caused during the movement of the patient during working hours (Machado et



al. 2003). The NiTi shape memory alloy has got other applications in the areas of fractures that occur in the case of the human bones. In this case, the alloy is used in the form of staples called orthopaedic staples (Machado et al. 2003). The staple in the open form is first placed in the place where the bones need to be joined. After placing the staple, an enormous amount of heat is applied from an external source that contracts the staple to its original shape and size thereby holding the fractured areas so as to ensure quick healing of the patients from the caused fracture.

The NiTi alloy is deployed in a number of cardiovascular applications, one of them being in the angioplasty of patients having collapsible blood vessels. The reason for performing the angioplasty on the patients is treating coronary heart disease and also ensuring that the blood flow is made proper in these cases. The procedure is carried out by making a thin wire holding a compressed stent through a collapsed artery till the wire just passes over the blockage. The stent used are nothing but metal cylinders, that are shape set and compressed during pushing the same with a guide wire through a collapsed artery.

### **2.3 Annealing of Nickel-Titanium Shape Memory Alloy**

Titanium alloys have been constituted as bio-materials because they are viewed to possess exceptional characteristics such as higher corrosion resistance, higher ultimate tensile strength and proven to be bio-compatible (Xavier et al. 2017). The Titanium alloy is observed to show allotropic transformation during heating performed on the same. The structure is noticed to transform from hexagonal closed packed to body centered cubic. The control of the micro-structure and mechanical properties was evident to be possible by performing heat-treatments (Li. 2004). Also, the process of heat-treating NiTi alloys is found to be critical. It is critical since the transformational temperatures need to be fine-tuned to suit the application. It is found that the heat-treatment temperature and time is observed to manipulate the different phases present in Nickel-rich alloys such as  $Ni_4Ti_3$  and  $Ni_{14}Ti_{11}$ . The release of the phases such as  $Ni_4Ti_3$  from the NiTi matrix is observed to contribute to increase the transformation temperature to suit the requirement (Pelton et al. 2003). It was proven by many manufacturers that a combination of cold working and heat-treatment is a must in controlling the overall properties of Nickel-Titanium alloy products. Walid et al. (2017)

has conducted an extensive review on the Nickel-rich NiTi alloys by studying the effect of heat-treatment on the phases present and also the types of heat-treatment processes. The author has mentioned the two main properties of the NiTi alloy. The thrust of the research is studying the effect of performing the annealing treatments on the shape memory as well as superelastic properties of the NiTi alloy. The effect of heat-treatment on the microstructure was carefully analyzed followed by its effect on the mechanical properties. The author mentioned the increasing of the Austenitic finish temperature ( $A_f$ ) by heat-treatments would bring the same, a little above the body temperature. This would ensure the alloy in a mixed phase of Austenite and martensite/R-phase. According to the literature, the alloy would exhibit the superelastic nature ensuring excellent flexibility and cyclic fatigue. The results looked to be promising in using the alloy as endodontic files in dentistry with improved fatigue and cyclic resistance.

Gusev et al. (2019) conducted a study on Nickel-rich NiTi alloy in terms of effect of heat-treatment. The author suggested the range of heat-treatment temperature to be in the range of 700°C to 1200°C. The effect of heat-treatment resulted in the grain growth of the austenitic phase as the temperature was increased. However, the superelastic tests did not show any significant changes in terms of the stress-strain curves. There was one major change observed during an increase in the heat-treatment temperature i.e. the stress needed to change from the austenitic to the martensitic phase was seen to increase upon an increase in the heat-treatment temperature. Also, the recovery strains upon unloading were seen to increase for an increase in the heat-treatment temperature. The heat-treatment temperature, when increased beyond 1100°C was seen to reduce the ductility property of the material drastically. The annealing temperatures when increased above 1100°C brought about a reduction in the fatigue properties also.

The effects of heat-treatment time duration and the temperature was observed by (M. Nishida et al. 1986) on Nickel-rich shape memory alloys and concluded that there are a lot of precipitations that take place during the ageing treatments. The precipitation sequence as seen are  $Ni_{14}Ti_{11}$ - $Ni_4Ti_3$ -  $Ni_3Ti$  and the ageing temperatures are of the range of 800°C to 1000°C for a time period of about 100 – 500 hours. This manipulation of the transformational temperatures that are carried out by a combination of ageing

treatments as well as cold working is done to suit various bio-medical applications (Pelton et al. 2000).

The ageing treatments along with the  $A_f$  also influence the ultimate tensile strength (Pelton et al. 2003). It is mentioned that the ageing performed between 300°C and 450°C are found to raise the ultimate tensile strength of the Nickel-rich alloy whereas high heat-treatment temperatures are seen to significantly lower the strength of the specimen, which could be due to recrystallization taking place.

The precipitates such as  $Ni_3Ti$  released during the ageing treatment according to (Pelton. A et al. 2000) is seen to act as barriers and prevent any kind of dislocation that could take place during the cold working of the alloy. Also, these precipitates not only prevent dislocation density to increase but also are observed as strain inducers that stabilize the R-phase formed during the cooling or heating cycle of the alloy. The heat treatment processes such as annealing, normalizing, Austempering, Martempering etc. are seen to activate the ageing process that causes rearrangement of the defects and dislocations that are formed in the material by utilizing the stored internal energy of the sample (Reed-Hill. 1992). According to (Reed-Hill. 1992), it is mentioned that in heavily cold-worked materials owing to dislocations, the annealing gets a higher driving force due to the stored internal energy in the cast material.

The heat-treatments performed on 30% and 50% cold worked materials were studied extensively by (Drexel et al. 2007) for the variation in their transformational temperatures. It was found out that in both the 30% and 50% cold-worked wires, the R-phase was stabilized by heat-treating at 450°C temperature for subtle time duration of 2 or 20 minutes. It clearly signifies that it is cold-working followed by the heat-treatment that stabilizes the transformational temperatures in alloy materials. The temperature of 450°C was found to be ideal in having the  $A_f$  temperatures increased due to the precipitates such as  $Ni_3Ti$  coming out of the solution (S M et al. 1990). From 450°C if the annealing temperature is further increased to 550°C, then the  $A_f$  for the samples is seen to be lowered. This lowering of the transformational temperature is found to happen probably due to the precipitates going back into the NiTi matrix. This

would increase the Nickel content thereby greatly lowering the temperature, studied by (Pelton et al. 2003).

However, the increase in the  $A_f$  temperatures occurs in the range of 400-450°C ageing with fairly shorter aging times. It was concluded that the highest  $A_f$  temperatures were found for the materials that are heavily cold-worked and they needed lower aging times to deplete excess Nickel from NiTi matrix according to (Drexel et al. 2007). Similarly, the similar phenomenon goes with the UTS of the NiTi alloy. According to (S M et al. 1990) the cold-working of the as-cast NiTi wires leads to a very high ultimate tensile strength as per the experimentation. (S M et al. 1990) suggested that the main reason for the high level of the UTS could be the stored internal energy in the cast samples. This internal energy gets accumulated due to sudden cooling taking place during the casting of the alloy samples. This high internal energy has prevented the alloy from showing the superelastic nature upon any particular load during the tensile testing (S M et al. 1990). Also, many other phenomena were observed such as the aging at a lowest temperature of 300°C resulted in a superelastic nature while aging at higher temperatures of 400 or 450°C showed signs of increased UTS. As at higher temperatures, transition as well as equilibrium precipitates such as  $Ni_{14}Ti_{11}$ ,  $Ni_4Ti_3$ ,  $Ni_3Ti$  etc. come out of the matrix as excess Nickel. These excess Nickel ions are seen to act as barriers preventing any sort of dislocation to take place in the micro-structure. The subsequent heat-treatments performed on the 50% cold-worked NiTi wire leads to a reduction in their Ultimate Tensile Strength. The reduction in the UTS is seen on account of a much greater stored internal energy that offers a great helping hand for the aging process. Hence it was confirmed by (S M et al. 1990) that it is the recrystallization that takes place in the material when the alloy is annealed at temperatures in the range of 500°C.

It was confirmed by (Drexel et al. 2007) that the 50% cold worked alloy showed greater response to the aging operations in terms of stress values than the 30% wires. This was stated by (Drexel et al. 2007) that the temperature of the aging processes along with its duration play a vital role during the manufacture of the alloy material for a particular application. The amount of the cold-working also needs to be considered for the same

as it results in a high storage of internal energy that activates the aging process and brings about a good change in the microstructure as well as mechanical properties.

The Nitinol alloy material has been extensively reviewed by (Pelton et al. 2000) where the optimization of the properties of the Nitinol wire are discussed with respect to the different processing parameters and the effects of heat-treatments. The use of Nitinol has seen to make a marked impact on the medical industry, in terms of transition of an open-heart surgery for a cardiovascular problem to minimally invasive technique (Brooks et al. 1998). In the medical industries after the discovery of Nitinol, many of the devices used by the medical professionals are noticed to use NiTi alloy as the material. The basic reason for using NiTi as the material was because of the superelastic behavior, that made it to be used in a wide number of applications such as the cardiovascular stents, endodontic tools, orthodontic arch wires and to name a few (Frank TG et al. 2000).

The superelastic performance of the NiTi alloy samples exhibited a marked improvement when subjected to a series of ageing treatments and cold-working according to (Duerig et al. 1990). It was proven by many of the researchers that the Nickel-rich alloys respond well to the ageing treatments done. The best ageing temperature range was discovered by (Nishida M et al. 1986) that were from 300°C to 500°C. The more appropriate range of ageing temperature, where the austenitic finish temperature is observed to vary is 350 - 450°C. In that temperature range, most of the precipitates were observed to come out of the NiTi matrix leading to a rise in the transformational temperatures.

The ageing treatment temperatures as well as the time duration have a profound effect on the mechanical properties as well. As per (Pelton et al. 2000) the ageing done in the temperature range of 300 – 450°C seem to have a major impact on increasing the ultimate tensile strength of the sample. The main cause for the increase in the UTS is the transition precipitates  $\text{Ni}_{14}\text{Ti}_{11}$  coming out of the matrix by diffusion phenomenon that act as barriers for dislocation of the atoms to take place upon loading. But similar to the transformation temperature, the ultimate tensile strength is observed to reduce upon increasing the ageing temperatures to 500°C and higher. That decrease in the

strength of the material is clearly the precipitates that go back into the matrix thereby the obstruction to the dislocation motion is gone, and the material deforms easily upon an external force. Hence, the aging temperatures and time greatly influence the transformation temperature as well as the mechanical properties in Nickel-rich alloys.

However, according to the (Chen et al. 2003), the materials engineers perform various operations in order to modify the characteristics of NiTi alloys to suit the needed application. These properties i.e. shape memory or pseudoelasticity can be zeroed on by modifying the transformational temperatures of the alloy. The main transformational temperature that is concentrated by the material researchers is the  $A_f$  according to (Chen et al. 2003). The temperature of  $A_f$  can increase to suit the pseudoelasticity application only when the excess Nickel gets depleted from the matrix thereby causing an increase in the atomic percentage of Titanium. Hence the experimental data obtained proved that the alloy was stable only above the temperatures of 630°C according to the phase diagram of NiTi alloy. The increase in the  $A_f$  temperature according to the T-T-T diagram states that the possibility of metastable precipitation to take place from the NiTi matrix for the transformational temperature to increase substantially according to (Nishida M et al. 1986). It was found by (Chen et al. 2003) that the minutest change in the composition of the Ni ion in the NiTi matrix can drastically change the property from being shape memory to pseudoelasticity and vice-versa. Also, it was mentioned by (Chen et al. 2003) that the principle of the changing of the  $A_f$  temperatures is ruled by the concept of grain growth taking place during the process of annealing and heat-treatment.

The microstructure followed by the grain size play a big role in manipulating the mechanical properties of the alloy. The manufacturing process selected and also the thermomechanical treatments given to the alloy make the grains finer and are observed to have a specific orientation. According to (F. M. Sanchez et al. 2008), from the different heat-treatments, grains of uniform sizes are formed and also precipitates of different types are released from the matrix. These are not found to be very stable and tend to mix with the elements in different proportions and come out of the matrix. Various transition as well as the equilibrium precipitates such as  $Ni_3Ti$  coming out from

excess Nickel raise the austenitic transformational temperature whereas the precipitates such as  $\text{Ni}_4\text{Ti}_3$  do affect the mechanical properties of the material.

(Pelton R et al. 2003) suggests that the NiTi material is cast using a VIM and VAR technique, followed by the casting process, the tubes of 50cm diameter are hot-rolled at temperatures of 600-800°C that drastically reduce the dimension of the tube. Cold work and a series of annealing processes are carried out in order to prevent work-hardening and achieve surface finish followed by dimensional accuracy. The properties of the material are optimized by carrying out a series of intermediate temperature ageing of around 300-500°C (Pelton R et al. 2003). The cold-working and heat-treatment procedures are responsible in achieving the desired properties of the NiTi material for bio-medical applications. The transformational temperatures are also so monitored so as to remain in the range of  $A_f$  to  $M_d$  to ensure pseudoelastic properties of the material (Pelton et al. 2001). Also, the effects of duration of the ageing done on the samples had a direct effect on the precipitates coming out of the matrix leading to an increase in the  $A_f$  temperatures so as to ensure superelasticity of the alloy wire. (Nishida M et al. 1986) suggested that the best ageing temperature range was 300-600°C with a typical duration ranging from 60 minutes to as high as 180 minutes for the main precipitates to come out of the NiTi matrix leading to an increase in the  $A_f$  and the matrix becomes enriched in Titanium rather than Nickel. Pelton et al. (2003) suggested that performing heat-treatments on Nitinol wires in the temperature range of 300-450°C enhance the mechanical property in terms of mechanical tensile strength. As in case of Nickel-rich alloys, the precipitates that come out of the matrix act as barriers for dislocation of the atoms thus yielding higher ultimate tensile strength.

According to (Molinari A et al. 2001) the cryogenic treatment is seen to enhance the cutting efficiency and also the cyclic fatigue resistance of the NiTi wires giving the alloy the needed thermal stability. The temperature range for performing the cryogenic treatment was found to be in the range of sub-zero range of -60°C to -80°C (Molinari A et al. 2001). The NiTi wire is cooled to sub-zero temperatures and then allowed to warm up to the room temperature of 37°C, the atmosphere being liquid Nitrogen in most of the cases (Huang J et al. 2003). This treatment of cooling the material in liquid nitrogen atmosphere has numerous benefits of increased fatigue resistance followed by an

increase in the cutting efficiency of the material (Huang J et al. 2003). It was studied and proven by (Kim J W et al. 2005) that the NiTi files that are treated using cryogenic treatment are seen to possess a higher level of microhardness than the files that are heat-treated by normal means. According to (George G K et al. 2011), the cryogenic treatment of the NiTi files is seen to improve the fatigue resistance by many folds.

According to (D. Treppmann et al. 1997), the class of smart materials i.e. Ni-Ti shape memory alloys are supposed to have specific properties such as pseudoelasticity, pseudoplasticity etc. to be used in a number of applications. Hence, the thermo-mechanical treatments are applied to tailor the micro-structure followed by the mechanical properties of the alloy material. The thermomechanical treatments necessary are so chosen after careful investigation of the application for which the alloy is being manufactured followed by the studying of the T-T-T diagrams. (D. Treppmann et al. 1997) suggests that the thermomechanical treatments carried out on the NiTi alloys have a wide range of temperatures ranging from the melting point of the material (1300°C) to as low as the martensitic finish temperature. The temperature range in between the process of the ausforming and marforming is of importance to carry out the treatments effectively so as to induce the necessary defects and dislocations in the alloy material making it resistant to any kind of diffusionless transformations.

D. Treppmann et al. (1997) says that there is a very complex form of the deformation of the microstructure that can take place when the temperatures are between  $M_f$  and  $M_d$ . The structure was found to be a combination of the one of ausforming and also marforming. The difficulties of the marforming can also be overcome by the process of tempering of the formed martensitic structure. This tempering needs to be carried out accordingly depending on the parameters such as the temperature at which the structure is activated, the percentage of the forming that is carried out and so on. According to (D. Treppmann et al. 1997), the tempering brought about various changes in the material in terms of the martensite being able to transform back into the austenitic structure followed by the controlled diffusion of the austenite grains. Finally, the growth of the austenitic grains take place within the structure of the material. The temperature and the time duration of the heat-treating play a very important role in the transformation of the martensite into austenite and also the growth of the grains. Copper



based alloys such as the CuZnAl shows also a two-stage transformation upon the thermal and mechanical treatment given to it. Overall, according to (D. Treppmann et al. 1997), the ausforming does not bring about any major change in the structure as well as the transformational properties. It is only in the case of marforming the structure as well as the properties take a major turn ensuring that the transformation back to the austenitic structure does not take place that easily. The time-temperature-reaction diagram plays a vital role in the shaping of the semi-finished materials also ensuring the strength and the transformational properties of the same.

D.A. Miller et al. (2001) has suggested that the thermomechanical treatments are seen to affect the mechanical behavior as well as the transformational temperatures of NiTi shape memory alloys in terms of the dislocations being introduced in them. It is suggested that the process of ausforming brings about a lot of improvement in the tensile strength of the alloy (Hombogen et al. 1997). Also, it was suggested by (Hombogen et al. 1997) that the process of ausforming needs to be done so as to ensure that the stress-induced-martensite should not take place above the  $M_d$ . But by the process of precipitation there might be small transformations of the phase that might occur due to the process of ausforming.

The cold working as well as the heat-treatments carried out have proven effects on the transformational properties of the NiTi alloys according to (A. S. Paula et al. 2008). It is observed by (A. S. Paula et al. 2008) that the percentage of cold-work has significant effect on the transformational properties of the alloy. The 10% cold-work has brought about a variation in the  $M_s$  and  $M_f$  temperatures upon an increase of the heat-treatment temperatures. A similar trend was found for the  $A_s$  and  $A_f$  temperatures upon increasing the ageing temperature. The austenitic start and the finish temperatures varied by decreasing and then increasing to a certain value when the ageing temperatures were increased to a high value of 800°C.

A. S. Paula et al. (2008) states that for a 20% cold-worked material the presence of R-phase is seen to occur at low ageing temperatures of about 477°C, whereas the R-phase disappears for slightly raised heat-treating temperatures of 647°C and is seen to come at highest temperature of about 750°C. Similarly, the other transformational

temperatures such as the  $A_s$ ,  $A_f$ ,  $M_s$  and  $M_f$  are seen to vary to quite an extent with the increasing annealing temperatures.

For a 30% and 40% cold-worked material, the types of phases and the variations in the transformational temperatures are seen to be similar as per (A. S. Paula et al. 2008). The R-phase is seen to appear only during the cooling cycles for the annealing temperatures of the order of 427 - 527°C. At slightly higher annealing temperatures, the 30% cold-worked samples are observed to exhibit higher  $A_s$  and  $A_f$  temperatures after annealing is carried out at 477°C or above. Whereas, the  $M_s$  and  $M_f$  temperatures are found to increase slightly for annealing at 527°C and reduce upon annealing beyond 727°C.

## **2.4 Transmission Electron Microscopic Studies of Nickel Titanium Alloy**

Transmission electron microscopy is carried out in many materials to reveal the internal structure that is of the order of few microns (Goodhew. 2011). The information that can be extracted from TEM depends upon resolving power of the equipment, the energy of electron beam, specimen thickness, composition and stability of the material. In a modern TEM, resolving power is in the order of nanometers. Hence the grain size of a severely plastic deformed material which is less than 100 nanometers can also be resolved. In a NiTi alloy, the structural changes caused by cold working and heat-treatments can be clearly understood through TEM. Along with the crystalline structure, stress, internal fractures and also dislocations can be studied using TEM technique.

The in-situ TEM techniques are employed in order to reveal the sub-microstructure of the samples under study. According to (Dominique Schryvers et al. 2004) it is still not clearly understood regarding the influence of the precipitates seen in the TEM that can influence the properties of NiTi. According to (E. Mohammad Sharifi et al. 2014) the cold rolling followed by annealing leads to formations of huge dislocation network as observed in TEM.

J. FERCEC et al. (2014) performed an analysis on six types of Orthodontic NiTi wires using Transmission Electron Microscopy (TEM). From the TEM it was observed that the Austenitic phase seemed to look like small particles. The microstructure revealed

that along with the Austenitic phase, the structure consisted of precipitates such as  $Ti_2Ni$  and also  $TiC$ . The precipitates seemed to possess greater grain sizes than the NiTi matrix. The austenitic phase consisted of fully crystallized grains having a grain size of the order of 50-160 nanometers.

G. Steiner et al. (2008) studied the microstructure of NiTi and NiTiHf alloys subjected to cold rolling and high-pressure torsion (HPT). The structure revealed both the Austenitic and Martensitic phases in certain amounts. But, the structure of the materials subjected to HPT showed the transformation of the austenitic to the martensitic phase.

X-G. Ma et al. (2007) studied the Microstructure and also the transformation of Nickel-rich NiTi alloys by performing in-situ TEM. The alloy samples were cooled and heated in the TEM apparatus to investigate the transformation behaviour and microstructure. The TEM revealed the presence of martensitic variants in the alloy matrix. Also, the sample showed superelastic property when tested under nano-indentation. This was probably due to the presence of martensitic twins in the matrix.

Remi Delville et al. (2009) performed the transmission electron microscopy on TiNiPd alloy to study the microstructural evolution that would influence reduction of the hysteresis and compatibility. The TEM images indicated the presence of martensitic structure. The martensitic variant being compatible with the parent phase austenitic variant showed reduction in the hysteresis of the alloy.

M Liu et al. (2002) studied the microstructures of NiTiHf alloy by performing a high-resolution transmission electron microscopy. The TEM showed self-accommodating martensitic twins formed on either side of melt-spun ribbons. According to (M Liu et al. 2002), along with the martensitic phase the amorphous phase was formed due to the process of melt-spinning. The presence of the amorphous phase along with martensite leads to the increased hardness and brittleness in the material.

Kurnia Hastuti et al. (2015) carried out research on the effect of annealing on the microstructure and the deformation behavior of Ni-rich NiTi alloys. The microstructural analysis of the as-received alloy material revealed the presence of dislocations that would have got produced during the manufacture of the alloy. According to their research, it was found that the annealing treatment of 400°C proved

to be beneficial in altering the microstructure in terms of removing the dislocations and also improving the ultimate tensile strength to be maximum. The annealing carried out in the temperature range of 300-400°C revealed the presence of the austenitic and the martensitic phase as well when examined under TEM. Annealing temperatures above 500°C was not preferred due to the absence of the martensitic phase as seen in microstructure leading to a reduction in the UTS.

R. Delville et al. (2011) made a thorough study of the sub microstructure of the Nickel-rich NiTi alloy. The alloy was subjected to different modes of heat-treatments and superelastic cycling was carried out on the as-received and heat-treated wires. The grain size of the sub-microstructure of the as-received wires were in the range of as low as 100nm. The heat-treatments brought in a subsequent change in the size of grains going as high as 200nm. The dislocations were seen to increase with an increase in the grain size. This increase in the grain size leads to a loss in the martensitic phase, when the wires were subjected to a superelastic cycling.

R. Santamarta et al. (2013) have carried out several investigations on Ni-rich NiTiHf and NiTiZr alloys. The alloys procured from a commercial manufacturer have been subjected to a series of solution and annealing heat-treatments and the microstructures have been analyzed using TEM. The TEM investigation revealed the presence of smaller precipitates when the alloys were heat-treated at lower temperatures in the range of 400-600°C. The precipitates were seen to be more prominent upon an increase in the heat-treatment temperature of the order of 800-1000°C.

Ghazal Tadayyon et al. (2016) made a study of the microstructure through TEM for the as-received and heat-treated Ti-rich NiTi alloys. The alloys were heat-treated at temperatures around and also above the recrystallization temperatures. A solution treatment was also carried out on the Ti-rich NiTi alloys. The microstructures revealed the daughter phase B19' to be viewed as self-accommodated plates at higher annealing temperatures. The Ti<sub>2</sub>Ni precipitates were observed in the TEM investigation that according to the literature is size controllable.

## 2.5 X-Ray Diffraction Studies of Nickel-Titanium Alloy

X-ray diffraction is a unique method for the determination of crystallinity of an alloy. In an XRD analysis, the atoms of a crystalline material create an interference pattern of waves present in the incident beam of x-rays. The planes present in a crystalline solid, act on the x-ray in a similar manner, as a uniformly ruled grating on a beam of light passing through it.

Z. Lekston et al. (2007) conducted an extensive research on TiNiCo and Nickel-rich NiTi alloys through phase analysis. This was carried out in order to analyze the phases present in the alloy in the as-received as well as the heat-treated condition. The author concluded that the NiTi alloy exhibited reversible martensitic transformation. The peaks of the martensitic, R-phase and the austenitic phase were found to occur in the  $2\theta$  angle of  $37 - 47^\circ$ . It was also found out that after heat-treating the alloy at  $450^\circ\text{C}$  temperature, the R-phase is seen to occur in the heating and cooling cycles and the same was exhibited in the X-Ray diffractogram.

Mohammad Honarvar et al. (2015) conducted investigation on various diameters of NiTi wires. The investigations conducted were on wires of diameter less than 0.19mm. It was confirmed that the wires when heat-treated to temperatures of  $70 - 80^\circ\text{C}$  yielded R-phase as the main phase with martensitic phase and no austenitic phase. The wires of diameters 0.24 – 0.29mm yielded martensitic phase when heat-treated to temperatures of  $70 - 80^\circ\text{C}$ . When the heat-treatment temperatures were increased to  $120 - 130^\circ\text{C}$  range, the R-phase was prominently observed in the wires of all the diameters.

Todd A. Thayer et al. (1995) have a thorough investigation on eight different NiTi wires of rectangular cross-section. The NITINOL wires underwent a superelasticity test ranging from 0 – 10% strain. The XRD patterns of each of the strained wires were analyzed. The wires without the 6% strain showed the Austenite as the main phase with traces of the daughter phase martensite. The wires undergoing 6% strain showed martensitic phase to appear in the XRD pattern. According to the literature, an increase in the percentage of the cold working carried out during the manufacturing of NITINOL indicated in the form of increased peak width. The author stated that the XRD results

clearly indicated that the cold work and heat-treatment form an important part of in the manufacturing of the product.

Iijima, M et al. (2004) performed an X-ray diffraction on two different orthodontic wires. There was a finding as per the literature, that the arch wire used in oral environment exhibited shape memory property, whereas, without oral environment was a superelastic one. The x ray diffractograms were obtained for a set of straight samples in the as-received condition. The straight samples clearly showed the presence of R-phase for the wire exhibiting shape memory property, while the wire exhibiting superelasticity did not show the R-phase. As per the author, the bent wires showed a clear presence of the martensitic phase. The changes noticed in the XRD patterns were found to be minimal for the superelastic wires.

J. Uchil et al. (2007) conducted a study on a 40% cold worked NiTi shape memory alloy by taking the as-received material and heat-treating the material at different temperature ranging from 200°C to 600°C. The XRD results were in the form of peaks within the  $2\theta$  angle range of 30 to 50 degrees. The XRD peak showed the Austenite as the main phase present in the alloy. According to literature, the peak intensity is seen to go up with an increase in the heat-treatment temperature. Also, the peaks narrowed with an increase in the peak intensity with increase in heat-treatment temperature from 200°C to 560°C.

Yun-xiang TONG et al. (2014) analyzed the X-ray diffractogram of the Nickel-rich NiTiCr alloy. It was found from the literature that annealing at temperatures of 300 to 450°C revealed the presence of precipitates. The austenitic phase appeared in the XRD at a  $2\theta$  angle between 40 and 45 degrees. The XRD showed the Ni<sub>4</sub>Ti<sub>3</sub> precipitates for the material when the heat-treatment temperature was increased to 450°C from 300°C. The as-received condition and lower heat-treatment temperatures happened to show austenitic peaks in the x-ray diffractogram.

## **2.6 Differential Scanning Calorimetric Studies of Nickel-Titanium Alloy**

The transformational temperatures of the alloy are characterized using Differential Scanning Calorimetry (DSC). Also, the specific heat and latent heat of the samples are

found out using DSC. DSC helps in ascertaining the property of the samples, being shape memory or superelastic depending upon the set of transformational temperature. Many applications prefer the superelastic property of the material. Hence, DSC for NiTi alloy provides a clear understanding of the transformation temperatures so as to ascertain the shape memory or superelastic property of the alloy depending on the working temperature.

According to (J A Shaw et al. 2008), the temperature-induced martensite or the stress-induced martensite is the phase change taking place in the alloy without the diffusion, hence, being made reversible. J A Shaw et al. (2008) state that the transformations taking place in the material totally depend on the mechanical history of the sample and many specimens that are found to be richer on the Nickel-side seem to exhibit a multi-phase transformation during the cooling to the martensitic phase by having the R-phase in the material. The temperature hysteresis found during the DSC measurements showed that in the case of rhombohedral phase present in the alloy, the hysteresis is much more in the martensitic transformation as compared to the one of R-phase. The compatibility is found more in the case of the R-phase as compared to the martensitic phase; hence, the hysteresis is lower in presence of R-phase (K B. 2003). The main cause for the high level of the temperature hysteresis is the nucleation energy barrier found in the microstructure that needs to overcome to proceed with the transformation either during heating or cooling as per (K B. 2003). J A Shaw et al. (2008) stated that in the DSC procedure, the sample preparation forms a very important parameter in ensuring good results. The heating and cooling rate also affect the types of results obtained in the DSC procedure.

DSC shows the reason for shape memory and superelastic behavior stating the different micromechanical mechanisms responsible for the same. There is hardly any change observed in the overall volume of the material upon changing from the austenitic phase to the martensitic phase according to (J A Shaw et al. 2008). The structure undergoes very minute change as far as the atomic positions are concerned during the cooling of the sample during DSC. In the shape memory effect, the martensitic phase gets formed upon crossing a threshold temperature by the formation of self-accommodating twins that are totally 24 in number. Further straining the martensitic structure gives rise to a

detwinned structure making the twins reorient in a specific direction. Overall, the ageing treatment also is seen to improve the resistance to the plastic deformation by slip phenomenon. This is mainly due to the release of  $\text{Ni}_4\text{Ti}_3$  equilibrium precipitates coming out of the matrix (Frick C P et al. 2005) and greatly enhancing the superelastic nature of the alloy material. This superelastic property is seen at temperatures ranging much above the  $A_f$ , wherein, the material can be transformed to martensite using stress and reverts back to the parent austenitic phase upon removal of the stress provided much of the plastic deformation has not occurred.

There are different observations noticed in Ni-Ti shape memory alloys during the DSC investigation in terms of the types of phases present in the alloy during cooling and heating. (Otsuka et al. 1990) stated that an additional R-phase can appear in the case of thermal investigation before the formation of Martensitic phase. As per the DSC investigations of the as-received and heat-treated specimens, (Kus et al. 2010) stated that the as-received sample showed specific transition peaks ensuring a two-stage transformation. An R-phase is found in both the cooling and heating curves.

Kus et al. (2010) also brought about the fact that the annealing temperatures ranging from  $400^\circ\text{C}$  to  $550^\circ\text{C}$  shows a two-peak transformation similar to the as-received material. Whereas the  $600^\circ\text{C}$  annealed specimen exhibited a single-stage peak as compared to the other annealed samples. There were small shifts noticed in the transition temperatures during the cooling of the alloy in terms of the formation of the R-phase. As the transformational temperatures increased to as high as  $600^\circ\text{C}$  the R-phase was seen to become unstable and disappeared from both the cooling as well as the heating cycles. The minute changes in the transformational temperatures could be due to the changes occurring in the microstructure of the alloy samples during the annealing treatment. Along with the annealing treatment, a prior cold-work is done that makes a remarkable effect on the shape memory property of the alloy (Fuentes J et al. 2002). It was found out and reported that the heat-treatment temperature followed by the time duration played a very important role in the regulation of the transformational temperatures (Yoon S et al. 2004). Fewer other studies proved that an increase in the heat-treatment duration saw a rise in the transformational temperature of the alloy (Eggeler G et al. 2005).



As far as the transformational temperatures are concerned, the increase in the  $M_s$  temperatures attributed to the formation of the internal stress fields. The formation of the precipitates such as the  $Ni_{14}Ti_{11}$ ,  $Ni_4Ti_3$  or  $Ni_3Ti$  that are out of the NiTi matrix form crystals leading to an increase in the martensitic start temperature upon the reduction of Nickel in the solution (Gall K et al. 1999). Eaton-Evans J et al. (2008) states that for the material samples that are hot worked followed by the cold working during manufacture, tend to show a two-stage transformation during cooling and a single stage transformation from martensite to austenite during the heating process. This phenomenon occurs without the heat-treatment carried out on the samples. H Sadiq et al. (2010) mentions that the samples that are aged between the temperatures of 500 to 600°C are found to display the R-phase during the cooling cycle along with the sample that was not annealed but only hot-rolled and cold-rolled. The ageing of the samples above 500°C are seen to reduce the lattice defects in the material thereby the movement of the crystals in the micro-structure is permitted leading to the formation of the martensitic phase directly from the austenitic phase (Nurveren K et al. 2008). The main cause of the defects being almost extinct from the microstructure was that the internal stresses get relieved from the material upon heating and air quenching and a great enlargement of the grains is seen in the structure (Gall K et al. 1999).

According to (Karaman et al. 2005), the low temperature annealing and severe plastic deformation leads to the deformed austenite as well as martensite upon the cooling process without a third phase when the deformation of the samples are carried out at room temperature. A similar trend of a single-stage transformation is observed to take place during the severe plastic deformation at 450°C followed by a low-temperature annealing. This is being carried out to improve the fatigue resistance of the alloy followed by its cyclic stability.

There are also suggestions given by (UCHIL et al. 2002) that DSC is a very effective technique to get a hold on the transformational temperatures of the alloy. It was mentioned by (UCHIL et al. 2002) that the heat-treatment process proved to be very beneficial to DSC in determining the transformational temperatures of the alloy. The heat-treatment temperatures are seen to play a key role in the determination of the number of phases that can be seen in the alloys namely the martensitic phase alone or

the martensitic phase with the R-phase. It is observed by (Uchil et al. 2002) that the ageing done in the range of 350-400°C is said to yield two phases, the R-phase and the martensitic phase, whereas, increasing the ageing temperature to around 600°C is said to yield a single martensitic phase upon cooling and vice-versa. Also, the straining of the samples by subjecting to a certain magnitude of tensile force also brought about a drastic change in terms of the disappearance of the R-phase from samples aged in the range of 400°C.

Lucas et al. (2015) clearly suggests that DSC performed on cold-worked materials superelastic in nature might not yield very accurate results and the transformational temperatures may not be detectable. DSC, according to (Lucas et al. 2015) proves itself to be useful for the specimens undergone an ageing process to have got relieved of its internal stresses to obtain the cooling as well as the heating curves. According to (N et al. 1999), NITINOL tubes that are superelastic in nature, are subjected to a lot of cold-work prior to its final dimensions that could lead to residual stresses in the specimen. There are lot of evidences about influencing the transformational temperatures of NITINOL by performing the alteration of heat-treatment time and temperatures according to (Y et al. 2001) (R et al. 2010). The ageing temperature range was selected as about 400 – 450°C to have a change in the transformational temperature (Pelton A R et al. 2003).

Palloma Viera Muterlle et al. (2014) performed low temperature annealing treatment on Nickel-rich NiTi alloys. The heat-treatment temperature according to the author was between 350°C and 600°C. The as-received samples were analyzed using DSC and a multiple step transformation was observed in the cooling cycle such as B2-R-B19'. The heat-treatment carried out at 350°C brought in the R-phase along with the austenitic phase at the room temperature. Since the alloy is a Nickel-rich alloy, the author mentioned that the transformational temperatures  $A_s$ ,  $A_f$ ,  $M_s$  and  $M_f$  got altered significantly with an increase in the heat-treatment temperature. Another important observation done by the author was that, upon an increase of the annealing temperature to 600°C made the intermediate R-phase to disappear.

X. B. Wang et al. (2014) has made a thorough review of the appearance of R-phase in binary NiTi alloys. The author has clearly mentioned that the R-phase is dependable on the thermomechanical treatments performed on the binary alloy. The literature mentions the increase in the thermal cycles of upto 250°C brings about the prominence of the R-phase in DSC. There could be the release of the Ni<sub>4</sub>Ti<sub>3</sub> precipitates in the matrix. The heat-treatment influences the presence of the R-phase depending upon the Nickel concentration. The literature further mentions the presence of the R-phase on post-annealing conditions is co-dependent on increase in the Nickel concentration in the alloy matrix.

M. Drexel et al. (2007) carried out detailed investigations on NiTi alloy and concluded that defects are formed during the cold working of the material and have an effect on the Austenitic to martensitic transformation. The dislocation occurrence due to cold working may make the grain structure so fine that the transformation from austenitic to the martensitic structure could be nearly impossible to observe.

Kus et al. (2010) mentioned that the heat-treatment done for the as-received material brought about significant changes to the transformational behavior of the alloy. The annealing treatments carried out below 600°C, in the range of 300 – 500°C yielded an R-phase during the cooling and heating cycles. Upon an increase of the annealing temperature to 600°C, the transformation was a single stage from a two-stage transformation.

The superelastic as well as the shape memory behavior of the wire has been brought about by relating with the transformational temperatures that the alloy undergoes a phase change while cooling as well as heating. Harrison et al. (1990) suggested that the method utilized to measure the transformation temperature of NiTi material needs to match the application that the NiTi wire is used for. The standard transformational temperature chosen to benchmark the superelastic property of the alloy was the A<sub>f</sub> temperature by many researchers. The location of the A<sub>f</sub> temperature clearly signified as per the researchers whether alloy was shape memory or a superelastic one. The main techniques were the Differential Scanning Calorimetry (DSC) and the bend-free-recovery test. The austenitic finish temperature can be ascertained using DSC where

the sample is cooled and heated to return back to its original austenitic state (W et al. 1992). Also, the bend free recovery testing although being similar to DSC involved the cooling of the sample, bending by the stress application and heating again to note the temperature at which the sample gets back to its original shape and size (Chen et al. 1997). According to (K et al. 1990) and (Tamura et al. 1992), the DSC as well as the bend-free recovery tests are seen to show similar results for investigating the  $A_f$  of the material. One-minute change observed was the presence of an extra R-phase along with the two important phases of the alloy during the DSC test, which was thought of as a shear result of the parent Austenitic phase of the material.

## **2.7 Mechanical Properties of Nickel-Titanium Alloy**

Mechanical testing of materials is carried out to determine various mechanical properties. The mechanical properties of the alloys determine the range of the service that can be expected from the material. The testing of the mechanical properties provides information on the strength, ductility, hardness and fracture toughness of the material. Nickel-Titanium alloy is tested for mechanical property in order to evaluate the yield strength, ductility and UTS. This is to ensure the suitability of the alloy for a particular application it is being used for.

Dalibor et al. (2010) carried out research on as-received, as well as, NiTi alloys, heat-treated at different temperatures and time durations. The author mentioned that as far as the time durations of the heat-treatment is concerned, annealing time of 2 mins to 16 mins influenced the tensile strength and the recovery stress. The annealing temperatures in the range of 400-450°C was seen to improve the tensile strength of the alloy material whereas higher annealing temperatures of more than 600°C was seen to reduce the strength. As per the author, the wire behaved in a superelastic manner even in the as-received condition. The alloy being Nickel-rich saw a big change in the tensile properties when subjected to a variety of heat-treatment conditions.

Praveen Sathiyamoorthi et al. (2018) carried out research on CoCrNi alloy by subjecting the same to heat-treatments in the temperature range of 700°C for a set of time durations. The durations range from 2 to 15 minutes. According to the literature, the strength of the samples annealed for 2 minutes exhibited low tensile strength and

fine-grained structure with recrystallization just started to take place. Annealing for longer durations at the same temperature caused grain growth to take place that impacted the mechanical properties of the alloy material. The tensile strength improved significantly as the alloy was annealed for a duration of 15 minutes.

KERMANPUR et al. (2018) made an extensive study of the tensile and the superelastic properties of NiTi alloys having nano-sized grains. It was seen that the alloys subjected to cold working of 70% followed by annealing treatments possessed exceptional ultimate tensile strength and also materials demonstrated a recoverable strain of nearly 12% when subjected to a cycle of loading and unloading.

Miura et al. (1986) conducted extensive research on the NiTi alloy wire. The NiTi wire was subjected to tensile loading to ascertain the ultimate tensile strength and stiffness of the alloy wire. The wire exhibited very good stiffness upon tension loading. More importantly, according to the author the wire delivered superelastic property. It was analyzed that the stress remained constant over any change in the strain. The alloy was found to be superelastic with the same improving with heat-treatment carried out on the alloy.

Mohamed E et al. (2009) conducted research on Nickel-rich NiTi alloys. The alloys were subjected to a cold work upto 40%. The material was annealed at temperatures ranging from 400°C upto 700°C at intervals of 100°C. According to the literature, annealing of the alloy material in the temperature range of 400 – 500°C was found to increase the Austenitic phase in terms of volume fraction and cause a decrease in the hardness. The hardness was noticed to go up with increased heat-treatment temperatures above 500°C. The reason for this increase meant the recrystallization taking place in the material beyond 500°C temperature.

Palloma Vieira Muterlle et al. (2015) conducted an extensive study on a set of two NiTi samples wherein one NiTi sample was possessing the superelastic nature and other NiTi sample possessing shape memory nature. As per the literature, the superelastic material was subjected to a set of heat-treatments at temperatures ranging from 350°C to 600°C. The Vickers hardness of the sample annealed at 350°C was showing the highest value compared to the as-received and the remaining heat-treated samples. An increase in the

heat-treatment temperature more than 350°C is found to reduce the hardness of the material. The alloy sample showing the shape memory effect is observed to display the least hardness.

R. Aliasgarian et al. (2011) conducted sliding wear tests on two sets of Nickel-rich NiTi alloys. The two sets of alloys were heat-treated at 400°C and 700°C. The findings state that the alloy sample heat-treated at 400°C temperature exhibited lower Rockwell hardness compared to the sample annealed at 700°C temperature.

M. Arciniegas et al. (2008) carried out extensive research on five different compositions of TiNi alloys. The alloys were manufactured and heat-treated at 500°C and air quenched. It was studied and concluded that the presence of precipitates in the Nickel-rich alloy such as Ni<sub>4</sub>Ti<sub>3</sub> had a great influence on the hardness and also the wear properties of the TiNi alloy. The wear was seen to reduce by the presence of precipitates thereby causing an increase in the hardness of the material.

## **2.8 Tribological Characteristics of Nickel-Titanium Alloy**

Wear test is carried out on materials in order to predict the wear performance and conduct the investigation of wear mechanism. It is well known that wear is not just a material property, but it is a tribo-system property. The wear property of a component is evaluated from a material point of view to confirm the suitability of the component for a specific wear application. The wear test is also carried out from surface engineering point of view since the potential of using a certain surface engineering technology is evaluated to reduce wear for a specific application.

In a wear analysis, the amount of material removed from a component is measured after the test. The amount of material removed is expressed in terms of mass loss, volume loss, type of wear and geometry and size of test material. The mass loss of a specimen is expressed in terms of the weight difference before and after the test. Other means of measuring the wear of a material is in terms of volume loss and dimension loss. The wear resistance of a material is expressed as an inverse of mass loss or volume loss. In the case of Nickel-Titanium alloy, the sample is evaluated for wear resistance since the material is being used in a number of bio-medical applications such as endodontic tools, orthodontic arch wires, cardiovascular stents and so on. In many applications, high wear

resistance of the material plays a vital role considering the longevity of the component. Since the component needs to be used repetitively for many cycles without frequent replacements. The suggested type of wear for Nickel-Titanium alloy is an abrasive wear considering the hardness of the material.

T. Abubakar et al. (2013) conducted a research by using 316LN stainless steel disc and coated Nickel-rich NiTi alloys on the same. Annealing processes were carried out on the same set of materials at two different temperatures 500°C and 600°C for different time intervals. The annealing processes produced nickel-rich precipitates to come out of the solution and the main phase existing was the austenitic phase. Pin-on-disc wear tests carried out on the same demonstrated that the coatings of NiTi alloy post-annealing had exceptionally good wear resistance and the same could be used in a number of mechanical applications.

Palloma Vieira Muterlle et al. (2015) conducted an extensive study on a set of two NiTi samples wherein one NiTi wire was possessing superelastic nature and other NiTi wire was possessing shape memory nature. As per the literature, the superelastic material was subjected to a set of heat-treatments at temperatures ranging from 350°C to 600°C. It was analyzed by conducting the micro abrasive wear tests that the pseudoelastic sample annealed at a temperature of 350°C showed the best wear resistance compared to the as-received superelastic sample. The Vickers hardness of the same was showing the highest value compared to the as-received and the remaining heat-treated samples.

R. Aliasgarian et al. (2011) conducted sliding wear tests on two sets of Nickel-rich NiTi alloys. The alloys were solution treated and annealed at two different temperatures of 400°C and 700°C. The NiTi alloy samples annealed at 400°C showed better wear resistance compared to the NiTi alloy heat-treated at 700°C. As per literature, the samples annealed at 400°C showed lower wear upon an increase of the loading from 20 to 60N. The author suggested that the lowering of the wear could be the formation of oxide layers TiO<sub>2</sub> on the surface of the wear specimen.

Fei Gao et al. (2007) conducted research on a Titanium-rich Ti<sub>2</sub>Ni/TiNi alloy. The alloy was a combination of Ti<sub>2</sub>Ni and TiNi and the manufacturing technique employed to produce was laser melt deposition. The alloy produced was confirmed by the author to

be superelastic in nature. The combination of the alloys was subjected to abrasive wear tests under a set of loading conditions. It was confirmed that the wear resistance of the alloy was poor at lower loads such as 7N, 13N and 25N loading whereas the wear resistance was found to improve greatly at higher loads of 49N.

M. Abedini et al. (2010) conducted a study on Nickel-rich NiTi alloy with respect to transformation temperature as well as mechanical and tribological properties. The wear test was conducted over a temperature range of 0°C to 80°C. The author tested and found out that wear resistance of the alloy improved upon increase of the testing temperature from 0 to 50°C. However, the literature suggested an improvement in the pseudoelastic property upon working temperature increase to 50°C. The testing at higher elevated temperatures of 80°C showed an improvement in the tribological properties owing to an elevated ultimate tensile strength.

Joseph Stokes et al. (2013) conducted an extensive research on Nickel-rich NiTi alloys. The NiTi alloy is produced in a powdered form and deposited on 316L stainless steel structure. As per literature, annealing was carried out at temperatures of 550 and 600°C at different time intervals. The annealing of the alloy indicated the presence of Ni<sub>3</sub>Ti precipitates and also the austenitic phase of the alloy; this was seen to improve the wear resistance of the alloy.

Fengxiang Zhang et al. (2019) carried out research on the addition of Nickel and Hafnium on the wear performance of Ni-rich NiTi alloys. There were four different alloy compositions that were fabricated. The wear results concluded that an increase in the Nickel as well as Hafnium elements contributed to the superior wear performance of the alloy. The nature of wear according to the literature proved to be abrasive in nature.

Yan et al. (2006) conducted a detailed research of examining the wear rate of NiTi alloys and compare the same with Stainless Steel. It was found out from the wear tests that maximum contact pressure exerted by the material on disc accounted for maximum wear; in other words, reduction in the wear resistance. According to the literature, it was proven that the superelastic property of the NiTi alloy contributed for exceptional wear resistance of the same to be used in a number of applications. However, the author



stated that the huge amount of strain recovered during the unloading played a vital role in the wear resistance. The Stiffness of the alloy contributed to the increase in the wear resistance compared to Stainless Steel.

L.M. Qian et al. (2005) conducted fretting wear tests on Nickel-Titanium alloys having superelastic property. The wear test was carried out at different amplitudes and was observed that the superelastic nature contributed to superior wear resistance of the alloy. The wear resistance of the alloy was compared according to the literature to GCr15 and was concluded that not only exceptional wear resistance, but the superelastic property of the NiTi alloy allowed for much lower hardness compared to GCr15.

Milena Arciniegas et al. (2008) conducted an extensive research on different compositions of NiTi alloys. The composition varied from being Titanium-rich to nickel-rich. The literature stated that the solution treatments followed by water quenching was carried out on the samples. The samples were then heat-treated at 500°C followed by air quenching. The alloy samples were examined for their microstructures. The best microstructure was chosen and the properties were tested in the form of hardness and wear. The alloy composition being on the Nickel-rich side showed the presence of precipitates of  $\text{Ni}_4\text{Ti}_3$  and  $\text{Ni}_3\text{Ti}$ . As per the author, the precipitates played a vital role in the improvement of wear resistance and the hardness. As per this literature, the precipitates acted as a strong barrier and prevented further grain growth and accommodation of the martensitic twins.

Pena, J. Solano et al. (2005) conducted research on NiTi alloys and brought about a comparison with the martensitic start temperature ( $M_s$ ) and the wear of the material. As per literature, the wear is measured in terms of mass losses and the same is correlated with the  $M_s$ . The literature states that the wear resistance is greatly improved by the superelastic property of the material. This property allows for the accommodation of the martensitic variants thereby being able to withstand huge plastic deformation of the material without getting permanently damaged by wear. The  $M_s$  temperature was found to highly influence the wear performance of the alloy. This  $M_s$  temperature was further co-dependent on the atomic percentage of Nickel in the alloy.

Yan et al. (2015) made a thorough study of the wear behavior of austenitic NiTi. The adhesive pin-on-disc wear tests were done varying the loading and also the temperature range. The wear resistance was seen to improve drastically in the temperature range between the austenitic finish temperature and the martensitic deformation temperature. The author examined and stated that the contact stresses between the Alumina wheel and the specimen caused the stress-induced martensitic transformation to occur improving the wear resistance. The second temperature range was above the martensitic deformation temperature. In this range, the superelastic property was observed to be lost thereby hindering the wear performance of the material. Overall, according to the literature, the wear resistance was dominated by the contact stresses. The contact stresses being high would lower the wear resistance.

Timothy J. Rupert et al. (2013) conducted research on Ni-W alloy by conducting the abrasive wear resistance of the material having nano-sized grains. According to the literature, the reduction in the grain sizes caused an increase in the wear resistance of the material. This was concluded with the reduction in the contact stresses which would have caused a dip in the wear of the samples. The fine microstructures that occur due to mechanical working of the material are found to introduce certain features called grain boundary dominated mechanisms that bring about big gains in the wear performance.

Lina Yan et al. (2003) conducted wear test on NiTi alloys that was in the martensitic state. It was a pin-on-disc test against Alumina wheel. The test was conducted under different loading conditions and also cycles. The observations found out were three different stages of wear taking place in the same material. The wear test began with a near-zero stage followed by a transition and an abrasive wear stage. The wear resistance of the alloy was observed to be good with less wear taking place owing to low contact stresses.

Oksuz, Y et al. (2014) conducted a research on NiTi alloys mixed with Aluminum oxide powder by the process of liquid metallurgy method. The aluminum oxide particles were of nano-size. The wear and hardness properties were investigated as per the literature. The wear of the samples mixed with  $Al_2O_3$  are seen to have reduced considerably due

to the increase in the hardness of the samples. According to the author, an increase in the loading caused an increase in the wear of the sample; thereby causing a dip in the wear resistance of the material.

Ni et al. (2004) conducted a research for the PhD work where microscopic shape memory effect and superelastic property was investigated. The mechanical properties of NiTi alloys were investigated using different techniques. A soft intermediate layer of NiTi alloy was examined that existed between the Aluminum substrate and a coating of CrN. The superelastic property of NiTi alloy proved to be a boon between the substrate and the coating thereby improving the wear resistance of the same. According to the author, the intermediate layer of the NiTi alloy was seen to have a huge elastic recovery ratio and that could be a boon in improving the wear resistance of the composite structure.

Qian L et al. (2008) conducted an extensive research on the fretting wear of the Nickel-Titanium alloy. The GCr15 steel ball was employed was employed for the fretting wear test. According to the literature, the martensitic transformation plays a vital role in the fretting wear characteristics of the alloy. Upon subjecting to wear testing, the martensitic transformation is said to take place that is reversible in fretting wear process. The author mentions about the martensitic transformation reaching a peak at certain number of fretting cycles and then stabilizes after fretting crosses a certain number of 1000 of cycles. The martensitic reorientation brings about a shielding effect on the alloy thereby causing low contact stress increasing the wear resistance.

There are literatures that discuss about the increase in the wear resistance of the NiTi material by ion implantation. It was mentioned that ion implantation increases the life of the instrument even after repeated uses (Ernesto Rapisarda et al. 2001). In this study, it was observed that the material without any implantation itself is highly wear-resistant, which is much needed for endodontic applications. Also, being a Titanium-rich material, the ageing has little or no effects on its wear properties that make it an ideal candidate for endodontic files.

## **2.9 Superelastic Behaviour of Nickel-Titanium Alloy**

Superelasticity is the property of a material by virtue of which the alloy can be strained far more than the normal elastic limit and recovered back upon unloading. In NiTi alloys, an external stress on the parent austenitic phase causes martensitic phase transformation. This transformation of NiTi alloy is athermal, without the application of heat. Superelasticity is of two types; linear superelasticity and non-linear superelasticity. The types of superelasticity are differentiated in terms of stress-strain curve. In linear type, the stress-strain curve is observed to be linear. Non-linear superelasticity refers to stress induced martensite transformation during the loading phase and reverting back to the parent phase during unloading following a hysteresis path. Non-linear superelasticity is called pseudoelasticity. NiTi alloys are examined for their superelastic behavior considering its suitability for a variety of applications. The applications include bio-medical, automobile, aerospace and to name a few. The material possessing superelastic property is essential in order to be tailored for minimally invasive surgical operations.

Narges Shayesteh Moghaddam et al. (2019) mentions that the fabrication methods used were exceptionally good compared to the regular manufacturing methods for the NiTi alloys. The manufacturing included a set of techniques namely usage of a high wattage laser, high scanning speed and a process named hatch spacing of 80 $\mu$ m. There were no heat-treatments carried out on the NiTi samples post-fabrication. The results obtained were phenomenal. The strain recovery was observed to be really high on an average level of 5.6%. The recovery ratio too was high on the level of nearly 100%. According to the literature, all this was being possible without heat-treatment done on the alloy material.

Abdy et al. (2014) has conducted a study on superelastic NiTi alloy material. As per the literature, the wires were procured from a commercial manufacturer of 1mm diameter and were subjected to low temperature annealing treatments at a temperature range of 200 – 400°C and the specimens were quenched in water. The author mentions that there are two tests conducted on the NiTi wires. The first test being the tensile tests on all the specimens and the second test is the recovery test on the heat-treated wires. The mechanical properties evaluated by tensile testing followed by the recovery stresses

were observed to improve greatly by heat-treatment. The ultimate tensile stress was noticed to be a maximum at the heat-treatment temperature of 350°C. The specimen that was found to be promising was the 350°C annealed specimen owing to its large recovery stress; be it the maximum and the minimum recovery stress. The annealing temperature of 400°C was seen to produce a lower recovery stress compared to the specimen annealed at 350°C.

Zupanc et al. (2018) conducted a review on different types of NiTi wires. The author stated that performing a set of thermomechanical treatments leads to the occurrence of the intermediate R-phase and the martensitic phase. In this research, different types of wires were examined for the phases present in the same for the clinical purposes. It was found that the two types of materials named M-wire and the R-phase types of wires were found to be in the austenitic state whereas the other types namely CM, gold and blue types had substantial amount of the martensitic phase present in the same. The findings from the research were that the wires which possessed the austenitic phase demonstrated the superelastic properties and also a high value of the torque at fracture. The wires possessing the martensitic phase were seen to possess low torque values at fracture but enhanced flexibility compared to the austenitic wires. The more preferred wires were the ones of the martensitic phase expecting curved paths in root canal treatment.

Mohammad et al. (2018) conducted a research on cast NiTi alloys. The alloys were produced by standard Vacuum Induction Melting followed by 70% cold work. The process of annealing preceded the cold-work. The analysis proved that the annealing at 400°C was beneficial in achieving nano-sized grains of the order of 20-70nm size. The greatest improvement according to literature was the recoverable strains of NiTi wire enhanced to 12% from the conventional 8%. Also, during tensile testing, it was observed that the stress to achieve the stress-induced-martensitic transformation is increased.

Ozbulut et al. (2018) conducted a research on Nickel-rich NiTi alloys. The alloy was procured from a commercial manufacturer and had a diameter of 5.5mm. The superelastic properties of the wires were evaluated by subjecting the same to cyclic

loading and unloading cycles. The main properties evaluated from the test were the maximum tensile stress followed by the residual strain. The results showed that when the wires were subjected to a strain of 6% or less, there was no noticeable residual strain. Upon stressing the wires to 10% strain, a very small residual strain of nearly 0.8% was seen. This concluded that the wire possessed a very good superelastic property. In addition, to the superelastic property, the fatigue property was analyzed. It was seen that the specimen possessed a very good fatigue resistance and was able to withstand more than 2500 cycles of loading and unloading.

Paryab et al. (2019) investigated the superelastic properties of Nickel-rich NiTi alloys. The procured alloys were aged at different temperatures ranging from 400°C to 800°C at various time durations. The superelastic properties were analyzed with respect to hardness and microstructures. The precipitates such as the Ni<sub>4</sub>Ti<sub>3</sub> and Ni<sub>3</sub>Ti looked to cause an increase in the hardness of the material. The hardness was seen to vary from high to low at a heat-treatment temperature range of 400 – 500°C and had a constant rise from 500-800°C. According to the literature, the best superelastic property was seen at 400°C annealing temperature.

Fujio Miura et al. (1986) conducted extensive research on NiTi alloys. The alloys were put to tension as well as 3-point bending tests to evaluate the superelastic as well as the tensile properties such as the Young's modulus and the Ultimate tensile stress. The results showed that the material possessed the exceptional property called superelasticity. The heat-treatment performed on the alloy samples caused an improvement in the superelastic property. The NiTi material compared to Chromium and Steel alloys demonstrated a constant proportionality between stress and strain. The stress was seen to be constant over an increase in the strain levels. The author also mentioned that the increase of the heat-treatment temperature to 500°C was seen to reduce the force needed for the superelasticity property to be exhibited.

## **2.10 Electrochemical Corrosion Characteristics of Nickel-Titanium Alloy**

Corrosion is a natural process of conversion of a pure metal into a chemically stable form such as oxide or sulphide. This takes place by means of chemical or electrochemical reaction with the environment. There are different treatments involved in reducing the rate of corrosion to metallic objects exposed to weather, salt water, acids and other environments. In the case of Nickel-Titanium alloys, exposure to the environment and also certain body fluids causes chemical attack and corrosion takes place. This chemical attack on the alloy by body fluids is also seen to cause Nickel poisoning, which is hazardous to patients. The corrosion needs to be prevented using suitable treatments such as surface treatments. A lot of care needs to be envisaged in sealing the surface defects such as cracks or pinhole defects through treatments. Also, thermal treatments performed on the alloy are seen to reduce the rate of corrosion.

Alana Witt et al. (2015) conducted an extensive research on the Nickel-rich NiTi alloys by performing electrochemical corrosion tests using different solutions. It was also mentioned by the author that the treatment of the surface of the alloy material being important considering the biocompatibility property of the same. The current research included the exposure of polished Nickel-Titanium alloy surfaces to different fluid compositions. The different types of solution were Hanks's solution, Hanks' balanced salt (HBSS) solution, saline body fluid (SBF) solution, and Ringer solution. According to the literature, there were two types of tests carried out namely, open circuit potential and voltammetry. The results of the tests with respect to each of the simulated body fluids were compared. The NiTi alloy was observed to show similar corrosion behavior in nearly all the body fluids. However, the HBSS and the Hanks's solution demonstrated similar results; the HBSS being the ideal solution to test the corrosive property of NiTi alloy.

Kharia Salman Hassan et al. (2015) studied the corrosion behavior of Aluminum alloys subjected to a process named shot peening. There were a set of specimens that were subjected to shot peening using Steel balls. A couple of experiments such as the mechanical tests were performed followed by the corrosion test on shot peened and also the cast specimens. The corrosion test was performed using the TAEFL extrapolation

method. The author claimed that the shot peened specimens had been induced with the compressive residual stresses leading to an increase in the hardening of the external surface layer. This increase in the surface hardening led to an increase in the corrosion resistance.

Madelina Capos et al. (2015) conducted corrosion studies on NiTi alloy by using an artificial saliva solution. The testing temperature and the pH was varied throughout the study. The aim of the study was to see the amount of Nickel ions release into the solution leading to Nickel poisoning. The author mentioned that the increase in the temperature of testing caused a reduction in the release of Nickel ions to the solution. According to the literature, the release of the Nickel ions did not get affected much by pH variation. The amounts of Nickel ions released into the solution were far less than the critical values that could cause allergies.

Trepanier et al. (2000) made a detailed study on the corrosion resistance and the biocompatibility of NITINOL. There was a lot of review done on the corrosion resistance of NiTi alloy under different circumstances. The study mentioned that NiTi alloy that is passivated showed a very high corrosion resistance compared to 316LN stainless steel. Also, the oxide layer coating formed on the outer surface of the alloy proved to enhance the corrosion resistance of the same by many folds. The oxide layer protection was seen to reduce the Nickel ions greatly after immersion of the material in a solution. The other surface treatment that was observed to enhance corrosion resistance thereby promoting bio-compatibility was electropolishing. The literature concluded the implantation of the material in a human system depended upon the passivation and the surface treatment.

Ingrid Milosev et al. (2012) have made an extensive study on the corrosion behavior of NiTi alloys. According to the literature, there were variations in the pH of the Hank's solution in terms of 4.5, 6.5 and 7.5. Further, there were preparations in terms of the surface. Three types of surfaces were used namely polished, ground and chemical etching. The composition of the Nickel and Titanium at the surface was seen to influence the corrosion resistance greatly. This difference in the surface composition originated from the preparations of the surface. The surface that had the highest corrosion resistance was the etched surface, since etching introduced pits with Titanium



seen in the NiTi matrix. The polished surface had a very good surface finish possessing a good corrosion resistance, while the surfaces put to grinding had a surface roughness nearly the same as the etched one. It was concluded that the polished and etched surfaces were least prone to corrosion attack than the ground surface. More importantly, a polished surface having a superior surface finish was recommended for practical applications.

G. Mealha et al. (2016) made a thorough study of the corrosion resistance of NITINOL in the Master's work. The material was subjected to heat-treatments in diversified environment as well as different temperatures. The temperatures ranged at 250°C and 350°C and the environments were air and N<sub>2</sub>. Hank's solution was used in order to analyze the corrosion behavior of the material. The corrosion of the heat-treated surface and the as-received was compared. The results concluded that the heat-treatment in Nitrogen atmosphere at 350°C rendered the best corrosion results. The main reason was an enhanced protection to the oxide layer by heat-treatment. The heat-treatment at 250°C had not brought any promising results as compared to the 350°C heat-treatment in N<sub>2</sub> atmosphere.

Sahar et al. (2014) conducted a corrosion behavior test by immersing the NiTi alloy in a virtual oral environment. The solution to replicate the oral environment was the Hank's solution containing epigallocatechin gallate (EGCG). According to the author, the application to be replicated is the orthodontic arch wires in the mouth. The corrosion resistance of the NiTi wire exposed to Hank's solution containing EGCG was seen to have improved by many folds. Comparing the corrosion resistance of NiTi alloy with pure Titanium, the NiTi alloy possessed superior corrosion resistance than the pure Ti.

D.O. Flamini et al. (2014) performed a unique study on the NiTi alloy by coating the surface with a combination of alkylsilane compound propyl trichlorosilane (C<sub>3</sub>H<sub>7</sub>SiCl<sub>3</sub>) and polypyrrole (PPy) doped with sodium bis(2-ethylhexyl) sulfosuccinate (Aerosol OT). The concept was to improve the surface characteristics of the material. The author concluded that the corrosion resistance of the material was greatly enhanced with the combination of two organic compounds preventing the entrance of Chlorine ions on the NiTi alloy.

Manju Chembath et al. (2014) conducted corrosion studies on NiTi alloys. The NiTi alloys subjected to electropolishing and passivation was compared with the mechanically polished NiTi alloy. The studies performed through electrochemical corrosion resistance clearly indicated that for the passivated alloy, the corrosion resistance was three-fold higher than that of the alloy subjected to electropolishing. The reason for the increase was formation of a layer of Titanium oxide. The immersion of the samples in Hank's solution proved that the Nickel release of the passivated sample was nearly half as compared to the polished samples. This confirms better stability of the passive layer as compared to mechanically polished samples.

Dalibor Vojtech et al. (2011) performed an extensive study on Nickel-rich NiTi alloys. The study was based on correlating various properties with each other, one being the corrosion resistance. The NiTi material was heat-treated in the temperature range of 450 – 600°C for a time duration of 10 minutes. The mechanical properties as well as the corrosion behaviour of the material were studied. According to the author, the corrosion resistance of the material was influenced greatly by the heat-treatment process. The literature states that the corrosion properties of the material are found to deteriorate at a fast pace upon an increase in the heat-treatment temperature from 450°C to 600°C. The heat-treatment was causing a defective oxide layer to form as an outer coating worsening the corrosion resistance of the material.

Further from the literature survey, it has been found that in case of Nickel-rich Nickel-Titanium alloys, there has been a enormous change observed in the microstructure as well as the mechanical properties of the NiTi alloy when subjected to heat-treatments in the temperature range of 300°C – 600°C. Though published information is available on various aspects of Nickel – Titanium alloys, all this information is limited to Nickel-rich Nickel-Titanium alloys. It appears that much published information is not available in the area of Titanium-rich Nickel – Titanium alloys.

## 2.11 Scope of the Present Investigation

Extensive survey of published information in the area of Nickel - Titanium also indicates that the alloy is made of equal amount of Nickel and Titanium in terms of atomic percentages. This alloy is known to exhibit certain superior properties such as Shape Memory Effect and Superelasticity. Although the alloy possesses superior properties, the manufacturing of this alloy calls for extremely tight compositional control since the properties are seen to get greatly influenced by minute changes in the compositional shifts. The Nickel-Titanium alloy is used in a variety of mechanical and bio-medical applications due to its extraordinary properties. A few popular mechanical applications of the NiTi alloy include the manufacture of the cellular phone antenna, the eye glass frame and to name a few. The popular bio-medical applications include the orthodontic arch wires, cardio-vascular stents, orthopedic applications, and a good number of surgical instruments.

Further from the literature survey, it has been found that in case of Nickel-rich Nickel-Titanium alloys, there has been a sea change observed in the microstructure as well as the mechanical properties of the NiTi alloy subjected to heat-treatments in the temperature range of 300°C–600°C. Though published information is available on various aspects of Nickel – Titanium alloys, all this information is limited to Nickel-rich Nickel-Titanium alloys. It appears that much published information is not available in the area of Titanium-rich Nickel – Titanium alloys.

Therefore, in the present investigation it has been proposed to systematically carry out studies on Titanium-rich Nickel-Titanium alloy in three stages. In the first stage, it has been proposed to evaluate the as-received Titanium-rich NiTi alloy in terms of its composition, mechanical properties, tribological characteristics, superelastic characteristics and corrosion characteristics.

In second stage, it has been proposed to subject the Titanium-rich NiTi alloy into low temperature annealing treatment at different temperatures and time and study all the above-mentioned properties/characteristics. It has been also proposed to find out the optimum combination of temperature and duration which yields superior properties.

In third stage, it has been proposed to compare all the properties exhibited by NiTi alloy subjected to optimum low temperature annealing heat-treatment with identical properties of as-received NiTi alloy and explore whether low temperature annealing heat-treatment is having any influence in improving said properties.

To be more specific, it has been envisaged to carry out the investigation systematically for two cases namely (a) as-received 50% Nickel – 50% Titanium alloy and (b) 50% Nickel – 50% Titanium alloy subjected to low temperature annealing heat-treatment at different temperatures. For both the cases, it has been proposed to carry out the following studies:

1. Evaluation of composition of the Nickel-Titanium alloy using EDAX as per ASTM F1375 - 92(2012) and perform low-temperature annealing heat-treatment on Nickel-Titanium alloy at 300°C, 350°C, 400°C and 450°C for one-hour duration in controlled Argon atmosphere.
2. To carry out Transmission Electron Microscopy on the Titanium -rich Nickel-Titanium alloy samples as per ASTM F86 to study the effect of heat-treatment on the sub-microstructure. Also, carry out phase analysis using X-Ray Diffraction on the material as per ASTM F2024 - 10(2016) and analyze the effect of heat-treatment on the same.
3. To evaluate the transformation temperatures through Differential Scanning Calorimetry on the Nickel-Titanium alloy as per ASTM D3418 and analyze the effect of heat-treatment on the transformational temperatures.
4. To evaluate the UTS of Nickel-Titanium alloy through tensile test as per ASTM E8 and confirm the effect of heat-treatment on the UTS. Also, to evaluate the Hardness of the alloy through Vickers Hardness test as per ASTM E92 – 17.
5. To evaluate the wear properties of Nickel-Titanium alloy through Abrasive wear test as per ASTM G-132a and study the effect of heat-treatment on the wear phenomenon. Also, to confirm the Superelastic Behavior of Nickel-Titanium alloy as per ASTM F2516-18 and to confirm the effect of heat-treatment on the same.

6. To evaluate the Corrosion Resistance of Nickel-Titanium alloy as per ASTM F-2129 using Hank's solution and study the effect of heat-treatment on the corrosion behavior.

Later, it has been proposed to compare the properties of NiTi alloy subjected to optimum low temperature annealing heat-treatment with the identical properties of as-received NiTi alloy.

## **CHAPTER 3**

### **EXPERIMENTAL WORK**

#### **3.1 Introduction**

In this chapter, the experimental methodology adopted for carrying out systematic investigation as explained in the previous chapter have been presented.

#### **3.2 Nickel-Titanium Alloys**

The binary NiTi rods of 16cm length and 3.04mm diameter were procured after contacting a vendor in China named Baoji Sunhope Titanium Industries Private Limited. This binary alloy was cast using the regular procedure of VIM followed by VAR. After casting the alloy in the form of the ingots, these were subjected to extensive hot forming operations that included hot swaging, hot rolling followed by cold rolling to obtain the final rods. The hot swaging was performed to reduce the dimensions of the cast ingot from as high as 25mm diameter to about 10mm diameter. Then the hot rolling was performed to further reduce the diameter to as low as 6-8mm at temperature as high as 800-900°C that is much above the recrystallization temperature of the material. Intermediate annealing was carried out between the hot rolling operations to achieve chemical homogeneity. Cold drawing of the rods was performed after the hot rolling in order to further reduce the diameter of the rods to as low as 3.04mm. This cold drawing of about 40% was done to achieve dimensional accuracy as well as a good surface finish. The entire cold drawing was performed in multiple stages to avoid cracks along the surfaces since the working temperature would be much lower than the recrystallization temperature of the material. The main aim of performing these thermomechanical treatments after the casting process was to have a good control over the dimensional accuracy thereby removing any effects of oxidation or the picking up of Carbon impurities during the melting of the alloy. According to the manufacturer the alloy is a shape memory alloy with a composition slightly above 50% of Titanium side and this composition given by the manufacturer was approximate. The experimental

methodology discussed in the following sections is common for both as-received samples and samples subjected to low annealing heat-treatment.

### **3.3 Conduction of Low Temperature Annealing Heat-Treatment**

The NiTi alloy samples were subjected to a low temperature aging treatment in the temperature range of 300 – 450°C to study the effect of annealing on the structure as well as the mechanical properties of the alloy material. The samples were heat-treated using the SIGMA box furnace at IIT Chennai in a controlled Argon atmosphere. The furnace is shown in figure 3.1.



Figure 3.1 SIGMA box furnace

The aging was carried out at temperatures of 300°C, 350°C, 400°C and 450°C temperatures in air. The ageing was done at respectively four-time durations of 15, 30, 45 and 60 minutes as illustrated in table 3.1. The furnace was switched ON and the temperature was set for 300°C. It was given time for the furnace to slowly heat up to 300°C at a slow heating rate from room temperature. The samples were inserted into the furnace upon touching 300°C temperature. The samples were placed vertically with the aid of glass wool since the heating coils were at the sides. The heat-treatment was carried out for a duration of 15 minutes and sample was removed from the furnace.

Table 3.1 Low Temperature Heat-treatment Temperature and Time Duration for 50% Nickel - 50% Titanium alloy for subjecting to Tensile Test

Heat-treatment temperature (°C)	Heat-treatment duration (minutes)			
300	15	30	45	60
350				
400				
450				

The next sample was inserted and the heat-treatment was carried out at 300°C for 30 minutes and sample was removed from the furnace and air quenched, similarly the process was repeated for the same temperature for 45 minutes and 60 minutes duration. A similar procedure was carried out for 350°C, 400°C and 450°C where the samples were heat-treated for four-time durations of 15, 30, 45 and 60 minutes. Among the four-time durations mentioned in table 3.1, the time duration of 60 minutes was chosen at each heat-treatment temperature for further studies (Pelton et al. 2000).

### 3.4 To Observe the Samples Under Transmission Electron Microscopy

The in-situ TEM was carried out for the as-received NiTi sample to evaluate the micro-structure and the dislocations present in the alloy due to 40% cold-working and analyze the effect of low temperature annealing heat-treatment of one-hour duration on the alloy samples. The TEM was carried out using the TECHNAI set-up at IIT Madras which is shown in figure 3.2. The equipment shown in figure. 3.2 is a TF20: Technai G2 200kV TEM. This set-up is suitable for cryo single particles or sections up to 100nm thickness electron microscopy and electron tomography. The TF20 is equipped with a Field Emission Gun (FEG) and +/-80 degrees tilted computer controlled LiN cryostage. This microscope features a TIETZ F415MP 4k x 4k multiport CCD camera with a 4-port readout and 15µm pixel size. Images could be recorded on plain film camera as well. This is a microscopy technique in which a beam of electrons is transmitted through a specimen to form an image. The specimen is most often an ultrathin section less than 100 nm thick. An image is formed from the interaction of the electrons with the sample as the beam is transmitted through the specimen. The image is then magnified and



focused onto an imaging device, such as a fluorescent screen, a layer of photographic film, or a sensor such as a scintillator attached to a charge-coupled device.



Figure 3.2 TECHNAI Transmission Electron Microscopy set-up

The sample preparation for Transmission Electron Microscopy is carried out as per ASTM F86. Samples of 300-micron thickness is sliced using an isomet slow speed diamond saw from the main sample. The samples are ground using emery papers to a thickness of about 100 microns. The sample is jet-polished using a Struers twin jet polisher to create a small hole in the center, of the order of a few nanometers diameter. The solution used in the jet polisher is a mixture of Perchloric acid and acetic acid at a temperature below zero degrees with liquid nitrogen for reaction for controlling the polishing. The sample was fixed to the sample holder in the jet polisher and the required tiny hole was obtained. The jet polished sample was mounted in the sample holder of the TEM machine and the necessary sub-microstructures and diffraction patterns were captured. The structures were then analyzed for the main phases present in the alloy along with the dislocation network. The structures were analyzed for nanometer range sizes.

### 3.5 EDS Analysis

The elemental compositions of the NiTi alloy samples were analyzed to ascertain the percentage of individual constituents and confirm whether the alloy is a Nickel-rich one or a Titanium-rich one. The analysis was carried out as per ASTM F1375 - 92(2012). Thin slices were sliced from NiTi rods using an isomet cutter to obtain pieces of approximately 5mm length using a slow speed diamond saw at about 100rpm. The slices were mounted on the EDS machine and a scan was done to indicate the approximate percentage of the individual constituents present in the alloy sample. The EDS was carried out using Neon-40 Carl Zeiss SEM machine at CMTI Bangalore which is shown below in figure 3.3.



Figure 3.3 Carl Zeiss Scanning Electron Microscopy set-up

The machine has a resolution of 1.2 nanometers at 30kV and had a magnification of 12x to 900kx. EDS was chosen for the analysis as it is rapid and would suffice for the check. It is known that even the best wet chemical analysis would not provide an accurate elemental composition of the alloy to confidently talk about its transformation temperatures or its mechanical properties. Both the as-received and heat-treated samples were analyzed using the set-up and elemental composition was obtained in the form of atomic percentages of Nickel and Titanium.

### 3.6 X-Ray Diffraction Studies

The X-ray diffraction (XRD) was carried out on the samples at CMTI Bangalore. The as-received NiTi and the low temperature heat-treated samples for one-hour duration were examined for the phases present as per ASTM F2024 - 10(2016). The XRD of all the NiTi samples was carried out on the D8 advance XRD set-up Bruker make as shown in figure 3.4.



Figure 3.4 D8 Advance X-Ray Diffraction set-up

The machine has a maximum usable angular range of  $110^\circ < 2\theta < 168^\circ$ , the smallest increment being  $0.0001^\circ$ . The anodes used in the same are Cu, Cr and Co for the different radiations. The applications of the machine are for the identification of crystalline materials, sample purity measurement, determination of unit cell dimensions, residual stress measurement and determination of degree of crystallinity. The samples were scanned at a  $2\theta$  angle range of  $30^\circ$  to  $50^\circ$  using  $\text{Cu-K}_\alpha$  radiation to identify the phases present in the alloy. The samples were inserted into the machine and scanned with an incremental step size of 0.01 degrees and the corresponding phases along with their respective angles ( $2\theta$ ) are noted. The results obtained from X-Ray diffraction was obtained in the form of peaks with different intensities. These peaks with different intensities were analyzed to ascertain the phases present in the alloy samples. The Differential Scanning calorimetry was carried out on all the NiTi samples

to confirm the results of the X-Ray diffraction as well as the superelastic property of the alloy, thereby making it suitable for a variety of mechanical as well as bio-medical applications.

### **3.7 Differential Scanning Calorimetric Studies**

The transformational temperatures of the as-received and the samples annealed for a duration of one-hour were investigated using the procedure of differential scanning calorimetry (DSC). The test was carried out as per ASTM D3418. A typical Perkin Elmer DSC set-up is shown in figure 3.5.



Figure 3.5 Perkin Elmer Differential Scanning Calorimetry set-up

The equipment used is LAB SYS-DSC 8500 at IIT Chennai. This is a double-furnace DSC, featuring our second-generation Hyper DSC technology. Now you can gain unlimited insight into the structure, properties, and performance of your materials. The equipments possess fast scanning rates of  $750^{\circ}\text{C}/\text{minute}$ . The highest temperature achievable in the machine is  $750^{\circ}\text{C}$  and the lowest being  $-180^{\circ}\text{C}$ . The readout rates in the machine are exceedingly quick at 100 points/second providing high data integrity. The equipment is used in a number of applications such as characterization of pharmaceutical materials, Process simulation in plastics and to name a few. The sample preparation was carried out by slicing small samples from the as-received rod as well as each of the heat-treated rods using the isomet slow speed diamond saw. Samples of very negligible thickness were cut from the samples

of approximately 20 mg weight. The set-up utilized the liquid nitrogen set-up which aided the equipment to go below Zero degrees temperature. Each of the samples were crimped into the Aluminum pan and placed into the apparatus. The temperature range was set from -50°C to 100°C for the operation to take place. The sample was cooled from room temperature to -50°C. From -50°C the heating was performed by heating the sample from -50°C to 100°C at a constant heating rate of 10°C/minute. Upon reaching the set temperature, the sample was cooled from 100°C to -50°C at a constant cooling rate of 10°C/minute. Upon reaching -50°C, the sample was brought back to room temperature and removed from the set-up. The respective heating and cooling peaks for the samples were obtained from the DSC set-up. The transformational temperatures of the austenite-martensite in the cooling cycle and martensite-austenite in the heating cycle could be interpolated and tabulated in degrees Celsius. This test would confirm the superelastic property or shape memory property of the alloy material.

### **3.8 Evaluation of Mechanical Properties**

#### **3.8.1 Evaluation of UTS**

The tensile tests were performed on a PC-2000 electronic tensometer at NMIT Bangalore at an ambient temperature of 30°C. The test has been carried out according to ASTM E8 standard. A typical electronic tensometer is shown in figure 3.6. This electronic Tensometer is a compact and versatile bench model horizontal Tensile Testing Machine of capacity 20 KN (2000kg). This instrument is used for testing tensile, compressive, Shear, Flexural properties of different materials. This combines the state-of-the-art computer technology and precision manufacturing techniques to offer unique mini horizontal Universal Testing Machine. The online test graph is displayed on the monitor. The as-received and the heat-treated samples were fixed in the set-up using the mechanical grippers in the tensometer. The gauge length of the sample was measured using a Vernier calipers. The needed inputs were fed to the software in the computer console such as the gauge length followed by the strain rate of  $8.3 \times 10^{-4} \text{sec}^{-1}$ . The set-up was switched on and the sample was elongated until failure. The results are evaluated in terms of stiffness in MPa and ultimate tensile

strength (UTS) in MPa. This is done to confirm the superelastic property of the material. The stress Vs strain graph is obtained from the test and is utilized for each sample to interpret the properties. The results of the as-received and the heat-treated samples, which are heat-treated at various temperatures and time duration are compared to bring about the ideal heat-treatment temperature for best properties.



Figure 3.6 PC-2000 Electronic Tensometer

The fractured surfaces of all the aged as well as the as-received samples were studied from the Carls Zeiss FESEM set-up. A small sample of 10mm thickness was cut from the fractured sample using a slow speed isomet. The fractured surface was placed under the SEM and the nature of the fracture was analyzed. The Micrograph obtained showed the nature of fracture taking place to ascertain the ductile nature of the material. The test followed by tensile is the Vickers hardness test. The reason for carrying out the Vickers Hardness was as per literature (Arciniegas et al. 2008), the hardness of the material to be very high, the Brinell hardness test would prove to be unsuitable and the Rockwell hardness would also not be suggested since the diameter of the indenter would be large. Hence, it was decided to carry out the Vickers hardness test on a minimal load.

### **3.8.2 Evaluation of Hardness**

The hardness of the as-received sample and the samples heat-treated for a duration of one hour were studied by performing the Vickers Hardness test with the hardness tester

at NMIT Bangalore. This hardness was carried out inspite of Rockwell and Brinell hardness tests being prevalent since the material is reported to be very hard as per the literature that could damage the indenters of Rockwell as well as Brinell hardness testers. The Vickers Hardness was carried out as per ASTM E92 – 17. A Vickers hardness tester is shown in figure 3.7.



Figure 3.7 Vickers Hardness Tester

This machine has a load range of 5kg to 120 kg. The height of the machine is 1000mm and the test specimen is limited to a height of 200mm. The machine has a scale least count of 0.001mm. The machine employs a diamond cone indenter having an angle of 135°. The samples of approximately 10 mm long were sliced using an isomet and the cut surfaces were polished to obtain a mirror finish to see clearly and measure the Vickers indentation. The sample is placed on the anvil and brought in contact with the indenter cup above and the cup is locked to hold the sample in place securely. A load of 5 Kg was applied using the loading arm and then released after full load was applied. The indentation in the form of a rhombus was observed using the scale and the length of the diagonals were measured and noted to obtain the size of the indentation. The Vickers Hardness Number was calculated using the suitable formula for the sample.

$$\text{VHN} = \frac{1.8544 * P}{d^2} \text{ Kg/mm}^2$$

Where, P = Load applied, Kg

$$D = \text{diameter of indentation} = \frac{d1+d2}{2}, \text{ mm}$$

The tribological properties of the as-received as well as the heat-treated samples were analyzed by performing the abrasive wear on all the NiTi samples. The wear test was carried out to analyze the abrasion resistance of the material to render it suitable for orthodontic and endodontic applications. The adhesive wear test was carried out but to know the wear of the samples was of the order of run-out of the machine.

### 3.9 Evaluation of Tribological Characteristics

The as-received and aged samples, that were heat-treated for a duration of one hour were tested for wear phenomenon. Abrasive wear test was carried out on a DUCOM wear testing machine at NMIT Bangalore since the samples hardly showed any sign of wear when tested for adhesive wear. The test conditions will approximately simulate the conditions met by endodontic tools when they are run against tooth and the associated tissues. The as-received as well as the annealed samples were subjected to wear test using pin-on-disc DUCOM machine as per ASTM G-132a. As per the standard, specimens of approximately 20mm thickness were cut from all the samples using a slow speed isomet. The cut surface was made flat to ensure a smooth and uniform wear to take place in the tribometer. The wear testing machine is shown in figure 3.8.



Figure 3.8 DUCOM Wear Testing Machine

An AA60 K5 V8 abrasive wheel of 60 grit size (alumina) was chosen for the test keeping in mind the working conditions that would be met by the endodontic files and



drills. The abrasive disc had 150mm outer diameter, 31.75mm inner diameter and was 6mm thick. We know the hardness of Dentin and synthetic alumina are 3 to 4 on the Mohs scale. The wheel is thoroughly cleaned for any impurities and debris that are sticking to it so as to not hamper the wear test. The cut sample is fixed to the sample holder and seen to it that the machine setting is completely flat to simulate the wear condition. The wear track diameter is set to 100mm and is kept constant throughout the test and also the wheel speed is set to 100rpm throughout the test. The abrasive wear tests were carried out with loads of 5, 15, 25, 35 and 45N, keeping the time duration constant for 10 minutes. The inputs corresponding to the test was fed to the WINDUCOMM software and the test was run to collect the corresponding readings of wear and coefficient of friction. The wear results were obtained in microns after the test was run for a duration of 600 seconds. The wear results were calculated in terms of wear mass loss expressed in grams was then calculated using the formula

$$\text{Density} = \text{Mass}/\text{Volume}$$

$$\text{Density} = 6.45\text{g}/\text{cm}^3$$

$$\text{Volume} = \frac{\pi}{4} * d^2 * L, \text{ where } d = \text{diameter of the sample}; L = \text{wear loss in cm}$$

$$\text{Mass} = \text{Density} * \text{Volume, grams}$$

A graph was plotted for all the samples of wear loss Vs load to get a fair idea of the increase or decrease of the wear with increase in the loading conditions.

Thin samples of 5mm thickness were sliced from the worn-out specimens using slow speed isomet and the worn surface was preserved carefully.

The specimen was placed in the SEM set-up and the worn surface was deeply examined under 2000X and 5000X to get a good idea of the nature of plough marks as well as density of the plough marks and also their depth to ascertain the degree of wear that has taken place in the samples. Also, an approximate elemental composition is analyzed using EDAX facility in the same experiment. The EDAX is taken both for a particular area as well as a region to analyze the nature of the constituents in the matrix. The main constituents that were looked for were  $\text{Ti}_2\text{Ni}$  precipitates as well as the Nickel and Titanium elements.

The NiTi material alloy samples were tested for various strain levels within 8% to confirm the superelastic property that were done previously using DSC, tensile test and the X-Ray diffraction studies. This test was carried out to have a clear idea and confirm the superelastic property of the alloy material to render it suitable for a variety of applications.

### 3.10 Study of Superelastic Behavior

The as-received as well as samples, heat-treated for one-hour duration were analyzed for their superelastic nature to replicate the pseudoelastic nature of endodontic files. The area under the stress strain curve depicts the elastic nature of the material. Also, the toughness is clearly analyzed by studying the stress curves. The NiTi files used in endodontic applications need to be superelastic in nature. Since they take huge stresses in the procedure, the files need to follow the path of the canal without damaging the human tooth as well as retaining their structure. The superelastic test was carried out as per ASTM F2516-18. The specimens were analyzed for 2%, 6% and 8% strains using 5582 INSTRON machine at National Aerospace Laboratories, Bangalore shown in figure 3.9.



Figure 3.9 5582 INSTRON Machine

This machine has a capacity of 100KN and can accommodate a sample of gauge length maximum 25mm. The as-received specimen was held on the machine using grippers having gauge length 25mm and tested at a strain rate of 1mm/second.

The extent of superelasticity of the specimens are quantified by calculating the net energy dissipated by the specimen during the loading and unloading cycle through measurement of the area under the stress-strain curve. The area under the loading and unloading cycle under the stress-strain curve represents the net energy dissipated. The same is expressed in terms of work done /unit volume as  $J/cm^3$ .

The as-received specimen was loaded with a tensile force upto 2% strain and made to unload. Similarly, the specimen was loaded upto 6% and 8% strains and made to unload. The variation in the curve was analyzed by measuring the hysteresis between the loading stress and unloading stress for all the predetermined strain values. The three consecutive loadings and unloading was done to ascertain the superelastic property of the material upto 8% strain without undergoing plastic deformation.

The similar procedure was repeated for the heat-treated samples. The samples were gripped for a gauge length of 25mm, loaded upto a strain of 2%, 6% and 8% strains and unloaded to analyze the superelastic property in terms of net energy dissipated.

### **3.11 Evaluation of Corrosion Characteristics**

The as-cast as well as the heat-treated samples were examined for corrosion in a medium that replicates the human system. The reason for carrying out the corrosion test was to confirm the effects of Nickel poisoning that can take place when the alloy material is exposed to the human blood during insertion into the arteries.

The corrosion test for the as cast and NiTi alloy samples, that were heat-treated for a duration of one-hour was carried out using 600E Electrochemical Analyzer as per ASTM F-2129 at Chemistry Dept NITTE Meenakshi Institute of Technology, Bangalore. The machine is illustrated in figure 3.10.



Figure 3.10 600E Electrochemical Analyser

The system contains a fast-digital function generator, a direct digital synthesizer for high frequency AC waveforms, high speed dual-channel data acquisition circuitry, a potentiostat and a galvanostat (available only in select models). The potential control range is  $\pm 10$  V and the current range is  $\pm 250$  mA. The instrument can measure current down to picoamperes. With the CHI200B Picoamp Booster and Faraday Cage (fully automatic and compatible with the CHI600E series), currents at sub-picoamperes can be measured. The instrument is very fast. The function generator can update at a 10 MHz rate. Two high speed and high-resolution data acquisition channels allow both current and potential (or an external voltage signal) to be sampled simultaneously at a rate of 1 MHz, with 16-bit resolution. The instrument provides a very wide dynamic range of experimental time scales. For instance, the scan rate in cyclic voltammetry can be up to 1000 V/s with a 0.1 mV potential increment or 5000 V/s with a 1 mV potential increment. The potentiostat/galvanostat uses a 4-electrode configuration, allowing it to be used for liquid/liquid interface measurements, and eliminating the effect of the contact resistance of connectors and relays for high current measurements. The data acquisition systems also allow an external input signal (such as spectroscopic) to be recorded simultaneously during an electrochemical measurement. The instrument is capable of a wide variety of electrochemical techniques and is available with integrated simulation and fitting software functions for both impedance and cyclic voltammetry. These features provide powerful tools for both electrochemical mechanistic studies and trace analysis.

Hank's solution was used for the testing purpose. The solution comprised of the following compounds:

1. NaCl;
2. KCl
3. CaCl<sub>2</sub>
4. MgSO<sub>4</sub>
5. MgCl<sub>2</sub>
6. Na<sub>2</sub>HPO<sub>4</sub>
7. KH<sub>2</sub>PO<sub>4</sub>
8. D-Glucose
9. NaHCO<sub>3</sub>

100ml of the Hank's solution was prepared by mixing suitable quantities of the ingredients and then poured into a beaker. The 50% Nickel – 50% Titanium sample of 3mm diameter and 16cm length was then inserted into the Hank's solution with 1cm<sup>2</sup> cross-sectional area of the sample being exposed to the solution. The electrochemical measurements were carried out for the alloy samples in the as-received and also the heat-treated condition. The test performed was Potentiodynamic Polarization Measurements test. The Potentiodynamic polarization measurements were carried out for the as-received 50% Nickel - 50% Titanium sample. In this measurement, the electrochemical character of the as-received alloy sample was analyzed by recording anodic and cathodic polarization curves in Hank's solution with an exposed area of 1cm<sup>2</sup>. A conventional three-electrode cell with Nickel-Titanium alloy as the working electrode, platinum foil as counter electrode and saturated calomel electrode as reference electrode. Potentiodynamic polarization curves were recorded after the immersion of the sample in Hank's solution for a period of 30 minutes with a scan rate of 0.4mV/sec. The linear TAEFL segments of anodic and cathodic curves were extrapolated to corrosion potential (E<sub>corr</sub>) to obtain the corrosion current densities (I<sub>corr</sub>). The corrosion rate was calculated using the formula as stated:

$$CR = \frac{I_{corr} * K * EW}{d * A}$$

Where:

CR = the corrosion rate in mm/year

$I_{\text{corr}}$  = the corrosion current in amps

$K$  = a constant that defines the units for the corrosion rate = 3272 mm/(amp-cm-year)

$EW$  = the equivalent weight in grams/equivalent = 106.56 g

$d$  = density in grams/cm<sup>3</sup> = 6.45 g/cc

$A$  = sample area in cm<sup>2</sup> = 1cm<sup>2</sup>

### **3.12 Conclusion**

In this chapter, the methodology adopted comprising of details of equipments used and procedure for assessing chemical composition using EDAX, different phases present using XRD, transformational temperatures using DSC for different heat-treatment cycles have been explained. Further, the methodology adopted for assessing the mechanical properties, wear characteristics and corrosion characteristics of the material for different heat-treatment cycles have also been explained.



## CHAPTER 4

### RESULTS AND DISCUSSION

#### 4.1 Introduction

In this chapter, the results of the systematic investigation on various aspects of Nickel-Titanium alloy such as results of observation of microstructure under TEM, evaluation of mechanical properties, tribological characteristics and evaluation of corrosion properties have been presented and discussed.

#### 4.2 Studies on Nickel-Titanium Alloy Without Any Heat-Treatment

##### 4.2.1 Microstructure observation under TEM

The Transmission electron microscopy micrographs of Ni-Ti alloy of the as-received sample at a magnification of 5000X has been presented in figure 4.1.

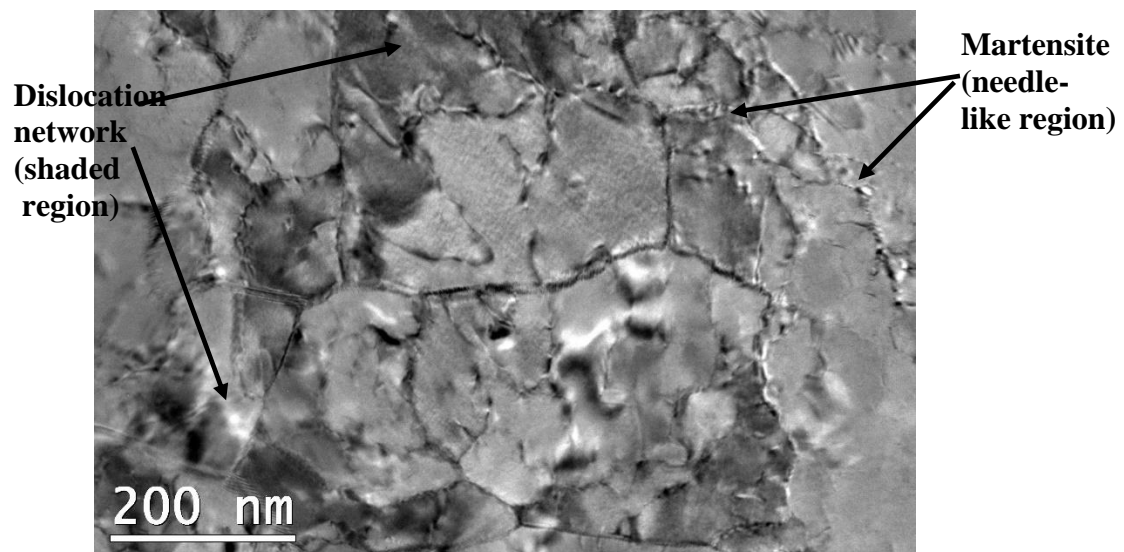


Figure 4.1 Microscopic image of as-received 50% Nickel - 50% Titanium alloy when observed under Transmission Electron Microscope

From this figure, presence of martensite which appears as a needle-like region can be observed. In addition, a shaded region indicating presence of dislocation network may also be observed.

In figure 4.2 the diffraction pattern of the as-received NiTi alloy under TEM has been presented.



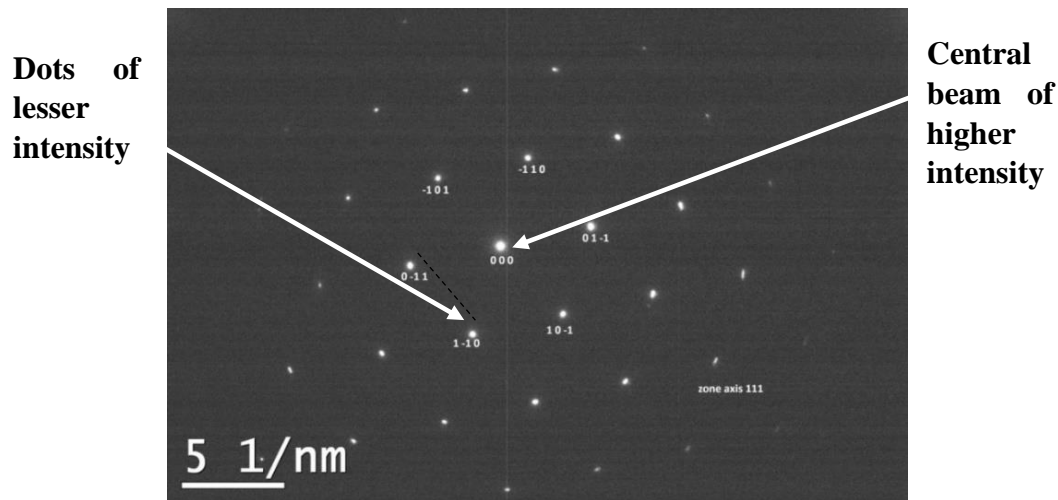


Figure 4.2 Diffraction Pattern of as-received 50% Nickel - 50% Titanium alloy used in this investigation when observed under Transmission Electron Microscope

It may be observed from figure 4.2 that the structure is hexagonal in nature having a central beam surrounded by six dots of lesser intensity. Thus, the microstructure and the diffraction pattern observed under TEM confirm that the alloy is a Nickel Titanium alloy existing in martensitic phase along with Austenitic phase at room temperature.

#### 4.2.2 EDS Analysis

The chemical composition of the constituents present in the alloy has been assessed by EDAX analysis. The graph of X-ray energy Vs number of counts per channel obtained for the NiTi alloy has been presented in figure 4.3. Similarly, the results of the chemical composition indicating atomic distribution of different elements obtained through EDAX analysis has been presented in table 4.1. From the study of both figure 4.3 and table 4.1, it can be observed that Titanium presence is 50.1% and Nickel presence is 49.9%. This confirms that the Ni-Ti alloy used in this investigation is a 50:50 Ti-Ni alloy which is well within the tolerance limit for 50:50 TiNi alloy as per ASTM F1375 - 92(2012). The alloy is found to be slightly on the Titanium-rich side.

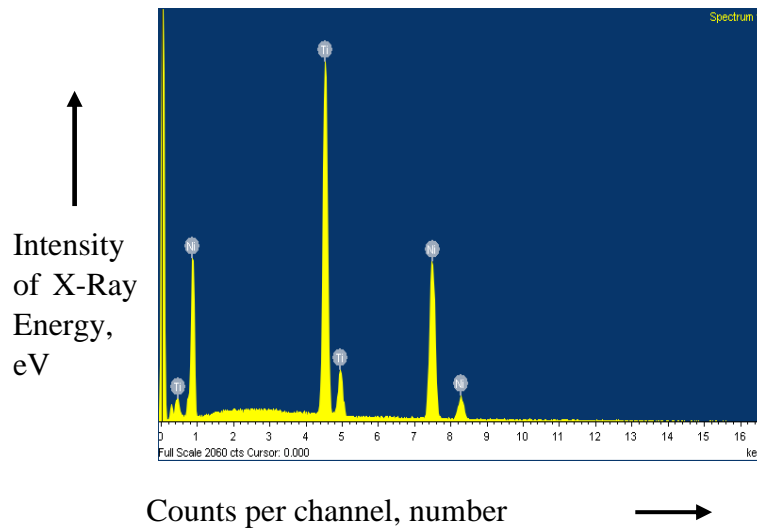


Figure 4.3 EDAX analysis spectrum of as-received 50% Nickel - 50% Titanium alloy used in this investigation

Table 4.1 Atomic Distribution of different elements obtained through EDAX analysis for the Ni-Ti alloy used in this investigation

S No	Element	Atomic Distribution (%)
(1)	(2)	(3)
1.	Titanium	50.1
2.	Nickel	49.9

#### 4.2.3 X-Ray diffraction studies

The X-ray diffractogram of the as-received Ni-Ti alloy has been presented in figure 4.4. From figure 4.4, it can be observed that the martensitic phase has appeared at  $2\theta$  value of  $39.24^\circ$ , whereas, the austenitic phase is noticed to appear at a  $2\theta$  value of  $42.1^\circ$ . Further, the energy intensity value of martensitic phase has been observed to be lesser than the energy intensity values of austenitic phase. The  $2\theta$  value range for appearance of these peaks in this investigation has been found to be in the range of  $30^\circ$  to  $50^\circ$ . The literature survey (Lekston et al. 2007) indicates that  $2\theta$  range for the appearance of peaks corresponding to Ni and Ti elements in Nickel-Titanium alloy is  $30^\circ$ - $50^\circ$ . The angle range for the appearance of peaks for the Nickel-Titanium alloy used in this

investigation confirm with the angle range for appearance of peaks for Nickel-Titanium alloy published in the earlier literature.

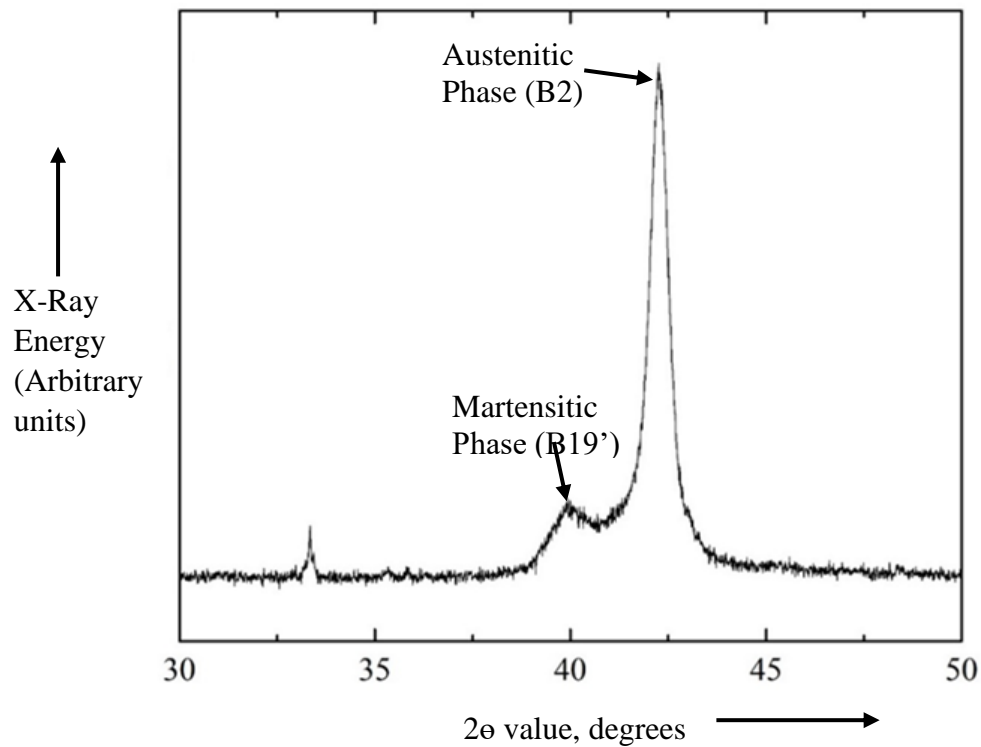


Figure 4.4 X-Ray Diffraction of as-received 50% Nickel - 50% Titanium alloy

#### 4.2.4 Differential scanning calorimetry

As mentioned earlier, the DSC tests are conducted as per ASTM D3418 / E1356 ISO 11357 on the material to evaluate the transformational temperatures of different phases present in the material. In this test, the sample is heated at a controlled rate and a graph of heat absorbed versus temperature i.e., thermal scan is plotted. From this scan, the transformational temperatures are investigated from the peaks obtained during the heating and cooling cycles. In this investigation, the DSC tests have been conducted on the Nickel-Titanium alloy to explore the different phases present in the alloy. Attempts have been made to record Austenitic phase start temperature ( $A_s$ ); Austenitic phase finish temperature ( $A_f$ ) were recorded. Similarly, Martensitic phase start temperature ( $M_s$ ) and Martensitic phase finish temperature ( $M_f$ ). The result of DSC test for as-received Nickel Titanium alloy obtained in terms of heating and cooling curves has been presented in figure 4.5.

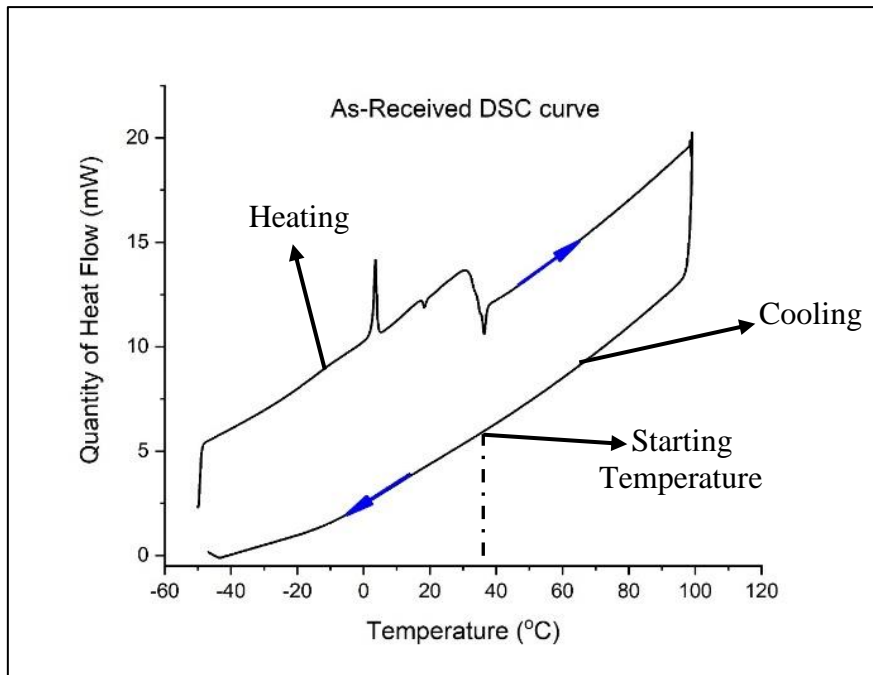


Figure 4.5 Differential Scanning Calorimetry curve of as-received 50% Nickel - 50% Titanium alloy

It is clear from figure 4.5 that there are no significant peaks observed in the heating as well as the cooling curves of as-received material indicating that there are no distinct phase transformations of either Austenite-Martensite or Martensite-Austenite present in the material. The absence of peaks in the material observed in this investigation may be the result of multi-step cold-working process performed on the material as reported by supplier Baoji Sunhope Titanium Industries Ltd. The process of cold-working performed on the material may have resulted in huge dislocation network in the grain structure inhibiting temperature-induced-martensitic transformation from taking place. Earlier investigators (Drexel et al. 2007) have published information on this aspect. They have reported that defects are formed during the cold working of the material and have an effect on the Austenitic to martensitic transformation. The stored strain energy on account of cold working probably makes the transformation from the austenitic to the martensitic structure nearly impossible to observe. Also, Pelton mentioned that the stored strain energy within the material due to cold working prevented the measure of the transformational temperatures performed by Bend Free Recovery Test (BFR). When trend of results obtained in this investigation has been compared with the trend of results reported by early investigators, it can be found that the trend of DSC test

results obtained in this investigation is similar to the trend of observations made by earlier investigators.

### **4.3 Mechanical Properties**

The as-received alloy is further analyzed for mechanical properties to ascertain Superelastic nature so as to be rendered suitable for many applications. The tension test is carried out as per ASTM E8 on PC-2000 tensometer to analyze the yield and ultimate strength of the material so that the tensile curve will indicate the presence or absence of pseudoelasticity.

#### **4.3.1 Ultimate tensile strength**

UTS is a measure of the maximum stress that an object/material/structure can withstand while being elongated, stretched, or pulled before breaking. It is found by performing a tensile test and recording the engineering stress versus strain curve. The highest point of the stress-strain curve is the UTS. The typical stress-strain diagram for the Nickel-Titanium alloy used in this investigation has been presented in figure 4.6. It can be observed that there are four distinct regions in the variation of stress with strain. In the literature (Vojtech et al. 2010) studies on the behavior of similar Nickel-Titanium alloys have been conducted. The tensile curve for Nickel-Titanium alloy having composition of nearly equi-atomic 50% Nickel and 50% Titanium as reported by (Vojtech et al. 2010) has been reproduced here as figure 4.6 for the sake of convenience of discussion. From this figure, it can be observed that they have reported that the alloy possesses four regions in the tensile curve. The first region shows the elastic deformation of the austenitic phase. The second region is the region where transformation from austenite to martensite is observed. The region III represents starting and ending of elastic deformation of martensite. Region IV represents further progression of plastic deformation of martensite. At the end of region IV, the material would have reached Ultimate stress where necking would have commenced and the material had failed at the respective breaking stress. The trend of results for the as-received Nickel-Titanium alloy used in this investigation is similar to the trend of results observed for Nickel-Titanium alloys reported by earlier investigators.

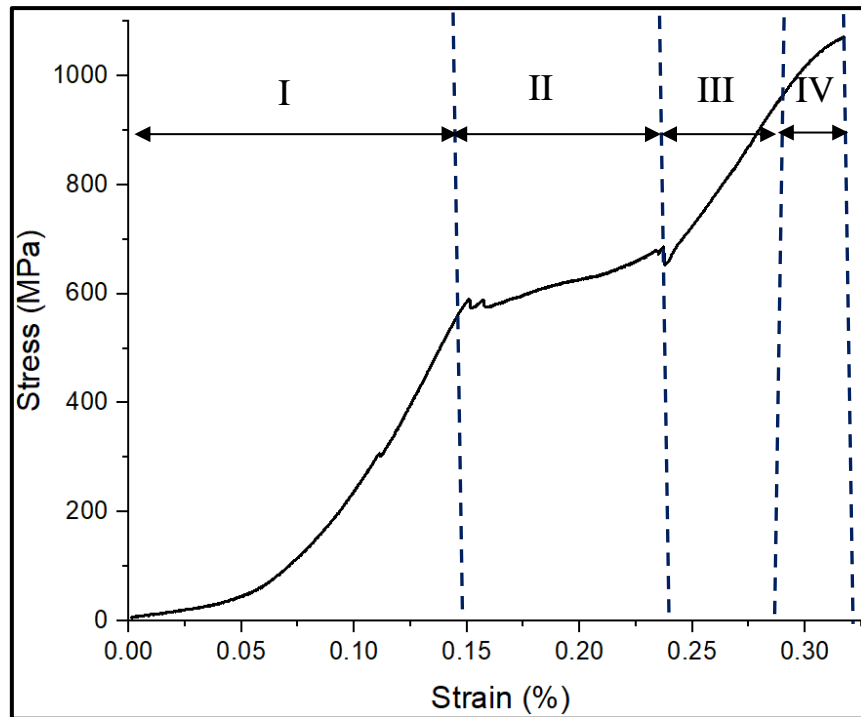


Figure 4.6 Tensile curve of as-received 50% Nickel - 50% Titanium alloy

Assuming similar phase transformation take place in the NiTi alloy studied in this research work, the typical stress-strain values corresponding to the commencement and completion of austenitic phase transformation to martensite have been presented in table 4.2. In the same table, the corresponding strain values and ultimate stress values have also been presented.

Table 4.2 Stress and strain values of as-received NiTi alloy during the assessment

Sl. No.	Stages of Assessment	Stress (MPa)	Strain (%)
(1)	(2)	(3)	(4)
1	Commencement of transformation from Austenitic phase	506	7
2	Completion of transformation to martensitic phase	547	17
3	Ultimate Tensile Stress (UTS)	966	24

It can be observed from table 4.2 that transformation of said austenite phase to martensite phase for this NiTi alloy commences at 7% and is completed at 17%. Further, the UTS value for the alloy has been found to be 966 MPa. Literature survey

(Mohammad et al. 2018, Fujio Miura et al. 1986) indicate that if the strength corresponding to transformation from austenite phase to martensite phase has commenced below 8% of strain value or in other words, if lower plateau strength (LPS) for NiTi alloy has commenced below 8% of strain value then the earlier researchers have observed that the alloy exhibits superelastic behavior. It is observed that from the table that the strength corresponding to transformation from said austenite phase to martensite phase has commenced below 8% of strain value or in other words, the said lower plateau strength (LPS) for NiTi alloy in this investigation has commenced at 7% of strain value which is less than 8% of superelastic strain value limit reported by the earlier investigators. This means that the material studied in this investigation appears to be super-elastic in nature. However, studies on superelastic behavior have been carried out on this material and the results have been presented and discussed in detail in later sections of this chapter.

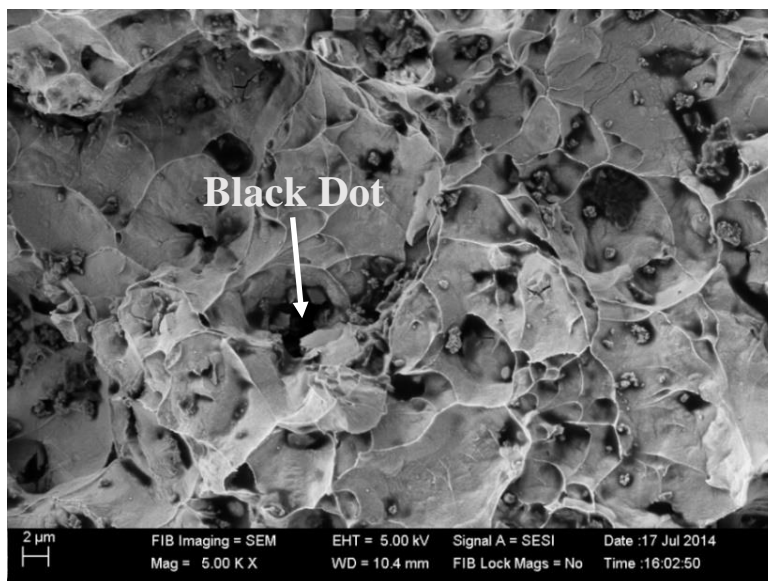


Figure 4.7 Fractograph of the as-received NiTi alloy when observed under SEM at a magnification of 5000X

Vojtech et al. (2010) has studied the stress-strain behavior of similar Nickel-Titanium alloys. They have reported that the LPS and UPS values are nearer to the values of the material reported in the investigation. The fractograph of the as-received NiTi alloy when observed under SEM at a magnification of 5000X has been presented in figure 4.7. It can be observed from figure 4.7 that the nature of fracture of the material appears as a transgranular fracture indicating that the material is ductile in nature which

appears as a black dot at its center. The black dot indicated in figure 4.7 could be the coalescence of micro voids and as the plastic deformation progresses the adjacent voids too are seen to have coalescence due to the plastic strain localization till the end of the cross-section leading to a fracture in the material.

#### 4.3.2 Hardness

As mentioned earlier, the published information on the hardness of Nickel-Titanium alloy material indicates that the material is having relatively higher hardness. Therefore, assessment of hardness in the form of Brinell hardness number may not be suitable and assessment of hardness in the form of Rockwell hardness number or in the form of Vickers Hardness number may be suitable. As the specimen sizes in this investigation were small, assessment of hardness of Nickel Titanium as-received material has been made in terms of Vickers Hardness number. The average representative values of Vickers Pyramid Number (VPN) of as-received NiTi alloy used in this investigation has been presented in table 4.3.

Table 4.3 Hardness Values of 50% Nickel - 50% Titanium alloy

Sl No	Material	Hardness value* VPN
(1)	(2)	(3)
1	As-received Nickel -Titanium alloy	421

\* Average Representative value

It can be observed from table 4.3 that VPN value of NiTi as-received material has been 421 VPN. From the published literature (Arciniegas et al. 2008), when the NiTi alloy has been manufactured by the process of cold rolling, it becomes a very hard material that is known to cut even the profile of a tooth for a root canal treatment. The reason for exhibition of high hardness could be the fine grain size that is seen as Nano-sized grains in the transmission electron micrographs presented in the earlier section.

#### 4.3.3 Tribological characteristics

As explained in previous chapter, abrasive wear behavior of as-received NiTi alloy was examined by subjecting the sample for different loads for a fixed sliding speed and



fixed test time. Wear mass loss has been used to grade the wear property of the test material i.e. in other words, if the wear mass loss is lower, then, higher is the wear resistance. The abrasive wear loss of the as-received NiTi alloy used in this investigation has been presented in table 4.4. The same values have been graphically presented in figure 4.8.

Table 4.4 Abrasive Wear characteristics of as-received 50% Nickel - 50% Titanium alloy

<b>S No</b>	<b>Load (P), N</b>	<b>Wear, Mass Loss, mg</b>
(1)	(2)	(3)
1	5	5.8
2	15	6.8
3	25	7.4
4	35	7.8
5	45	8.2

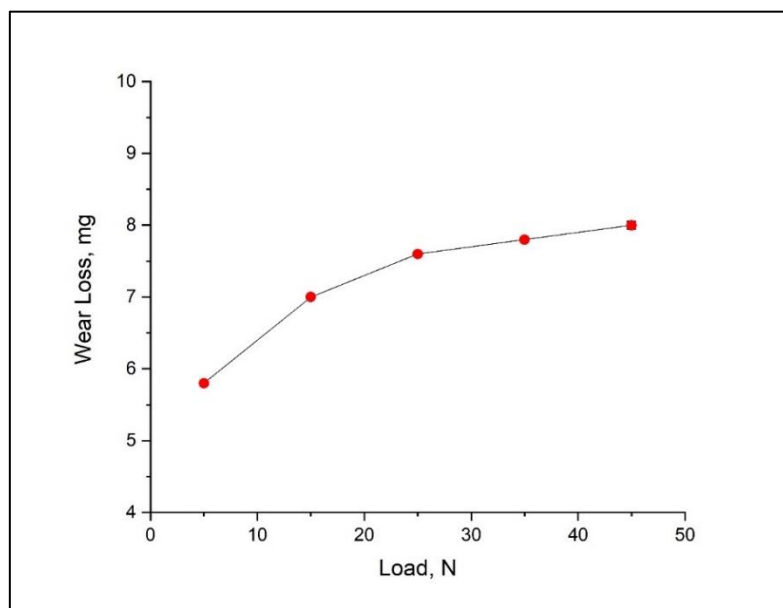
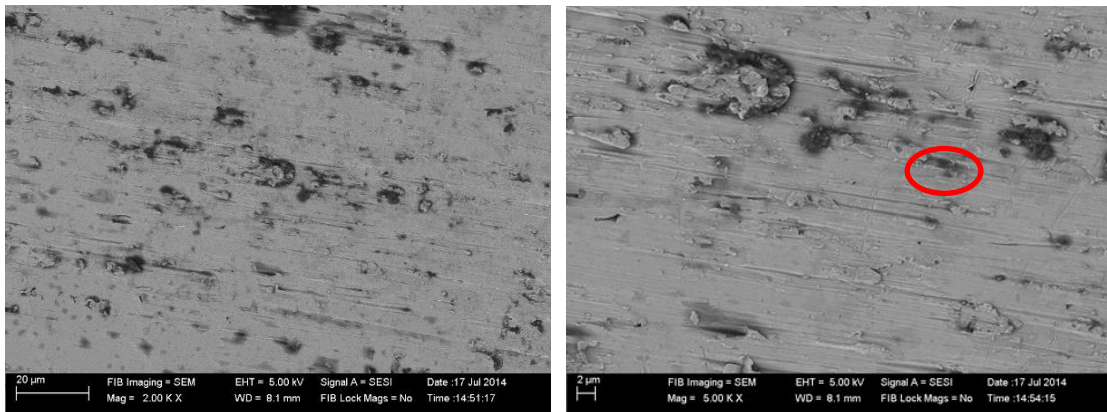


Figure 4.8 Wear Mass Loss of as-received 50% Nickel - 50% Titanium alloy

It can be observed from the figure 4.8 that within the scope of the investigation, when the load is increased from 5N to 15N, the wear mass loss rate is relatively at a higher rate. With further increase in the load, the wear mass loss rate is relatively at a slower rate.

Earlier investigators (Gao Fei et al. 2007) have studied abrasive wear behavior of different wear resistant materials using similar experimental set-up. The trend of results of variation of wear mass loss with the increase in the load observed in this investigation has been found to be similar to the trend of results reported by previous investigators. The worn surface of as-received NiTi alloy at typical test load of 15N at magnification of 2000X and 5000X have been presented in figure 4.9.



(a) Magnification 2X

(b) Magnification 5X

Figure 4.9 Worn surface of as-received 50%Nickel - 50%Titanium at 2000 and 5000 when observed under Scanning Electron Microscope

From these photographs, it can be observed that material is getting worn by the Alumina wheel. The presence of plough marks indicates wear due to Alumina wheel. As observed in figure 4.9 (b), initially when the surface is worn by the Alumina wheel, the material is shifted to the sides of the wear groove and not removed from the surface. This phenomenon refers to ploughing of the NiTi alloy surface. Further, since the material is ductile, a chip was observed to form during the test and material was removed such that the volume of material removed is equivalent to the volume of the wear track (groove). Thus, it can be inferred that the wear mechanism of NiTi alloy when subjected to the abrasive wear test appears to be micro-cutting and ploughing in nature.

#### 4.3.4 Superelastic Behaviour

As explained earlier, the stress-strain curves for as-received NiTi alloy specimens have been determined for different levels of predetermined strain values. The variation of

strain for different levels of stress during loading and after release of the load at predetermined strain value of 2% has been presented in figure 4.10.

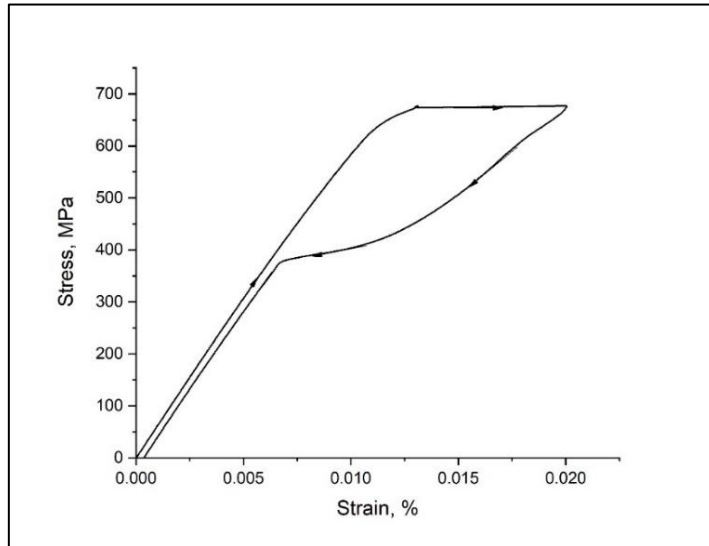


Figure 4.10 Stress verses strain graph for as-received 50% Nickel - 50% Titanium alloy at 2% pre-determined strain level during loading and release of load Similarly, variation of strain for different levels of stress during loading and after release of load at a predetermined strain value of 6% and 8% has been presented in figures 4.11 and 4.12 respectively.

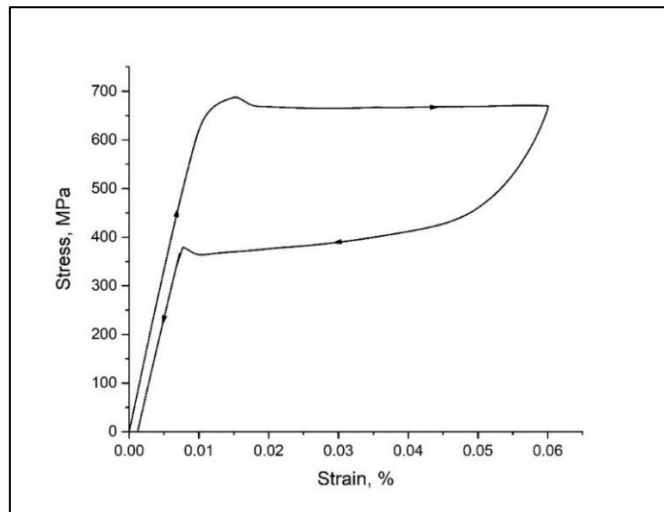


Figure 4.11 Stress verses strain graph for as-received 50% Nickel - 50% Titanium alloy at 6% pre-determined strain level during loading and release of load

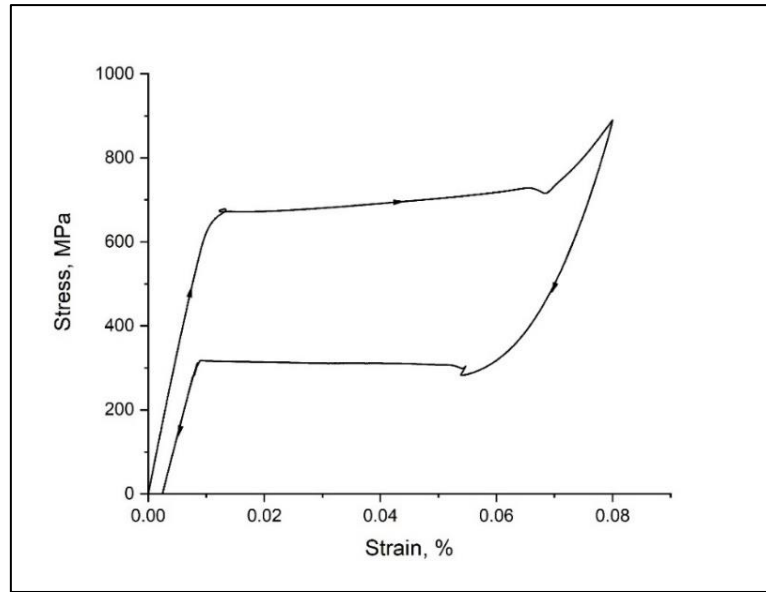


Figure 4.12 Stress versus strain graph for as-received 50% Nickel - 50% Titanium alloy at 8% pre-determined strain level during loading and release of load

It can be seen from the study of figures 4.10 to 4.12 that the material even after loading upto a stress level of 700 MPa does not break but returns back to the original stress value after release of the load. In other words, the unloading curve follows a hysteresis path compared to loading curve, returning back to the same point. This means that the material is exhibiting superelastic behavior. This has been found true at all the predetermined strain levels studied within the scope of this investigation. When we compare the results presented in figure 4.10 with the results presented in figure 4.11 and similarly the results presented in figure 4.11 with the results presented in figure 4.12, it can be observed that stress level during loading of the load, increases from 650 MPa to 700 MPa and further upto 800 MPa as the predetermined strain level has been increased from 2% to 6% and further to 8%, respectively.

Further, when we compare the results presented in figure 4.10 with the results presented in figure 4.11 and similarly the results presented in figure 4.11 with the results presented in figure 4.12, it can be observed that stress level during release of the load, decreases from 450 MPa to 375 MPa and further upto 300 MPa as the predetermined strain level has been increased from 2% to 6% and further to 8%, respectively. This indicates that hysteresis curve has broadened showing a much-lowered stress in the unloading cycle at 8% predetermined strain level as compared to 2% predetermined strain level and 6%

predetermined strain level. The superelastic performance is expressed as the net energy dissipated by the as-received alloy material when subjected to different predetermined strain levels. This is calculated as net energy dissipated during the loading and unloading cycle by measuring the area enclosed between the same in table 4.5.

Table 4.5 Net energy dissipated expressed as area enclosed within loading and unloading curves of stress vs strain diagram for as-received 50% Nickel - 50% Titanium alloy for different pre-determined strain rates

<b>S No</b>	<b>Pre-determined strain rate, %</b>	<b>Net energy dissipated, (J/cm<sup>3</sup>)</b>
(1)	(2)	(3)
1	2	6.2
2	6	14.2
3	8	13.1

From table 4.5, it can be seen that the net energy dissipated between the loading and unloading cycle for as-received 50% Nickel - 50% Titanium alloy for different predetermined strain rates varies from 6.2 J/cm<sup>3</sup> to 14.2 J/cm<sup>3</sup>. Further, among the different predetermined strain rates studied, the area enclosed within loading and unloading curves for 6% strain rate is maximum at 14.2 J/cm<sup>3</sup>. The results presented in this section indicates that as-received NiTi alloy exhibits superelastic behavior in the cold-worked condition by exhibiting the nature of stress induced transformation as presented in this section upto 8% strain, the superelastic performance being the maximum at 6% predetermined strain. The published information in the area of superelastic behavior of NiTi alloys carried out by earlier investigators (Narges Shayesteh et al. 2019) (Muhammad M Sherif et al. 2018) (Mostafa Tazarv et al. 2015) indicates that the nature of stress-induced transformation behavior observed in this research work is similar to the nature of stress-induced transformation behavior reported by earlier investigators.

#### 4.3.5 Corrosion characteristics

The electrochemical corrosion rate for as-received 50% Nickel - 50% Titanium alloy samples has been determined as explained in the previous section. The TAEFL plot i.e. semi log plot of current on log scale vs potential on plain scale for as received 50%Nickel - 50%Titanium alloy in a corrosive medium of pH value 7.5 has been presented in figure 4.13.

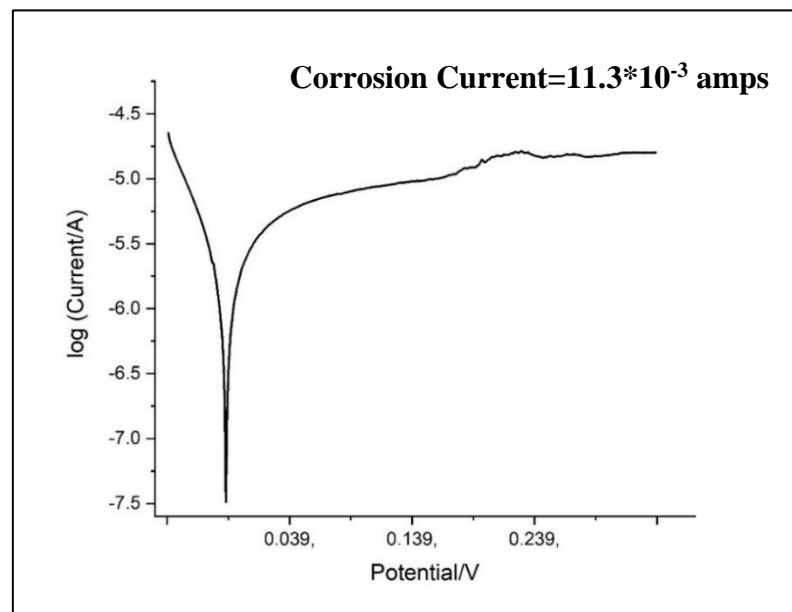


Figure 4.13 TAEFL plot for as received 50%Nickel - 50%Titanium alloy subjected to the corrosive medium of Hank's solution

As explained in the previous section, the intersection points of extended anode current line and extended cathode current line indicating the corrosion current for the material under consideration has been determined by feeding all the values into the software and has been mentioned in figure 4.13 and in table 4.6. The corrosion current for as-received 50% Nickel - 50% Titanium alloy has been found to be  $11.3 \times 10^{-3}$  amperes. Further, by substituting this value of corrosion current in the equation explained in the earlier section, the corrosion rate has been determined and has been presented in table 4.6.

Table 4.6 Electrochemical corrosion rate for as-Received 50% Ni - 50% Ti alloy

S No	Material	Corrosion Current (I) Amps	Electrochemical Corrosion Rate (CR) mm/year
(1)	(2)	(3)	(4)
1	As-received 50% Nickel-50% Titanium alloy	$11.3 \times 10^{-3}$	0.0613

The electrochemical corrosion rate for as-received 50% Nickel - 50% Titanium alloy has been found to be 0.0613 mm/year.

#### 4.4 Studies on Nickel-Titanium Alloy Subjected to Low Temperature Annealing Heat-Treatment

As explained in the previous chapter, the as-received Nickel Titanium alloy specimens have been subjected to four different low temperature annealing heat-treatments namely at 300°C, 350°C, 400°C and 450°C. Later, systematic study similar to the study reported in the previous section has been carried out, reported, and discussed in the following sub-sections.

##### 4.4.1 Microstructure observation under TEM

The typical Transmission electron microscopy micrographs of Ni-Ti alloy subjected to different low temperature annealing heat treatments for one-hour duration at a magnification of 2000X has been presented in figures 4.14 to 4.17.

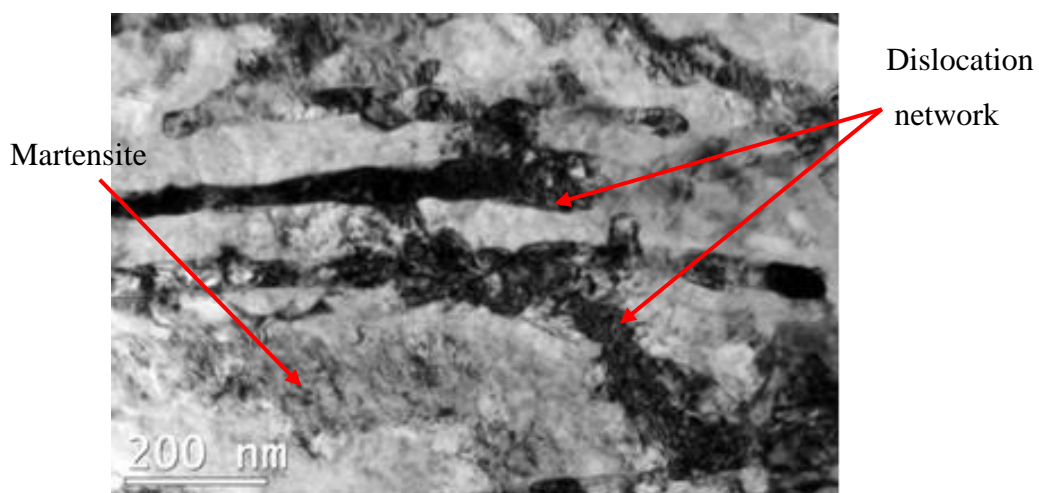


Figure 4.14 Microscopic image of 50% Nickel - 50% Titanium alloy subjected to low temperature annealing heat treatment at 300°C when observed under Transmission Electron Microscope

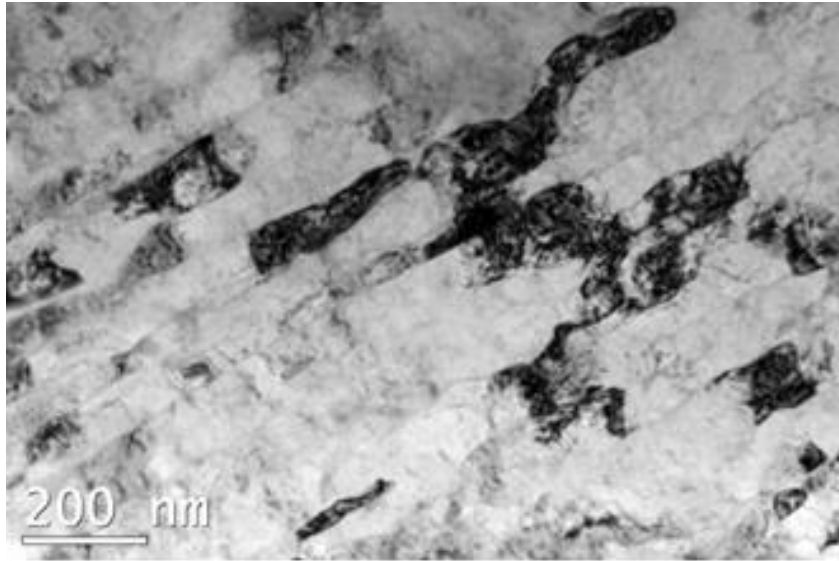


Figure 4.15 Microscopic image of 50% Nickel - 50% Titanium alloy subjected to low temperature annealing heat treatment at 350°C when observed under Transmission Electron Microscope

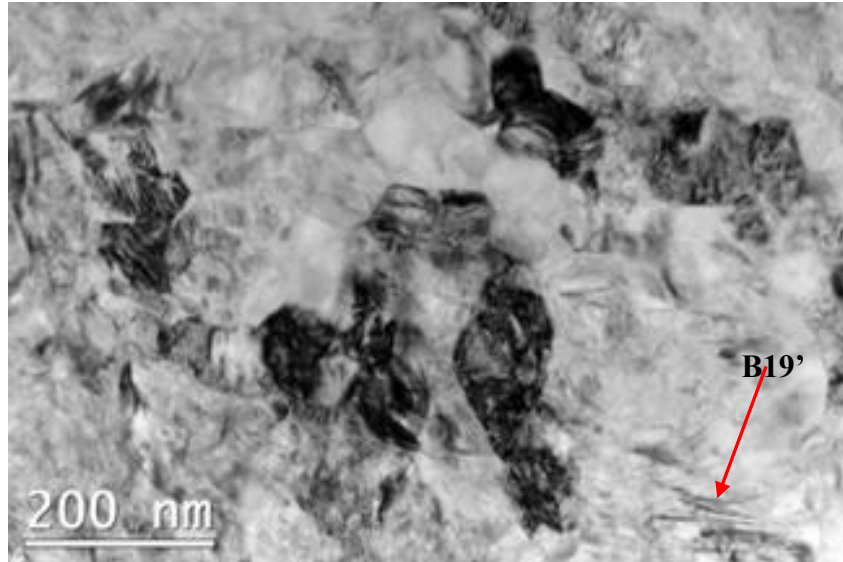


Figure 4.16 Microscopic image of 50% Nickel - 50% Titanium alloy subjected to low temperature annealing heat treatment at 400°C when observed under Transmission Electron Microscope



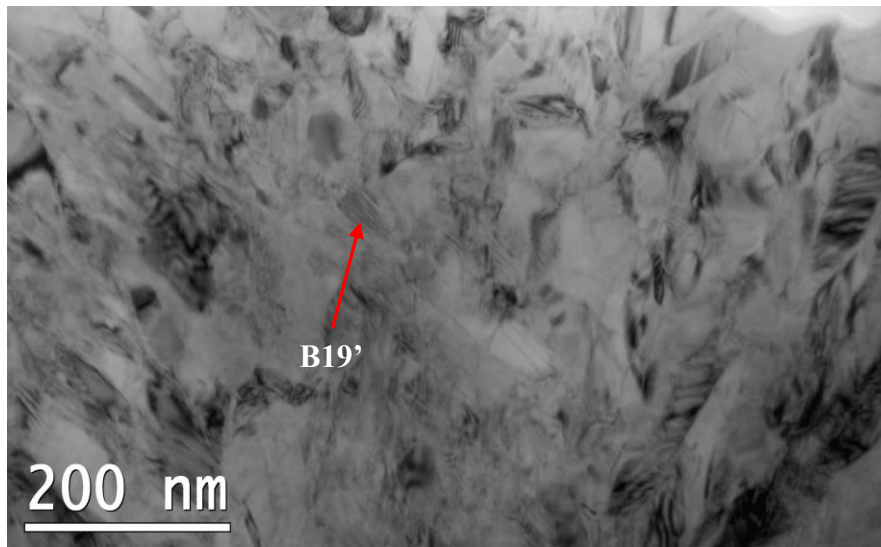


Figure 4.17 Microscopic image of 50% Nickel - 50% Titanium alloy subjected to low temperature annealing heat treatment at 450°C when observed under Transmission Electron Microscope

When the test specimens of NiTi alloy subjected to low temperature annealing heat treatment at 300°C, i.e., from figure 4.14, the presence of martensite which appears as a needle-like region can be observed. In addition, a shaded region indicating presence of dislocation network may also be observed. When the test specimens of NiTi alloy subjected to low temperature annealing heat treatment at 350°C were observed, i.e., from figure 4.15, the presence of martensite, dislocation networks and formation of NiTi alloy grains have been found. When the NiTi alloy subjected to low temperature annealing treatment at 350°C has been compared with that of 300°C, it appears that the extent of dislocation network has relatively reduced and the grain size of NiTi alloy has relatively increased. When the test specimens of NiTi alloy subjected to low temperature annealing heat treatment at 400°C were observed, i.e. from figure 4.16, the presence of martensite, dislocation networks and formation of NiTi alloy grains have been found. When the NiTi alloy subjected to low temperature annealing treatment at 400°C has been compared with that of 350°C, it appears that the extent of dislocation density has relatively reduced and the grain size of NiTi alloy has relatively increased. When the test specimens of NiTi alloy subjected to low temperature annealing heat treatment at 450°C were observed, i.e. from figure 4.17, the presence of martensite, dislocation networks and formation of NiTi alloy grains have been found. When the

NiTi alloy subjected to low temperature annealing treatment at 450°C has been compared with that of 400°C, it appears that the extent of dislocation network has relatively reduced and the grain size of NiTi alloy has relatively increased.

The above discussion indicates that within the scope of the investigation, when the NiTi alloy has been subjected to low temperature annealing heat treatment, as the annealing heat treatment temperature is increased, there has been a decrease in the extent of dislocation network and increase in the grain size of NiTi alloy. However, among the test specimens subjected to heat-treatment at different temperatures, it appears that the presence of martensitic phase is relatively more in specimens of 50% Nickel – 50% Titanium alloy subjected to low annealing heat-treatment at 350°C.

#### **4.4.2 EDS analysis**

As the low temperature annealing heat-treatment appears to have negligible effect on the chemical composition of the 50% Nickel – 50% Titanium alloy, EDAX analysis for the NiTi alloy subjected to low temperature heat-treatment at different temperatures has been excluded in this systematic investigation.

#### **4.4.3 X-Ray diffraction studies**

The X-ray diffractogram of the 50% Nickel – 50% Titanium alloy subjected to a heat-treatment of 300°C for a duration of one-hour has been presented in figure 4.18. From this figure, it can be observed that both austenitic phase and martensitic phase are present. It can also be observed that the martensitic phase has appeared at a  $2\theta$  value of 39.24°, whereas, the austenitic phase is seen to appear at a  $2\theta$  value of 42.8°. Further, the energy intensity value of martensitic phase has been observed to be lesser than the energy intensity values of austenitic phase. The  $2\theta$  value range for appearance of these peaks for this heat-treated alloy has been found to be in the range of 30° to 50°. The X-ray diffractogram of the 50% Nickel – 50% Titanium alloy subjected to a heat-treatment of 350°C for a duration of one-hour has been presented in figure 4.19. From this figure, it can be observed that both austenitic phase and martensitic phase are present. Apart from this, it appears that an additional phase named R-phase is present in the specimen.

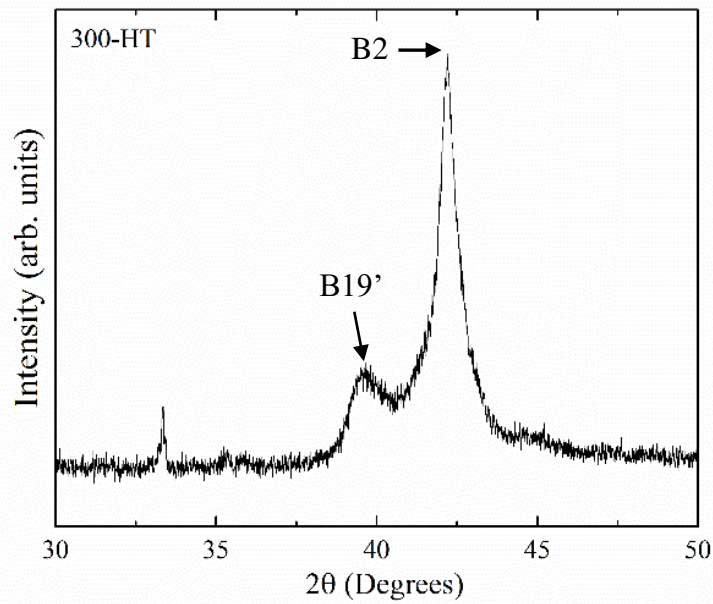


Figure 4.18 X-Ray Diffractogram of 50% Nickel - 50% Titanium alloy subjected to low temperature annealing heat treatment at 300°C

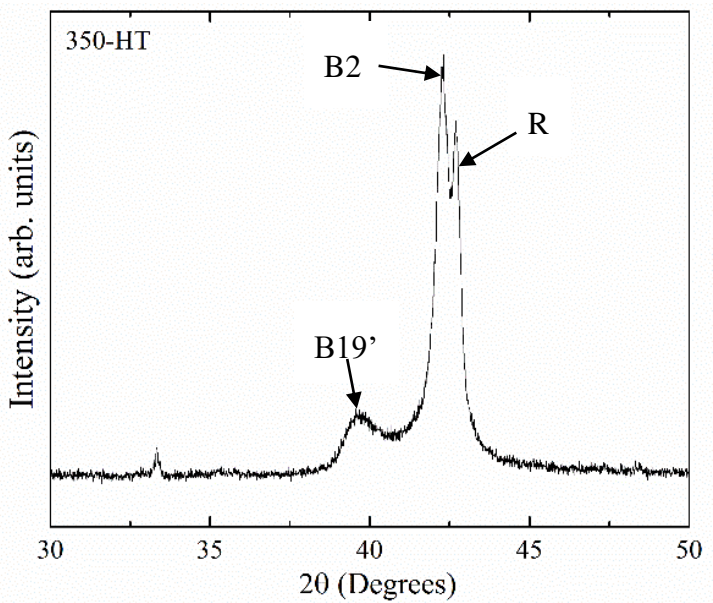


Figure 4.19 X-Ray Diffractogram of 50% Nickel - 50% Titanium alloy subjected to low temperature annealing heat treatment at 350°C

It can also be observed that the martensitic phase has appeared at a  $2\theta$  value of  $39.24^\circ$ . Whereas, the austenitic phase is observed to appear at a  $2\theta$  value of  $42.4^\circ$  and the Rhombohedral phase (R-phase) is found to appear at a  $2\theta$  value of  $43.1^\circ$ . Further, the

energy intensity value of martensitic phase has been observed to be lesser than the energy intensity values of austenitic phase. The energy intensity value of Rhombohedral phase has been observed to be in between the energy intensity value of martensitic phase and the austenitic phase. The  $2\theta$  value range for appearance of these peaks for this heat-treated alloy has been found to be in the range of  $30^\circ$  to  $50^\circ$ .

The X-ray diffractogram of the 50% Nickel – 50% Titanium alloy subjected to a heat-treatment of  $400^\circ\text{C}$  for one-hour duration has been presented in figure 4.20.

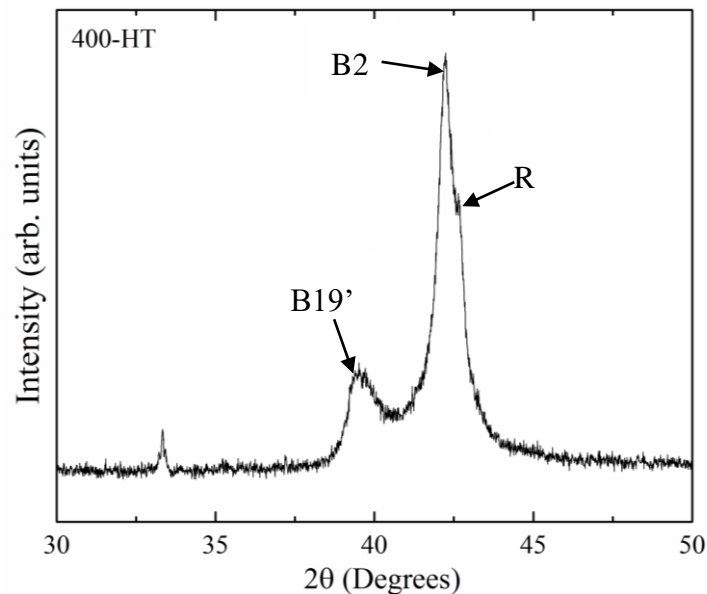


Figure 4.20 X-Ray Diffractogram of 50% Nickel - 50% Titanium alloy subjected to low temperature annealing heat treatment at  $400^\circ\text{C}$

From this figure, it can be observed that both austenitic phase and martensitic phase are present. Apart from this, it appears that an additional phase named Rhombohedral phase slightly present in the specimen. It can also be observed that the martensitic phase has appeared at a  $2\theta$  value of  $39.24^\circ$ . Whereas, the austenitic phase is found to appear at a  $2\theta$  value of  $42.4^\circ$  and the Rhombohedral phase (R-phase) is observed to appear slightly at a  $2\theta$  value of  $43.1^\circ$ .

Further, the energy intensity value of martensitic phase has been observed to be lesser than the energy intensity values of austenitic phase. The energy intensity value of Rhombohedral phase has been observed to be in between the energy intensity value of

martensitic phase and the austenitic phase. The  $2\theta$  value range for appearance of these peaks for this heat-treated alloy has been found to be in the range of  $30^\circ$  to  $50^\circ$ .

The X-ray diffractogram of the 50% Nickel – 50% Titanium alloy subjected to a heat-treatment of  $450^\circ\text{C}$  for a duration of one-hour has been presented in figure 4.21.

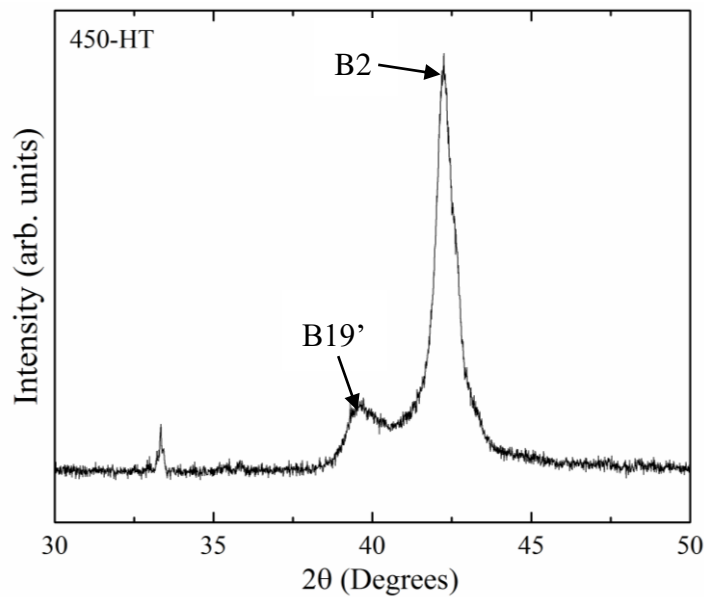


Figure 4.21 X-Ray Diffractogram of 50% Nickel - 50% Titanium alloy subjected to low temperature annealing heat treatment at  $450^\circ\text{C}$

From this figure, it can be observed that both austenitic phase and martensitic phase are present. Interestingly, it appears that an additional phase named Rhombohedral phase is absent in the specimen. It can also be observed that the martensitic phase has appeared at a  $2\theta$  value of  $39.24^\circ$ , whereas, the austenitic phase is noticed to appear at a  $2\theta$  value of  $42.4^\circ$ . Further, the energy intensity value of martensitic phase has been observed to be lesser than the energy intensity values of austenitic phase. The  $2\theta$  value range for appearance of these peaks for this heat-treated alloy has been found to be in the range of  $30^\circ$  to  $50^\circ$ .

The above discussion indicates that within the scope of the investigation, when the NiTi alloy has been subjected to low temperature annealing heat treatment, as the annealing heat treatment temperature is increased, the presence of Rhombohedral phase has been observed at  $350^\circ\text{C}$  and  $400^\circ\text{C}$ . With further increase in the annealing temperature to  $450^\circ\text{C}$ , there has been a marginal presence of Rhombohedral phase. In addition, the

intensity of the Rhombohedral phase appears to decrease with increase in heat treatment temperature 350°C to 400°C.

The literature survey (Lekston et al. 2007) indicates that  $2\theta$  range for the appearance of peaks corresponding to Ni and Ti elements in Nickel-Titanium alloy is 30°-50°. The angle range for the appearance of peaks for the Nickel-Titanium alloy subjected to low temperature heat treatment at different temperature, confirm with the angle range for appearance of peaks for Nickel-Titanium alloy published in the earlier literature.

#### **4.4.4 Differential scanning calorimetry**

As mentioned earlier, the DSC tests are conducted as per ASTM D3418 / E1356 ISO 11357 on the material to evaluate the transformational temperatures of different phases present in the material. In this test, the heat-treated specimens are heated at a controlled rate each for a duration of one-hour and a graph of heat absorbed versus temperature i.e., thermal scan is plotted. From this scan, the presence of different phases is found out.

In this investigation, the DSC tests have been conducted on the Nickel-Titanium alloy subjected to low temperature annealing heat-treatment at different temperatures keeping the time duration constant at one hour, to explore the different phases present in the alloy. Attempts have been made to record Austenitic phase start temperature ( $A_s$ ), Austenitic phase finish temperature ( $A_f$ ). Similarly, Martensitic phase start temperature ( $M_s$ ) and Martensitic phase finish temperature ( $M_f$ ) have been recorded.

The result of DSC test for Nickel Titanium alloy subjected to low temperature annealing heat-treatment at different temperatures and one-hour duration obtained in terms of heating and cooling curves has been presented in figures 4.22 to 4.25. Further, from these figures the transformation temperatures of different phases present in the alloy have been recorded and have been presented in table 4.7.

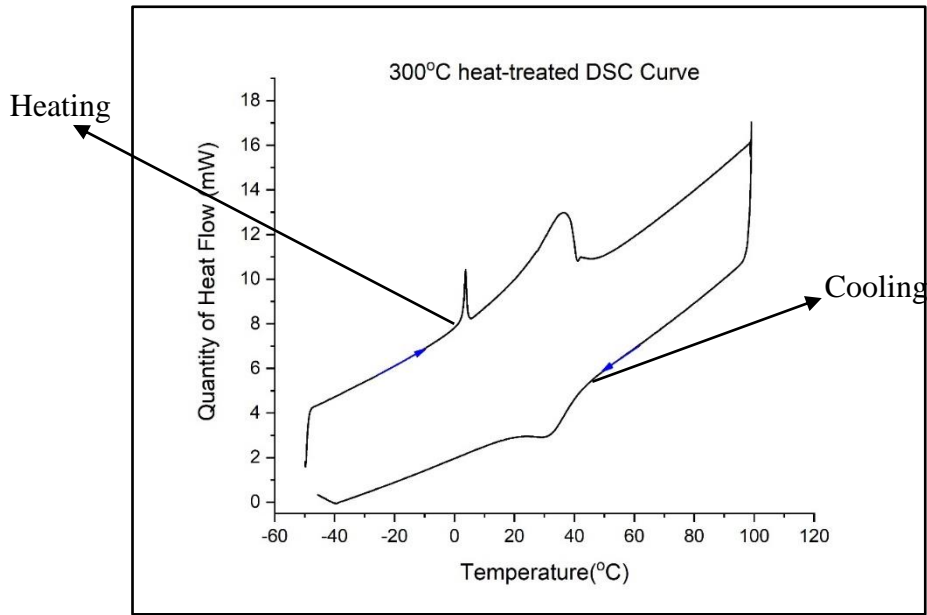


Figure 4.22 DSC Thermogram of 50% Nickel - 50% Titanium alloy subjected to low temperature annealing heat treatment at 300°C

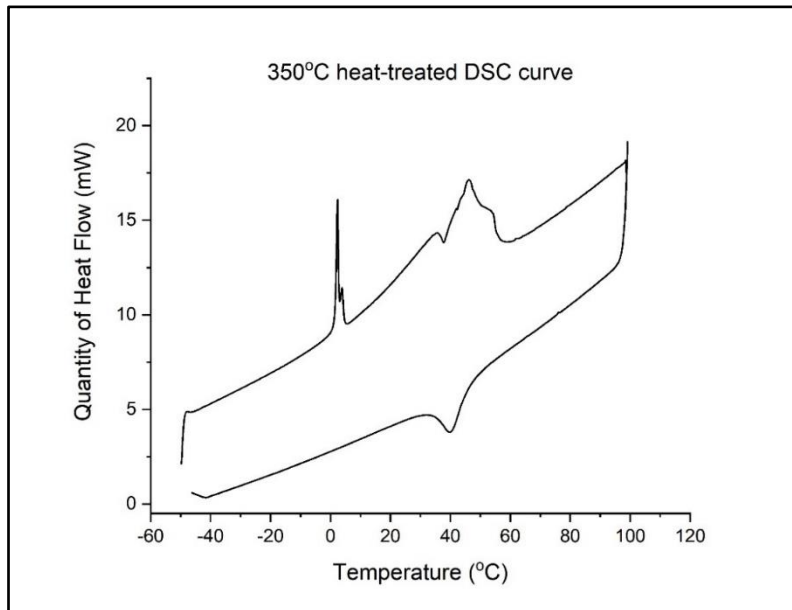


Figure 4.23 DSC Thermogram of 50% Nickel - 50% Titanium alloy subjected to low temperature annealing heat treatment at 350°C

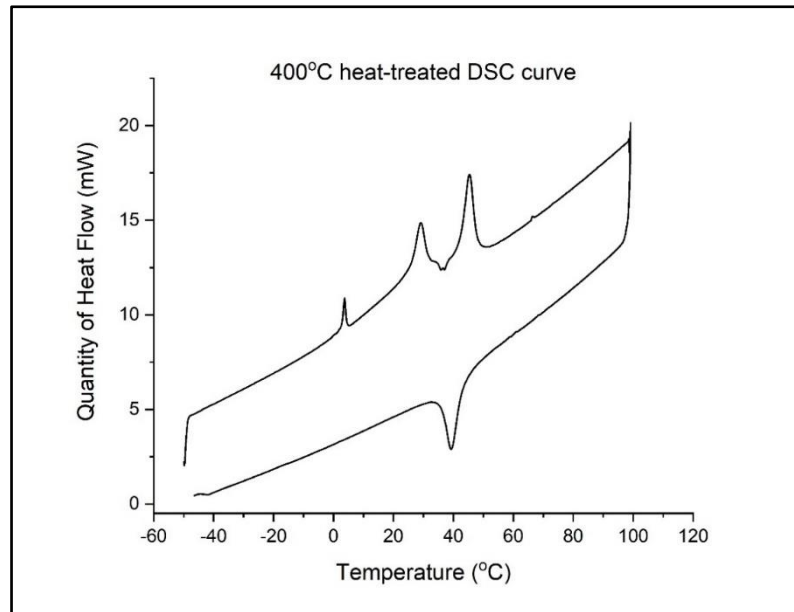


Figure 4.24 DSC Thermogram of 50% Nickel - 50% Titanium alloy subjected to low temperature annealing heat treatment at 400°C

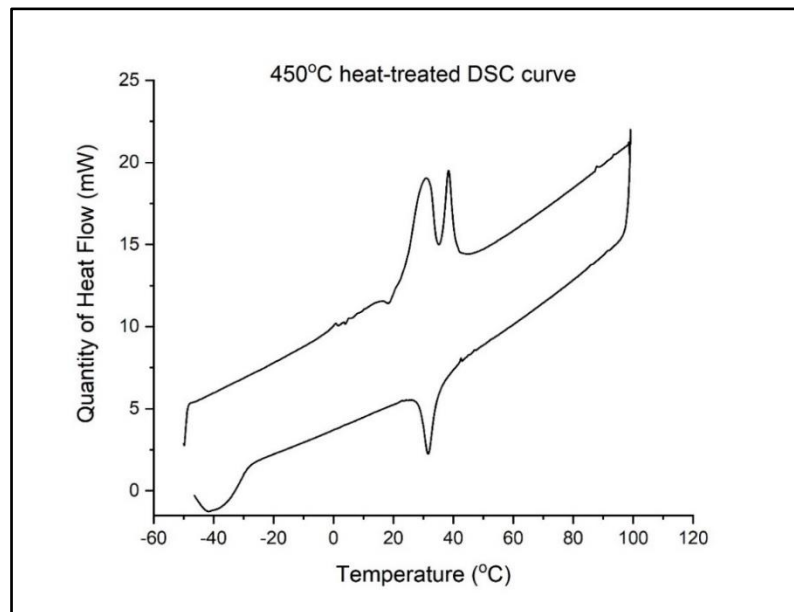


Figure 4.25 DSC Thermogram of 50% Nickel - 50% Titanium alloy subjected to low temperature annealing heat treatment at 450°C



Table 4.7 Transformation temperatures of different phases in 50% Nickel - 50% Titanium alloy when subjected to low temperature annealing heat-treatment at different temperatures

Sl. No.	Temperature at which low temperature annealing heat-treatment has been carried out °C	Transformation Temperatures					
		Martensitic phase		Rhombohedral phase		Austenitic phase	
		Start temp	Finish temp	Start temp	Finish temp	Start temp	Finish temp
		$M_s$	$M_f$	$R_s$	$R_f$	$A_s$	$A_f$
		°C	°C	°C	°C	°C	°C
(1)	(2)	(3)	(4)	(5)	(6)	(7)	(8)
1	300	47	16	-	-	23	48
2	350	44	33	17	37	38	53
3	400	43	35	21	29	37	46
4	450	32	27	18	24	37	43

It can be observed from figure 4.22 and table 4.7 that when Nickel Titanium alloy is subjected to low temperature annealing heat-treatment at 300°C, the specimens show a single-stage transformation from austenite phase to martensite phase in the cooling cycle and transform back to austenite in the heating cycle. The transformation temperatures for start and finish of martensite phase i.e.,  $M_s$  and  $M_f$  have been found to be 47°C and 16°C, respectively. Similarly, the transformational temperatures for start and finish of Austenite phase i.e.  $A_s$  and  $A_f$  has been found to be 23°C and 48°C. This observation indicates that at room temperature, both Austenite phase and Martensite phase are present in the alloy. This observation of DSC tests confirms the results of X-ray diffraction studies presented and discussed in the previous section.

It can be observed from figure 4.23 and table 4.7 that when Nickel Titanium alloy is subjected to low temperature annealing heat-treatment at 350°C, the specimens show a single-stage transformation from austenite phase to martensite phase in the cooling cycle and a two-stage transformation from martensite phase to rhombohedral phase and rhombohedral phase to austenite phase in the heating cycle. The transformation

temperatures for start and finish of Martensite phase i.e.  $M_s$  and  $M_f$  have been found to be 44°C and 33°C, respectively. Similarly, the transformational temperatures for start and finish of Rhombohedral phase i.e.  $R_s$  and  $R_f$  has been found to be 17°C and 37°C. This Rhombohedral phase transformation has been followed by transformation into Austenite phase. The transformational temperatures for start and finish of Austenite phase i.e.  $A_s$  and  $A_f$  has been found to be 38°C and 53°C. This observation indicates that at room temperature, Martensite phase, Austenite phase and Rhombohedral phase are present in the alloy. This observation of DSC tests confirms the results of X-ray diffraction studies presented and discussed in the previous section.

It can be observed from figure 4.24 and table 4.7 that when Nickel Titanium alloy is subjected to low temperature annealing heat-treatment at 400°C, the specimens show a single-stage transformation from austenite phase to martensite phase in the cooling cycle and a two-stage transformation from martensite phase to rhombohedral phase and rhombohedral phase to austenite phase in the heating cycle. The transformation temperatures for start and finish of Martensite phase i.e.  $M_s$  and  $M_f$  have been found to be 43°C and 38°C, respectively. Similarly, the transformational temperatures for start and finish of Rhombohedral phase i.e.  $R_s$  and  $R_f$  has been found to be 21°C and 29°C. This Rhombohedral phase transformation has been followed by transformation into Austenite phase. The transformational temperatures for start and finish of Austenite phase i.e.  $A_s$  and  $A_f$  has been found to be 40°C and 44°C. This observation indicates that at room temperature, Martensite phase, Austenite phase and Rhombohedral phase are present in the alloy. This observation of DSC tests confirms the results of X-ray diffraction studies presented and discussed in the previous section.

It can be observed from figure 4.25 and table 4.7 that when Nickel Titanium alloy is subjected to low temperature annealing heat-treatment at 450°C, the specimens show a single-stage transformation from austenite phase to martensite phase in the cooling cycle and a two-stage transformation from martensite phase to rhombohedral phase and rhombohedral phase to austenite phase in the heating cycle. The transformation temperatures for start and finish of Martensite phase i.e.  $M_s$  and  $M_f$  have been found to be 32°C and 27°C, respectively. Similarly, the transformational temperatures for start and finish of Rhombohedral phase i.e.  $R_s$  and  $R_f$  has been found to be 18°C and 36°C.

This Rhombohedral phase transformation has been followed by transformation into Austenite phase. The transformational temperatures for start and finish of Austenite phase i.e.  $A_s$  and  $A_f$  has been found to be 37°C and 43°C. This observation indicates that at room temperature, Martensite phase, Austenite phase and Rhombohedral phase are present in the alloy. This observation of DSC tests confirms the results of X-ray diffraction studies presented and discussed in the previous section.

The above discussion indicates that within the scope of the investigation, when the NiTi alloy has been subjected to low temperature annealing heat treatment, as the annealing heat treatment temperature is increased, the presence of Rhombohedral phase has been observed at 350°C and 400°C. With further increase in the annealing temperature to 450°C, there has been a marginal presence of Rhombohedral phase. In addition, the intensity of the Rhombohedral phase appears to decrease with increase in heat treatment temperature from 350°C to 400°C.

Table 4.8 Phase Transformation temperature range for 50% Nickel - 50% Titanium alloy when subjected to low temperature annealing heat-treatment at different temperatures

S No	Temperature at which low temperature annealing heat- treatment has been carried out °C	Phase Transformation Temperature Range		
		Martensitic phase	Rhombohedral phase	Austenitic phase
		Start temp - Finish temp [( $M_s$ - $M_f$ )] °C	Start temp - Finish temp [( $R_f$ - $R_s$ )] °C	Start temp- Finish temp [( $A_f$ - $A_s$ )] °C
(1)	(2)	(3)	(4)	(5)
1	300	31	-	25
2	350	11	20	15
3	400	8	8	9
4	450	5	6	6

The Phase Transformation temperature range for 50% Nickel and 50% Titanium alloy when subjected to low temperature annealing heat-treatment at different temperatures keeping the heat-treatment duration constant at one-hour has been presented in table 4.8. From this table, it can be observed that as the annealing heat-treatment temperature is increased from 300°C to 450°C, the martensite phase transformation temperature range i.e. the difference in start temperature and finish temperature of martensitic phase has been found to decrease from 31°C to 5°C. On similar lines, as the annealing heat-treatment temperature is increased from 300°C to 450°C, the austenite phase transformation temperature range i.e. the difference in start temperature and finish temperature of austenite phase has been found to decrease from 25°C to 6°C. However, no rhombohedral phase was observed when the NiTi alloy is subjected to low temperature heat-treatment at 300°C. But, as the annealing heat-treatment temperature is increased from 350°C to 450°C, the rhombohedral phase transformation temperature range i.e. the difference in start temperature and finish temperature of rhombohedral phase has been found to decrease from 20°C to 6°C.

The above discussion indicates that phase transformation temperature range for 50% Nickel and 50% Titanium alloy when subjected to low temperature annealing heat-treatment at different temperatures, within the scope of this investigation, as the annealing temperature is increased there has been a decrease in the range of phase transformation temperature. This trend has been found true in all the three phases namely martensite phase, rhombohedral phase and austenite phase observed in this investigation.

When trend of results obtained in this investigation has been compared with the trend of results reported by early investigators namely (Krzysztof Kus et al. 2010), it can be found that the trend of DSC test results obtained in this investigation is similar to the trend of observations made by earlier investigators.

The literature survey (Lekston et al. 2010) indicates that the existence of multiple phases has been observed in Nickel Titanium alloys when subjected to heat-treatment. The trends of results observed in this investigation have been found to be similar to the trend of results observed by earlier investigators.

## 4.5 Mechanical Properties

The as-received alloy is further analyzed for mechanical properties to ascertain Superelastic nature so as to be rendered suitable for many applications. The tension test is carried out as per ASTM E8 on PC-2000 tensometer to analyze the yield and ultimate strength of the material so that the tensile curve will indicate the presence or absence of pseudoelasticity.

### 4.5.1 Ultimate tensile strength

The variation of the Ultimate tensile strength (UTS) of NiTi alloy at different temperatures and heat-treatment for different duration is presented in table 4.9.

Table 4.9 Stress and strain values of heat-treated NiTi alloy during the assessment

Heat-treatment temperature (°C)		Heat treatment duration (mins)			
		15	30	45	60
300	UTS (MPa)	1252	1258	1263	1275
350		1380	1395	1387	1378
400		1278	1287	1293	1305
450		1256	1263	1262	1258

The variation of the UTS for the 300°C heat-treated sample was found to follow a trend such that upon an increase of the heat-treatment time from 15 minutes to 60 minutes, the UTS was observed to go up from 1252MPa to 1275 MPa. In the case of 350°C heat-treated sample, the UTS was found to increase from 1380 to 1395 MPa upon increase of the heat-treatment duration from 15 to 30 minutes. Upon further increase of the heat-treatment duration at the same temperature, the UTS was found to reduce from 1395 MPa to 1378 MPa. For the sample heat-treated at 400°C, the UTS appears to go up at a steady rate from 1278MPa and 1305MPa, when the heat-treatment duration is increased from 15 minutes to 60 minutes. Similarly, the sample heat-treated at 450°C, the UTS is observed to increase from 1256MPa at the heat-treatment time duration of 15 minutes to maximum of 1263MPa at the heat-treatment duration of 30 minutes. A further

increase in the duration of heat-treatment is seen to lower the UTS of the sample. From above results, it appears that within the scope of investigation low temperature annealing heat-treatment for a duration of 60 minutes exhibit superior mechanical properties.

The tensile curve for nickel-titanium alloy subjected to low temperature annealing heat-treatment, at different temperatures, keeping the heat-treatment duration constant at one-hour have been presented in figures 4.26 to 4.29. The tensile curve for Nickel-Titanium alloy subjected to low temperature annealing treatment at 300°C has been presented in figure 4.26.

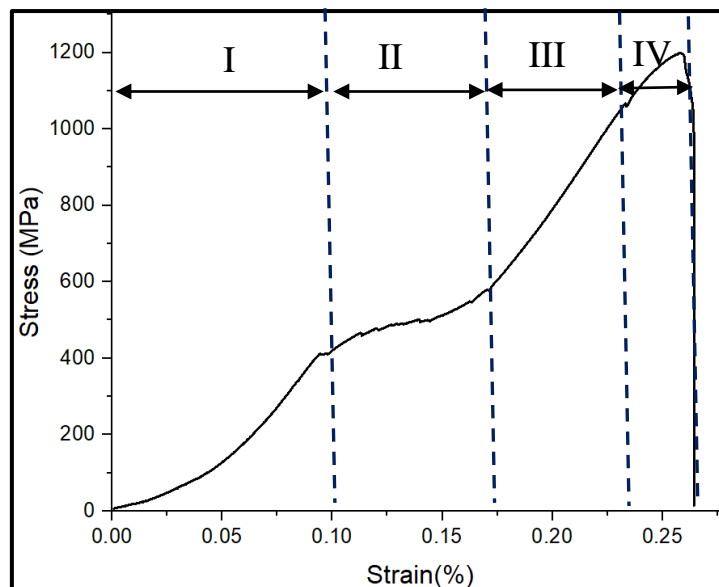


Figure 4.26 Tensile Curve of 50% Nickel - 50% Titanium alloy subjected to low temperature annealing heat treatment at 300°C

It can be observed that there are four distinct regions in the tensile curve. The region I refers to the elastic deformation of the austenitic phase, region II refers to the transformation of austenite to the martensite phase, region III refers to elastic deformation of martensite and region IV refers to plastic deformation of the martensitic phase. Similarly, the tensile curves of the NiTi alloy heat-treated at temperatures of 350, 400 and 450°C samples as illustrated in figures 4.27 – 4.29 show similar behavior as the 300°C sample.

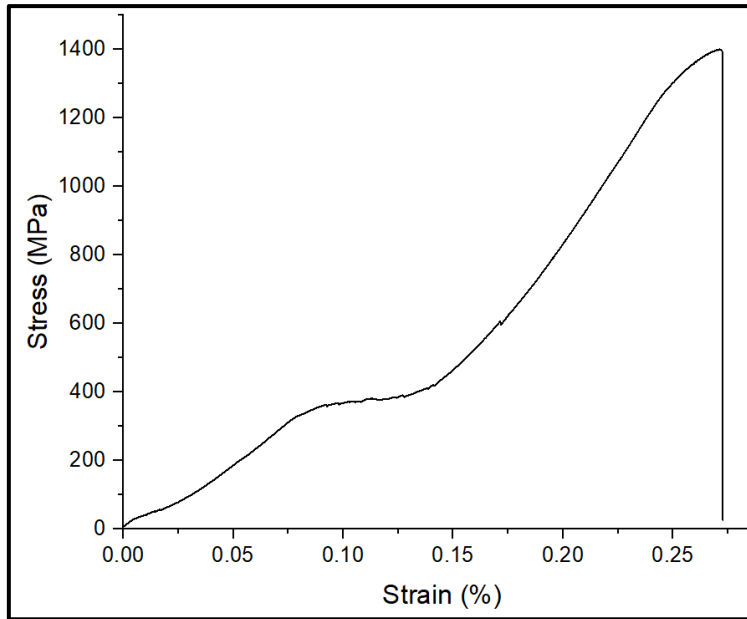


Figure 4.27 Tensile Curve of 50% Nickel - 50% Titanium alloy subjected to low temperature annealing heat treatment at 350°C

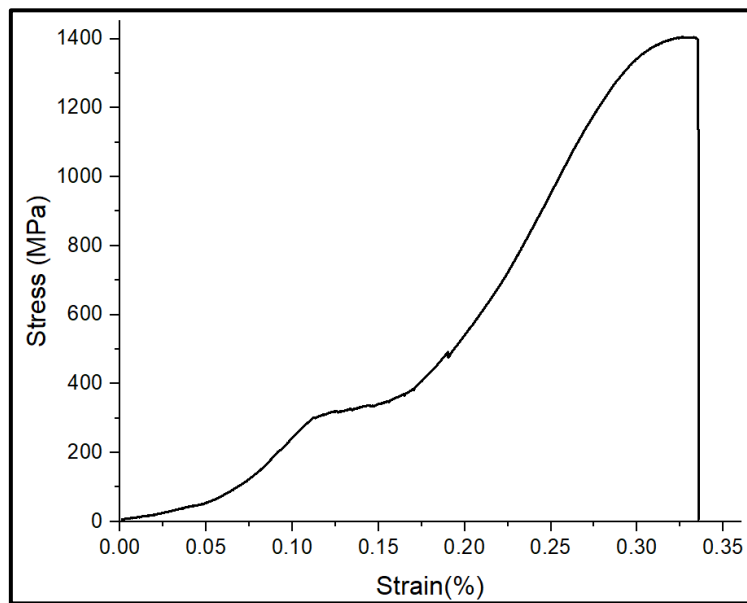


Figure 4.28 Tensile Curve of 50% Nickel - 50% Titanium alloy subjected to low temperature annealing heat treatment at 400°C

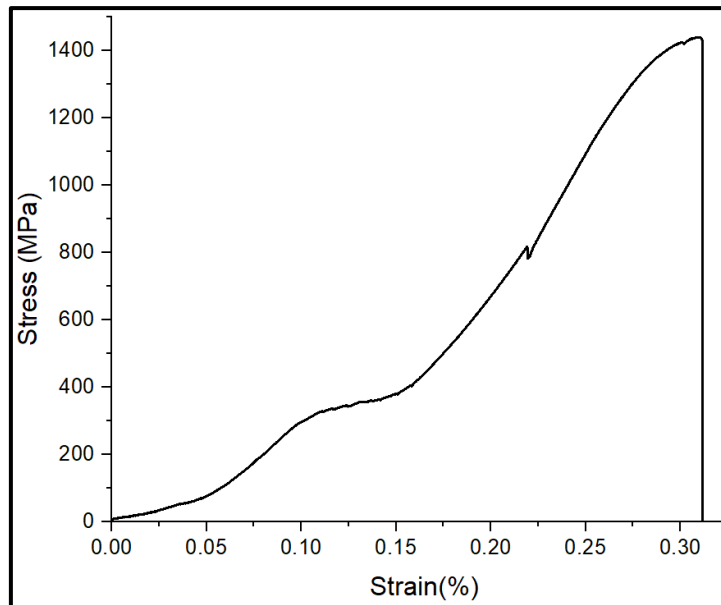


Figure 4.29 Tensile Curve of 50% Nickel - 50% Titanium alloy subjected to low temperature annealing heat treatment at 450°C

From the tensile curves of the heat-treatment samples, it has been seen that the 350°C heat-treated sample exhibits superior mechanical properties in terms of toughness. The fractograph of the 50% Nickel – 50% Titanium alloy heat-treated at 300°C for a duration of one-hour when observed under SEM at a magnification of 5000X has been presented in figure 4.30.

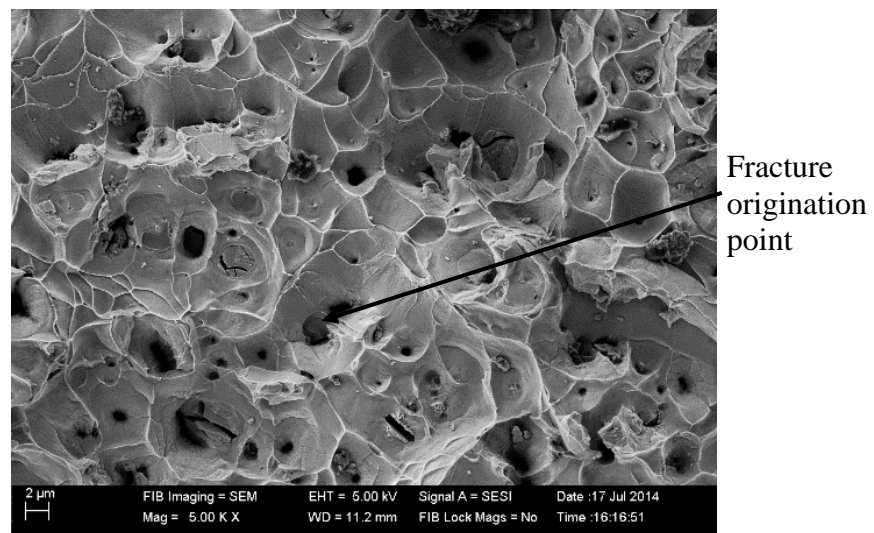


Figure 4.30 Fractograph of 300°C heat-treated NiTi alloy when observed under SEM at a magnification of 5000X



It can be observed from figure 4.30 that the nature of fracture of the material appears as transgranular indicating that the material may be ductile in nature. The fracture might have originated at the central point as indicated in fig 4.30 and progressed till the end of the cross-section. The fractograph of the 50% Nickel – 50% Titanium alloy heat-treated at 350°C for a duration of one-hour when observed under SEM at a magnification of 5000X has been presented in figure 4.31.

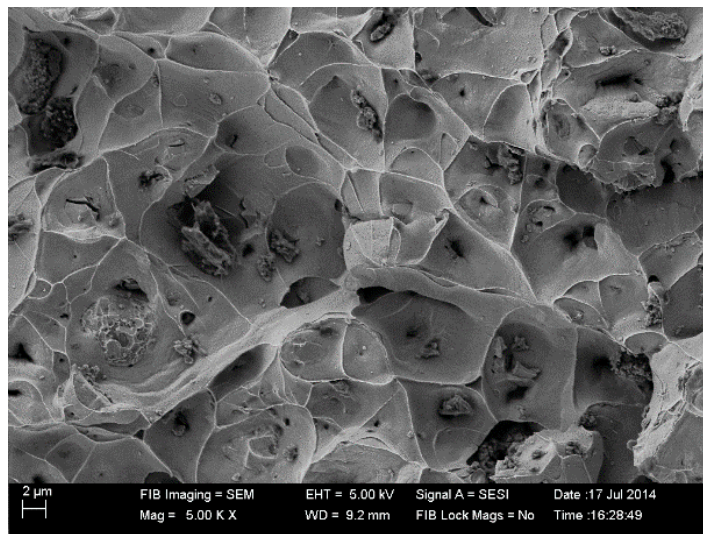


Figure 4.31 Fractograph of 350°C heat-treated NiTi alloy when observed under SEM at a magnification of 5000X

It can be observed from figure 4.31 that the nature of fracture of the material appears as a transgranular fracture indicating that the material may be ductile in nature. The grains seen under SEM appear to have enlarged size as compared to figure 4.30. Also, there are fewer grains observed for the fractured specimen indicating a smoother fractured surface. This might indicate the ductility and toughness of the material to be higher than that of 300°C heat-treated sample.

The fractograph of the 50% Nickel – 50% Titanium alloy heat-treated at 400°C for a duration of one-hour when observed under SEM at a magnification of 5000X has been presented in figure 4.32.

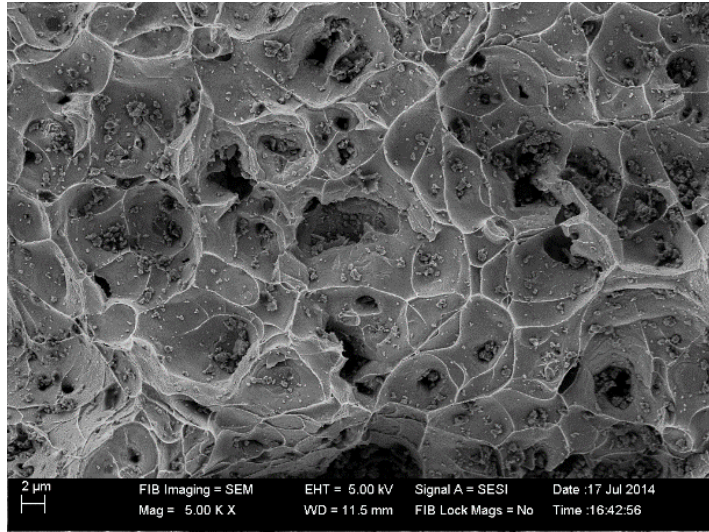


Figure 4.32 Fractograph of 400°C heat-treated NiTi alloy when observed under SEM at a magnification of 5000X

It can be observed from figure 4.32 that the nature of fracture of the material appears as a transgranular fracture indicating that the material may be ductile in nature. The fractured surface appears to be uneven i.e. the grains are of varied sizes. This may indicate that the ductility of the material has reduced marginally owing to a slight high temperature in the heat-treatment.

The fractograph of the 50% Nickel – 50% Titanium alloy heat-treated at 450°C for a duration of one-hour when observed under SEM at a magnification of 5000X has been presented in figure 4.33.

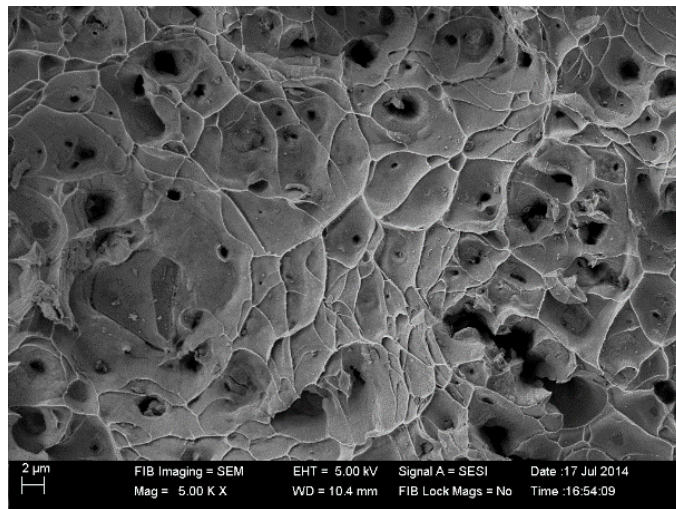


Figure 4.33 Fractograph of 450°C heat-treated NiTi alloy when observed under SEM at a magnification of 5000X

It can be observed from figure 4.33 that the nature of fracture of the material appears as a transgranular fracture indicating that the material may be ductile in nature. The fractured surface observed under SEM appears to be further uneven stating that the fracture may not be uniform throughout the cross-section of the material. This could attribute to further increase in the heat-treatment temperature rendering the sample to be less ductile compared to the 400°C sample. The fractograph shows a transition between grains of smaller size on the left to grains of marginal bigger sizes to the right of the picture.

Vojtech et al. (2010) have studied the behavior of heat-treated Nickel-Titanium alloys. They have reported that the heat-treatment temperature range of 410 – 460°C yields a strengthening in the Nickel-Titanium wire sample. An increase in the heat-treatment temperatures had resulted in lowering of the UTS of the sample. The annealing time of 2 minutes was found to reduce the strength in the sample whereas higher annealing time duration was found to increase the strength of the sample.

The trend of variation of UTS with the variation of temperature and time of heat-treatment found in the present investigation appears to be similar to the trend of variation of UTS with the variation of temperature of heat-treatment reported by earlier investigators for Nickel-Titanium alloy of different composition.

#### **4.5.2 Hardness**

As mentioned in earlier section, the assessment of hardness has been made in the form of Vickers Hardness number. The average representative values of Vickers Pyramid Number (VPN) of 50%Nickel and 50%Titanium alloy heat-treated at different temperatures for a duration of one-hour has been presented in table 4.10. It can be observed from table 4.10 that VPN value of NiTi alloy subjected to low temperature annealing heat treatment at 300°C has been found to be 438 VPN. When the same alloy has been subjected to low temperature annealing heat treatment at 350°C, the hardness has increased to 482 VPN. Whereas when the NiTi alloy has been subjected to a low temperature annealing heat treatment at 400°C, the hardness has decreased to 427 VPN. With further increase in the low temperature annealing heat-treatment to 450°C, the hardness value has further decreased to 365 VPN.

Table 4.10 Hardness of heat-treated 50% Nickel - 50% Titanium when subjected to low temperature annealing heat-treatment at different temperatures

S No	Heat Treatment Specification		Hardness VHN
	Temperature (°C)	Duration (Hours)	
(1)	(2)	(3)	(4)
1	300	1	438
2	350	1	482
3	400	1	427
4	450	1	365

The VHN value of NiTi alloy annealed at 450°C is found to be 365 VHN. Similar to the 400°C heat-treated sample, the trend of the hardness value is observed to be inverse of 300°C and 350°C annealed samples. A further increase in the heat-treatment temperature to 450°C might make the grains grow bigger compared to the 400°C heat-treated sample, with recrystallization taking in the sample. Also, it could be the grain growth taking place at an elevated annealing temperature to have further reduced the hardness.

As discussed in section 4.2.1, when the test specimens of NiTi alloy subjected to low temperature annealing heat treatment at 350°C has been compared with that of at 300°C, it appears that the grain size of NiTi alloy has relatively increased. This increase in grain size may have contributed for increased hardness of the NiTi alloy when subjected to low temperature annealing heat-treatment at 350°C compared with that of at 300°C. Published information (Dieter et al. 1961) indicates that when recrystallization occurs after heat-treatment, the metal softens resulting in lower hardness. Dieter et al. (1961) mentions that recrystallization is replacing the grains in the cold-worked material with a different set of grains that are in the strain-free condition. The literature (Byrne et al. 1965) mentions that the nuclei of the grains that are strain free grow with time and the new grains replace the grains in the matrix that was cold worked. Thus, the hardness in the material gets reduced due to the phenomenon of recrystallization. In the present investigation, when NiTi alloy is subjected to low temperature annealing heat-treatment

at 400°C and 450°C, recrystallization might have taken place resulting in softening of metal and reduced hardness as compared to that of 350°C.

### 4.5.3 Tribological Characteristics

The abrasive wear loss of 50% Nickel - 50% Titanium alloy subjected to low temperature annealing heat-treatment at different temperatures for a duration of one-hour has been presented in table 4.11 to table 4.14 for the sake of clarity, the values in the table have been presented in the form of graph in the figures 4.34 to 4.38.

From table 4.11 and fig 4.34, it can be observed that within the scope of the investigation, when the load is increased from 5N to 15N, the wear mass loss rate is relatively at a higher rate. With further increase in the load from 15N to 25N and 25N to 35N, the wear mass loss rate is relatively low and from 35N to 45N the wear loss rate appears to be relatively still at a lower rate.

Table 4.11 Abrasive Wear characteristics of 50% Nickel - 50% Titanium alloy subjected to low temperature annealing heat-treatment at 300°C for one hour

<b>S No</b>	<b>Load (P) N</b>	<b>Wear Mass Loss, mg</b>
(1)	(2)	(3)
1	5	3.9
2	15	4.8
3	25	5.5
4	35	5.9
5	45	6.1

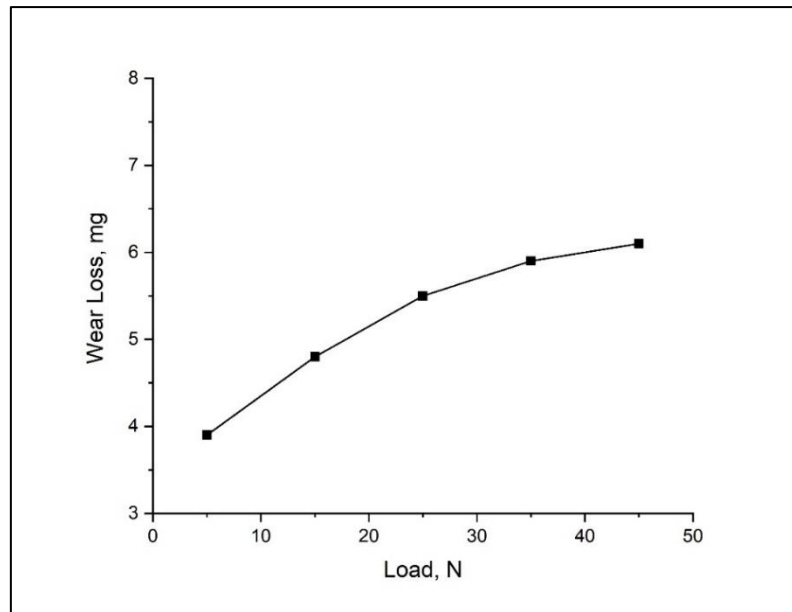


Figure 4.34 Abrasive Wear characteristics of 50% Nickel - 50% Titanium alloy subjected to low temperature annealing heat-treatment at 300°C for one hour

Table 4.12 Abrasive Wear characteristics of 50% Nickel - 50% Titanium alloy subjected to low temperature annealing heat-treatment at 350°C for one hour

<b>S No</b>	<b>Load (P) N</b>	<b>Wear Mass Loss, mg</b>
(1)	(2)	(3)
1	5	3.04
2	15	3.8
3	25	4.5
4	35	4.9
5	45	5

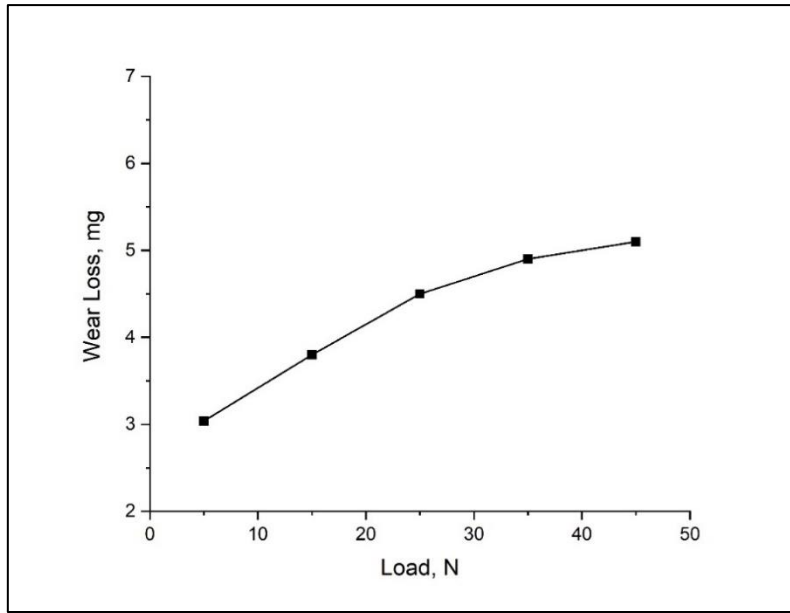


Figure 4.35 Abrasive Wear characteristics of 50% Nickel - 50% Titanium alloy subjected to low temperature annealing heat-treatment at 350°C for one hour

Table 4.13 Abrasive Wear characteristics of 50% Nickel - 50% Titanium alloy subjected to low temperature annealing heat-treatment at 400°C for one hour

<b>S No</b>	<b>Load (P) N</b>	<b>Wear Mass Loss, mg</b>
(1)	(2)	(3)
1	5	4
2	15	4.9
3	25	5.4
4	35	5.7
5	45	5.9

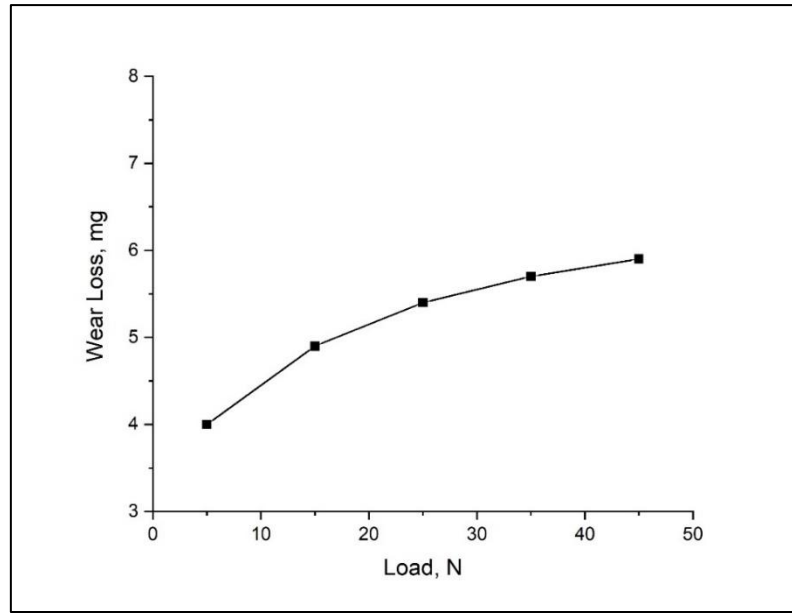


Figure 4.36 Abrasive Wear characteristics of 50% Nickel - 50% Titanium alloy subjected to low temperature annealing heat-treatment at 400°C for one hour

Table 4.14 Abrasive Wear characteristics of 50% Nickel - 50% Titanium alloy subjected to low temperature annealing heat-treatment at 450°C for one hour

<b>S No</b>	<b>Load (P) N</b>	<b>Wear Mass Loss, mg</b>
(1)	(2)	(3)
1	5	3.8
2	15	4.6
3	25	5.1
4	35	5.4
5	45	5.6



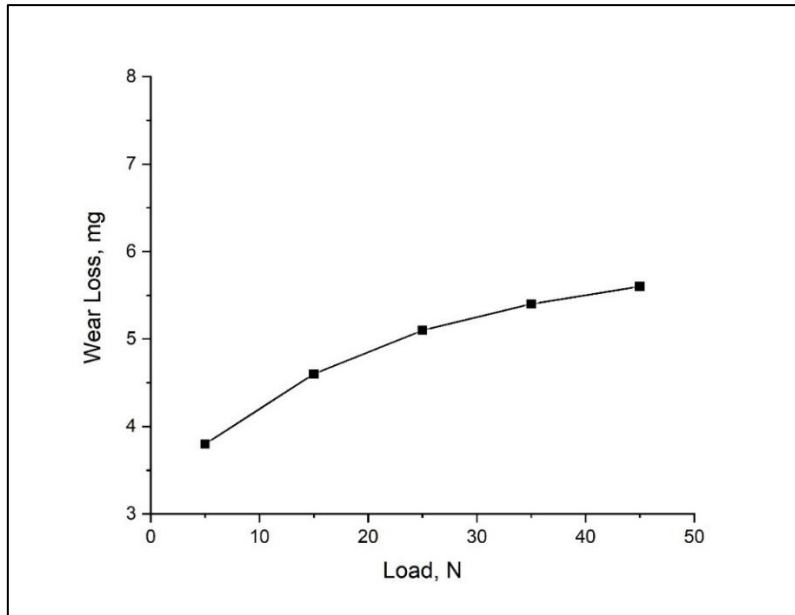


Figure 4.37 Abrasive Wear characteristics of 50% Nickel - 50% Titanium alloy subjected to low temperature annealing heat-treatment at 450°C for one hour

The trend of variation of wear loss rate with respect to the variation of load observed in 50%Nickel – 50%Titanium alloy subjected to low temperature annealing heat-treatment at 350°C, 400°C and 450°C appears to be similar to the trend of variation of wear loss rate with respect to the variation of load observed in the alloy subjected to low temperature annealing heat-treatment at 300°C. However, when the wear loss rate at different annealing temperatures for a particular load have been compared, it has been found that the wear loss was lowest when annealing temperature was 350°C. This has been found true at all load levels investigated within the scope of this study. However, literature (Aliasgarian et al. 2011) made a study on the wear resistance of Ni-rich NiTi alloys by subjecting them to a high temperature annealing treatment. It was found that the wear of the samples annealed at temperatures as low as 400°C showed reduced wear rate upon an increase in the axial load. However, according to (R. Aliasgarian et al. 2011), the wear of samples increased to a higher value when heat-treated at 700°C. This confirms with our study on the heat-treated 50%Nickel-50%Titanium alloy annealed at 400°C within the scope of investigation showing lower wear rates. Zhiqiang S et al. (2005) mentions the superior wear behavior of Aluminum alloys when subjected to wear under Silicon Carbide particles.

The worn surface of 50% Nickel – 50% Titanium alloy subjected to low temperature annealing heat-treatment temperatures for a duration of one-hour at a typical test load of 15N at magnification of 2000X and 5000X have been presented in figures 4.38 to 4.41. The wear micrograph of the 300°C annealed sample is presented in figure 4.38.

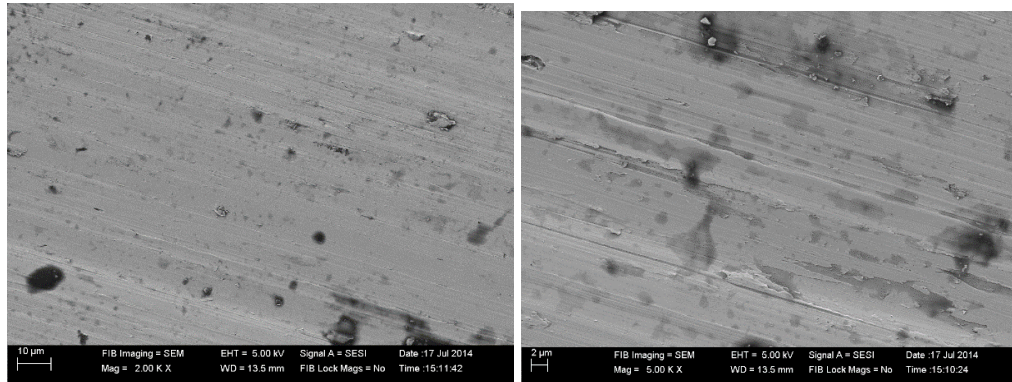


Figure 4.38 Worn surface of 50% Nickel - 50% Titanium heat-treated at 300°C at 2000 and 5000 when observed under Scanning Electron Microscope

From figure 4.38, it can be observed that material is getting worn by the Alumina wheel. It appears that the debris are formed on the worn surface of the NiTi alloy, which contain a major portion of NiTi alloy in the form of small chips with a small percentage of Alumina ( $Al_2O_3$ ) material from the disc. These debris are generated as a result of one surface penetrating the other. The wear debris particles protrude from the harder surface to the softer surface depending on their size and this in turn could lead to an increase in the wear of the material. A careful analysis of the wear debris is needed to assess its effect on the wear of the material. The size of the wear debris is directly proportional to the size of the particles in the abrading medium. If the size of the debris is too large, there is a possibility of component failure. The debris are found to be more prominent in 5000X magnification as compared to that of in 2000X magnification. Thus, it can be inferred that the wear mechanism of heat-treated NiTi alloy when subjected to the abrasive wear test appears to be micro-cutting and ploughing in nature similar to the phenomenon as observed in the NiTi as-received sample.

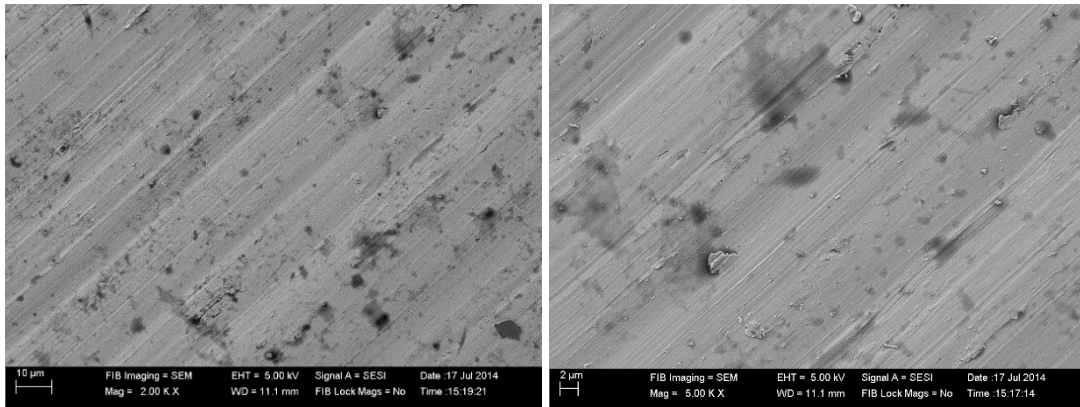


Figure 4.39 Worn surface of 50% Nickel - 50% Titanium heat-treated at 350°C at 2000 and 5000 when observed under Scanning Electron Microscope

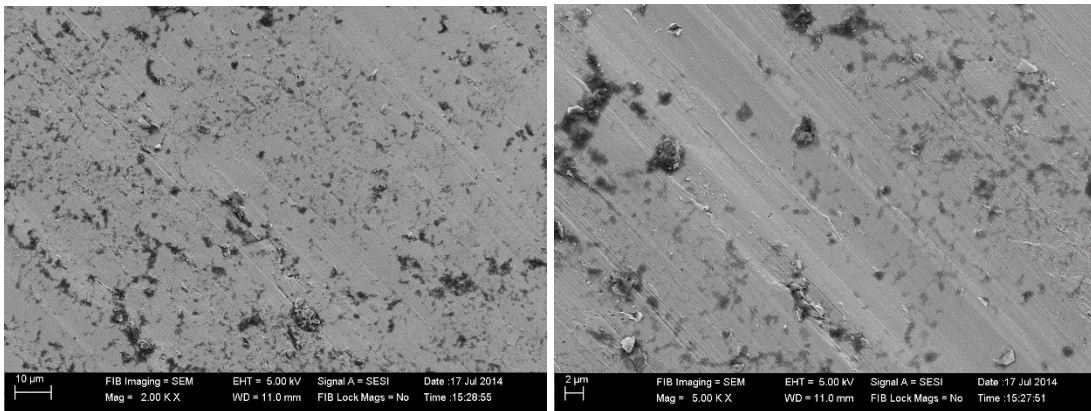


Figure 4.40 Worn surface of 50% Nickel - 50% Titanium heat-treated at 400°C at 2000 and 5000 when observed under Scanning Electron Microscope

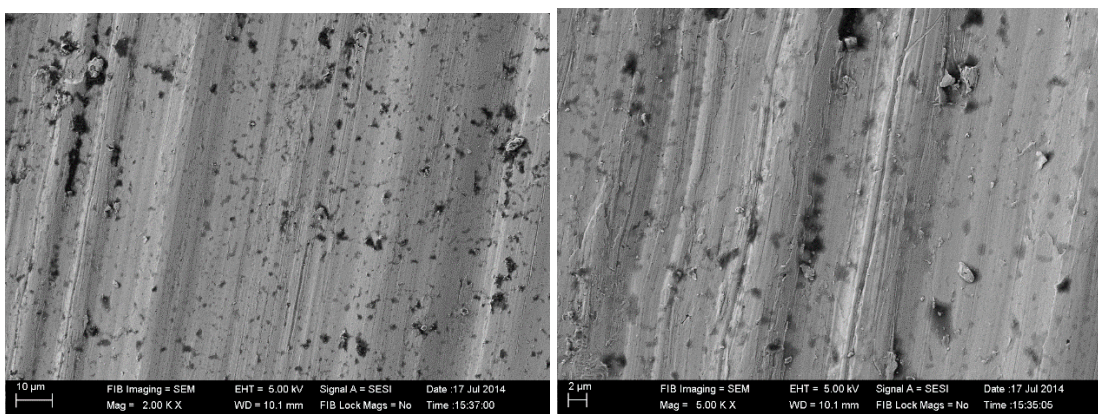


Figure 4.41 Worn surface of 50% Nickel - 50% Titanium heat-treated at 450°C at 2000 and 5000 when observed under Scanning Electron Microscope

When the worn surfaces of NiTi alloy subjected to low annealing heat-treatment at 350°C, 400°C and 450°C presented in figures 4.39 to 4.41 have been observed, it appears that the wear mechanism is predominantly due to micro-cutting and ploughing in nature. This has been found true at all annealing heat-treatment temperatures studied.

When the worn surfaces of NiTi alloy subjected to low annealing heat-treatment at 300°C, 350°C, 400°C and 450°C presented in figures 4.38 to 4.41 have been compared, it appears that in case of worn surfaces subjected to low annealing heat-treatment at 350°C, the groove marks are seen to be shallower compared to the groove marks at remaining all temperatures namely 300°C on lower side and 400°C and 450°C on higher side. This indicates that the NiTi alloy exhibits increased wear resistance when subjected to low temperature annealing heat-treatment at 350°C. As presented in section 4.2.5, the hardness of test specimens of NiTi alloy subjected to low temperature annealing heat treatment at 350°C has been found to be highest than hardness of test specimens heat-treated at remaining three temperatures namely 300°C on the lower side and 400°C, 450°C on the higher side. In this section, it has been found that in case of the worn surfaces subjected to low annealing heat-treatment at 350°C, the groove marks seem to be shallower compared to the groove marks at remaining all temperatures. This indicates that there exists a correlation between the hardness of the material and the tribological characteristics of the material. In this research work, it has been found that within the scope of the investigation, the NiTi alloy subjected to low temperature annealing heat-treatment at 350°C has exhibited superior hardness and consequently superior wear resistance property.

#### **4.6 Superelastic Behaviour**

As explained earlier, the stress-strain curves for 50% Nickel - 50% Titanium alloy samples subjected to low temperature annealing heat treatment at different temperatures for a duration of one-hour have been determined for different levels of predetermined strain values and have been presented in figures 4.42 - 4.53.

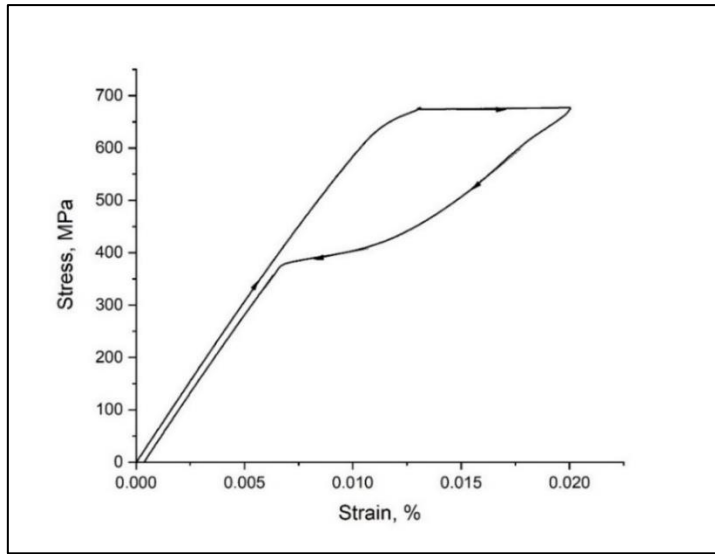


Figure 4.42 Stress versus strain graph for 50% Nickel - 50% Titanium alloy subjected to low temperature annealing heat treatment at 300°C at 2% pre-determined strain level during loading and release of load

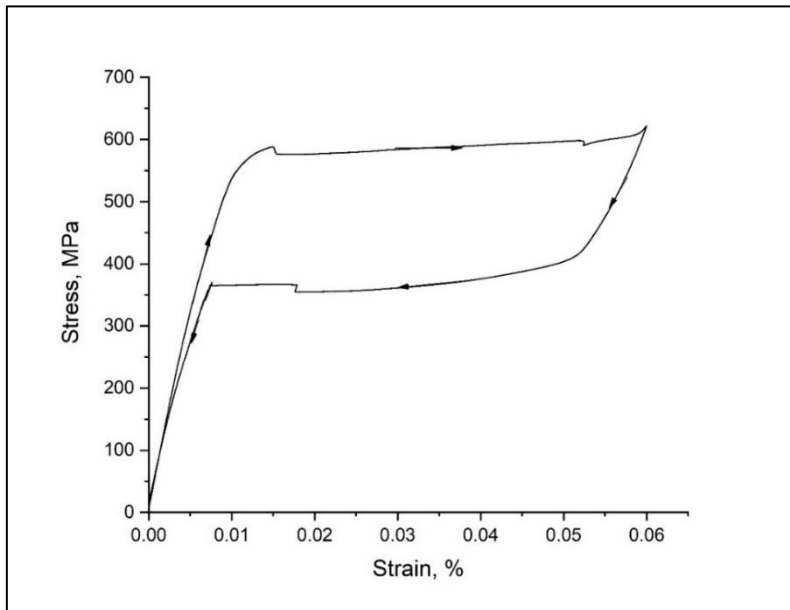


Figure 4.43 Stress versus strain graph for 50% Nickel - 50% Titanium alloy subjected to low temperature annealing heat treatment at 300°C at 6% pre-determined strain level during loading and release of load

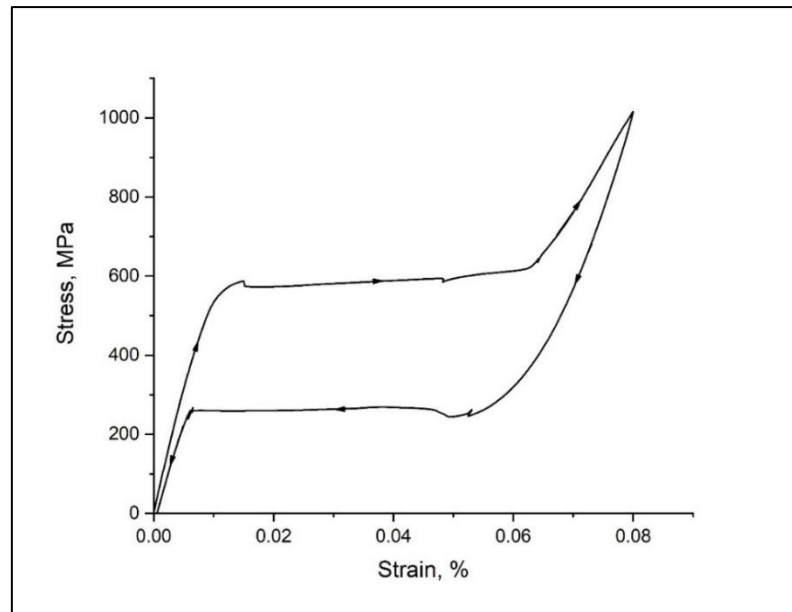


Figure 4.44 Stress versus strain graph for 50% Nickel - 50% Titanium alloy subjected to low temperature annealing heat treatment at 300°C at 8% pre-determined strain level during loading and release of load

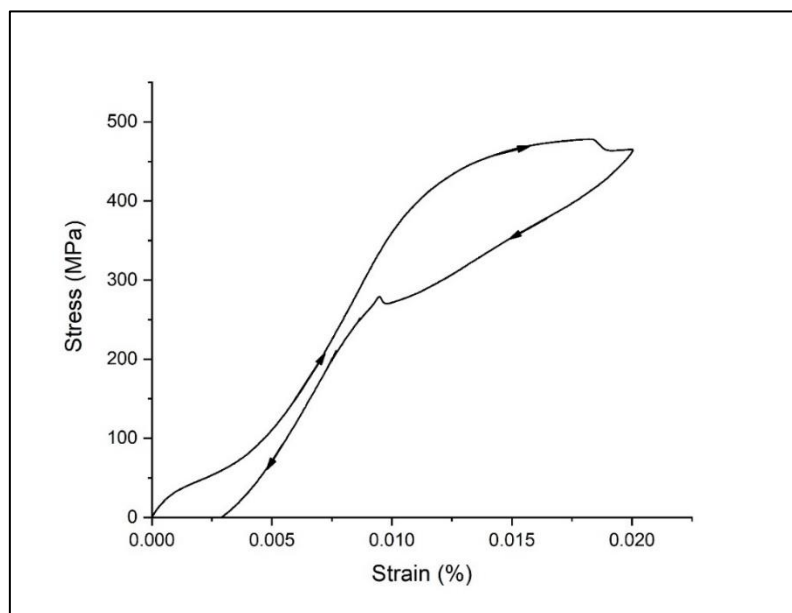


Figure 4.45 Stress versus strain graph for 50% Nickel - 50% Titanium alloy subjected to low temperature annealing heat treatment at 350°C at 2% pre-determined strain level during loading and release of load

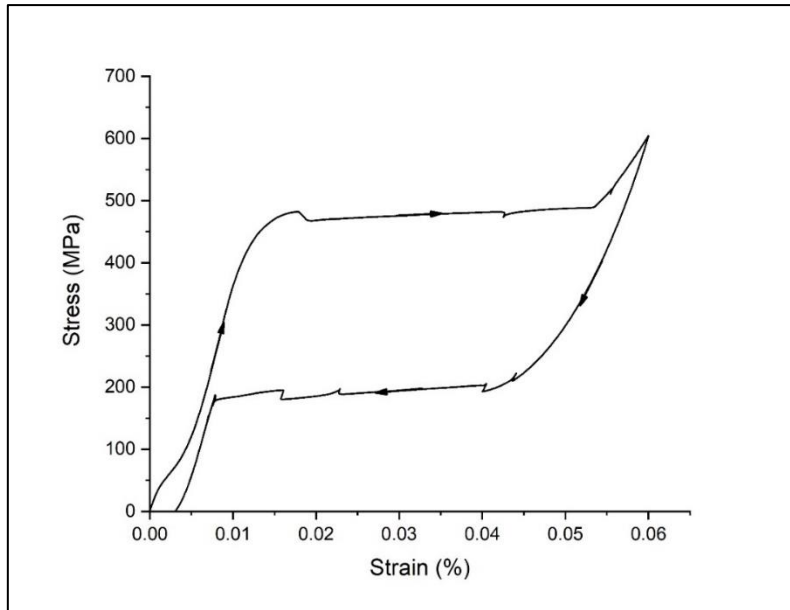


Figure 4.46 Stress versus strain graph for 50% Nickel - 50% Titanium alloy subjected to low temperature annealing heat treatment at 350°C at 6% pre-determined strain level during loading and release of load

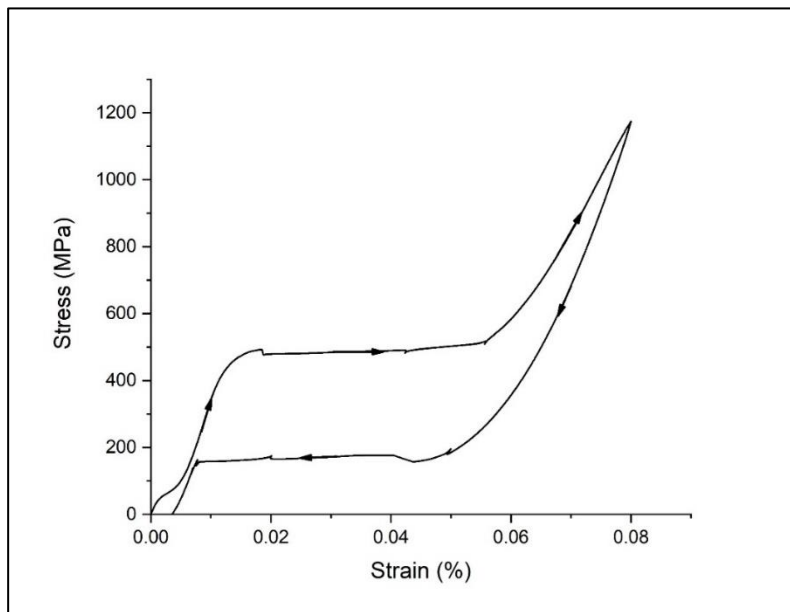


Figure 4.47 Stress versus strain graph for 50% Nickel - 50% Titanium alloy subjected to low temperature annealing heat treatment at 350°C at 8% pre-determined strain level during loading and release of load

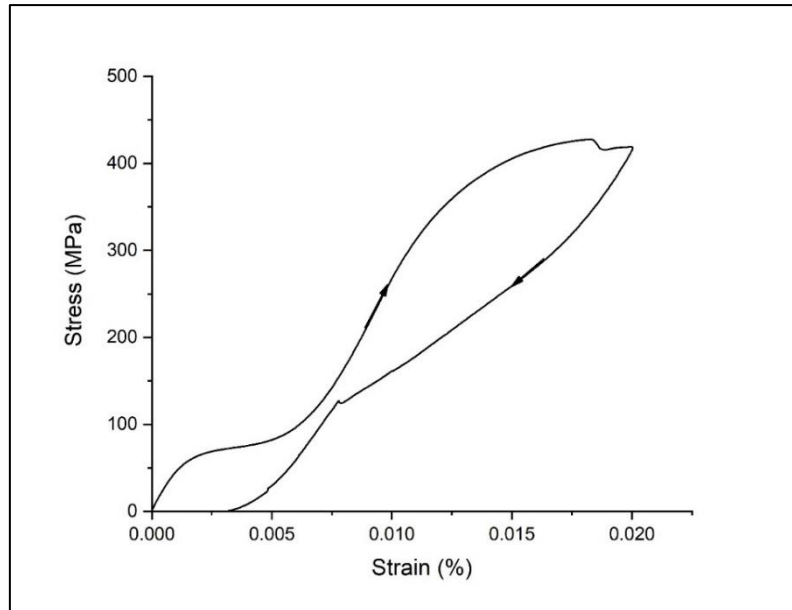


Figure 4.48 Stress versus strain graph for 50% Nickel - 50% Titanium alloy subjected to low temperature annealing heat treatment at 400°C at 2% pre-determined strain level during loading and release of load

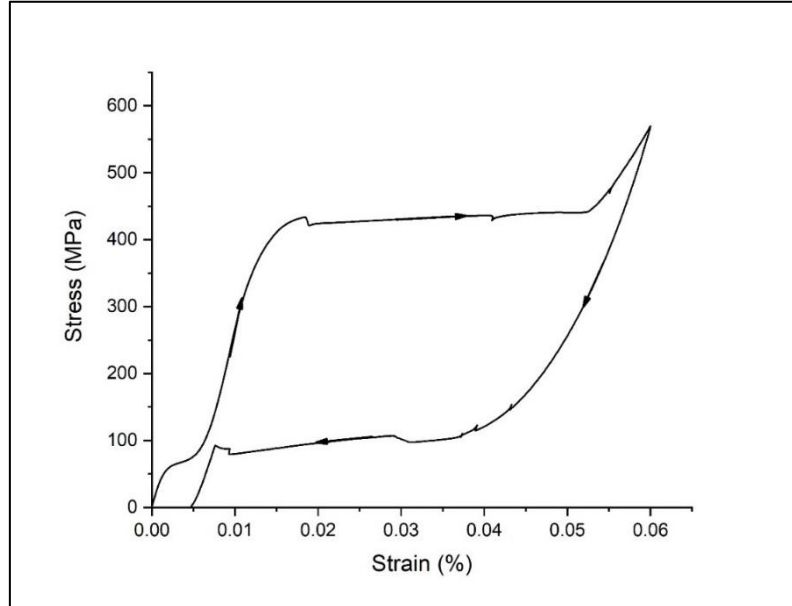


Figure 4.49 Stress versus strain graph for 50% Nickel - 50% Titanium alloy subjected to low temperature annealing heat treatment at 400°C at 6% pre-determined strain level during loading and release of load



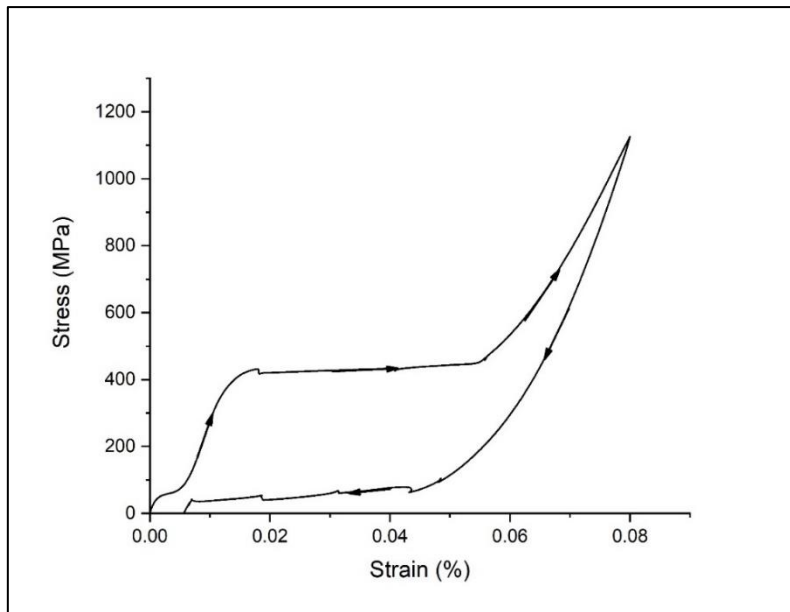


Figure 4.50 Stress versus strain graph for 50% Nickel - 50% Titanium alloy subjected to low temperature annealing heat treatment at 400°C at 8% pre-determined strain level during loading and release of load

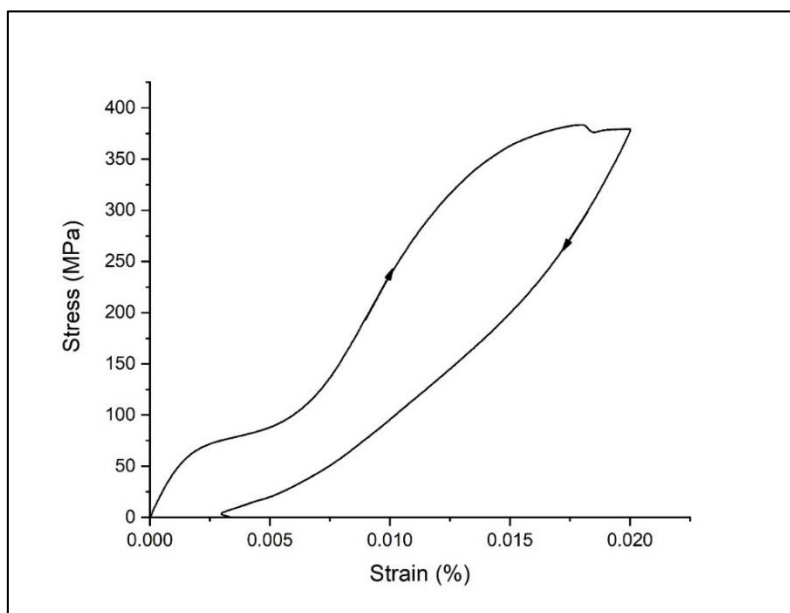


Figure 4.51 Stress versus strain graph for 50% Nickel - 50% Titanium alloy subjected to low temperature annealing heat treatment at 450°C at 2% pre-determined strain level during loading and release of load

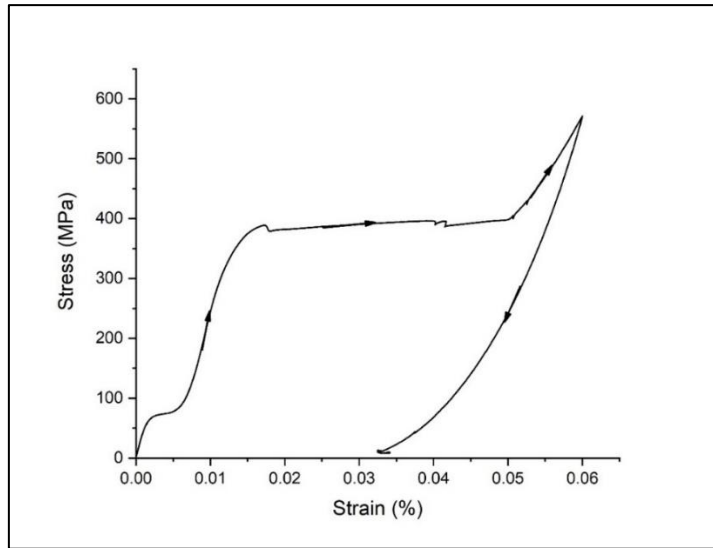


Figure 4.52 Stress versus strain graph for 50% Nickel - 50% Titanium alloy subjected to low temperature annealing heat treatment at 450°C at 6% pre-determined strain level during loading and release of load

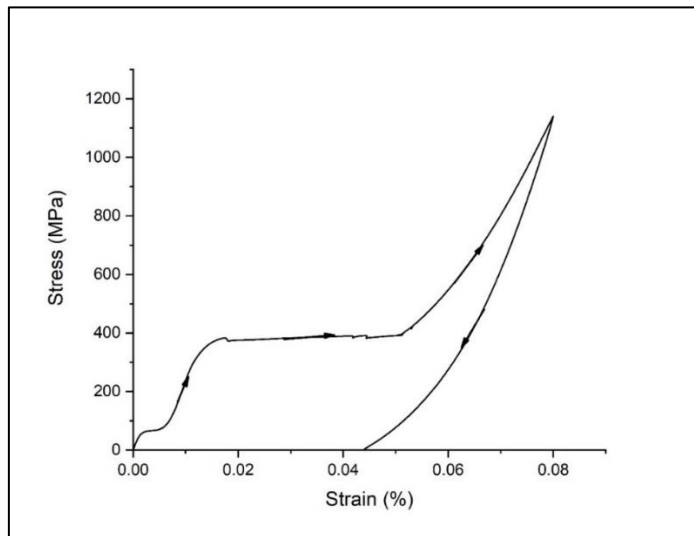


Figure 4.53 Stress versus strain graph for 50% Nickel - 50% Titanium alloy subjected to low temperature annealing heat treatment at 450°C at 8% pre-determined strain level during loading and release of load

It can be observed from figures 4.42 – 4.53 that the material after loading does not break but returns back to the original stress value after release of the load. In other words, the unloading curve follows a hysteresis path compared to loading curve, returning back to the same point. This means that the material after subjecting to low temperature annealing heat temperature at different temperatures and for different levels of

predetermined strain values, is exhibiting superelastic behavior. This trend has been found true at all the predetermined strain levels studied and at all low temperature annealing heat treatment temperatures studied within the scope of this investigation. From the data in figures 4.42 – 4.53, the net energy dissipated by the heat-treated samples annealed at different temperatures for one-hour duration between the loading and unloading cycles is expressed as area enclosed within the loading and unloading curves of stress vs strain diagram at different predetermined strain rates has been computed as explained in the previous chapter and has been presented in table 4.15 to table 4.18.

Table 4.15 Net energy dissipated expressed as area enclosed within loading and unloading curves of stress vs strain diagram for NiTi alloy annealed at 300°C for different pre-determined strain rates

Sl. No	Low temperature annealing heat treatment condition		Pre-determined strain rate %	Net energy dissipated J/cm <sup>3</sup>
	Temperature °C	Duration Hours		
(1)	(2)	(3)	(4)	(5)
1	300	1	2	5.8
2	300	1	6	14.8
3	300	1	8	13.0

Table 4.16 Net energy dissipated expressed as area enclosed within loading and unloading curves of stress vs strain diagram for NiTi alloy annealed at 350°C for different pre-determined strain rates

Sl. No	Low temperature annealing heat treatment condition		Pre-determined strain rate %	Net energy dissipated J/cm <sup>3</sup>
	Temperature °C	Duration Hours		
(1)	(2)	(3)	(4)	(5)
1	350	1	2	6.57
2	350	1	6	17.7
3	350	1	8	13.1

Table 4.17 Net energy dissipated expressed as area enclosed within loading and unloading curves of stress vs strain diagram for NiTi alloy annealed at 400°C for different pre-determined strain rates

Sl. No	Low temperature annealing heat treatment condition		Pre-determined strain rate %	Net energy dissipated J/cm <sup>3</sup>
	Temperature °C	Duration Hours		
(1)	(2)	(3)	(4)	(5)
1	400	1	2	11.3
2	400	1	6	23.5
3	400	1	8	14.6

Table 4. 18 Net energy dissipated expressed as area enclosed within loading and unloading curves of stress vs strain diagram for NiTi alloy annealed at 450°C for different pre-determined strain rates

Sl. No	Low temperature annealing heat treatment condition		Pre-determined strain rate %	Net energy dissipated J/cm <sup>3</sup>
	Temperature °C	Duration Hours		
(1)	(2)	(3)	(4)	(5)
1	450	1	2	12.1
2	450	1	6	25.2
3	450	1	8	20.25

From table 4.15, it can be noticed that the net energy dissipated for 50% Nickel - 50% Titanium alloy subjected to low temperature annealing heat-treatment at 300°C for a duration of one-hour for different predetermined strain rates varies from 5.8 J/cm<sup>3</sup> to 14.8 J/cm<sup>3</sup>. Further, among the different predetermined strain rates studied, the net energy dissipated for the 6% strain rate is maximum.

From table 4.16, it can be found that the net energy dissipated for 50% Nickel - 50% Titanium alloy subjected to low temperature annealing heat-treatment at 350°C for a duration of one-hour for different predetermined strain rates varies from 6.57 J/cm<sup>3</sup> to

17.7 J/cm<sup>3</sup>. Further, among the different predetermined strain rates studied, the net energy dissipated for the 6% strain rate is maximum.

From table 4.17, it can be viewed that the net energy dissipated for 50% Nickel - 50% Titanium alloy subjected to low temperature annealing heat-treatment at 400°C for a duration of one-hour for different predetermined strain rates varies from 11.3 J/cm<sup>3</sup> to 23.5 J/cm<sup>3</sup>. Further, among the different predetermined strain rates studied, the net energy dissipated for the 6% strain rate is maximum.

From table 4.18, it can be observed that the net energy dissipated for 50% Nickel - 50% Titanium alloy subjected to low temperature annealing heat-treatment at 450°C for a duration of one-hour for different predetermined strain rates varies from 12.1 J/cm<sup>3</sup> to 20.25 J/cm<sup>3</sup>. Further, among the different predetermined strain rates studied, the net energy dissipated for the 6% predetermined strain rate is maximum.

Hence, it is seen that the area enclosed within the loading and unloading curves of stress vs strain diagram may represent the resilience of the material and in turn may be an index of the level of Superelasticity behavior exhibited by the material.

Thus, within the scope of this investigation, among the different low temperature annealing heat-treatment temperatures studied, and among the different predetermined strain rates studied, the net energy dissipated for 50% Nickel - 50% Titanium alloy is maximum for 6% predetermined strain rate at an annealing temperature of 450°C. In other words, among the different predetermined strain rates studied, the superelastic behavior for 50% Nickel - 50% Titanium alloy is superior for 6% predetermined strain rate when subjected to low temperature annealing at 450°C.

The published information in the area of superelastic behavior of Nickel - Titanium alloys subjected to different types of heat-treatment carried out by earlier investigators (Stockel. 1988) (Robertson et al. 2012) indicates that the nature of heat-treatment influences the superelastic behavior. In this research work also, it has been observed that the predetermined strain rate and annealing temperature is having influence on the superelastic behavior of the 50% Nickel - 50% Titanium alloy.

## 4.7 Corrosion Characteristics

The electrochemical corrosion rate for 50% Nickel - 50% Titanium alloy samples subjected to low temperature annealing heat-treatment at different temperatures has been determined as explained in the previous section.

The TAEFL plot i.e., semi log plot of current on log scale vs potential on plain scale for 50% Nickel - 50% Titanium alloy subjected to low temperature annealing temperature of 300°C in a corrosive medium of pH value 7.5 has been presented in figure 4.54.

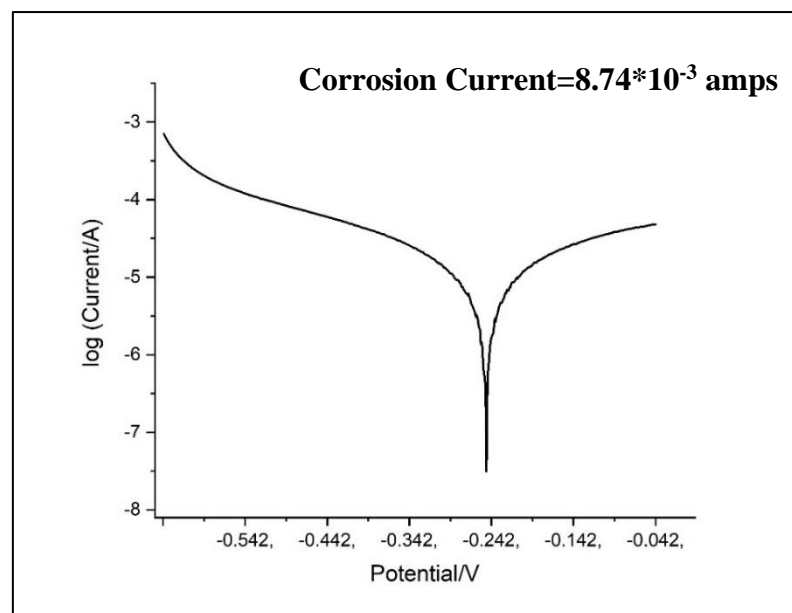


Figure 4.54 TAEFL plot i.e. semi log plot of current on log scale vs potential on plain scale for 50% Nickel - 50% Titanium alloy subjected to low temperature annealing temperature of 300°C in a corrosive medium of pH value 7.5

As explained in the previous section, the intersection points of extended anode current line and extended cathode current line indicating the corrosion current for the material under consideration has been determined by feeding all the values into the software and has been mentioned in figure 4.54 and in table 4.19. The corrosion current for the 50%Nickel-50% Titanium alloy subjected to low temperature annealing heat-treatment at 300°C has been found to be  $8.74 \times 10^{-3}$  amperes.

Table 4.19 Corrosion Current and Electrochemical corrosion rate for 50% Nickel - 50% Titanium alloy subjected to low temperature annealing heat-treatment at 300°C

Sl.No.	Low temperature annealing heat treatment condition		Corrosion Current (I) Amps	Electrochemical Corrosion Rate (CR) mm/year
	Temperature °C	Duration Hours		
(1)	(2)	(3)	(4)	(5)
1	300	1	$8.74 \times 10^{-3}$	0.0471

Further, by substituting this value of corrosion current in the equation explained in the earlier section, the corrosion rate has been determined and has been presented in table 4.19. The electrochemical corrosion rate for the 50% Nickel - 50% Titanium alloy subjected to low temperature annealing heat-treatment at 300°C has been found to be 0.0471 mm/year. The TAEFL plot i.e. semi log plot of current on log scale vs potential on plain scale for 50% Nickel - 50% Titanium alloy subjected to low temperature annealing temperature of 350°C in a corrosive medium of pH value 7.5 has been presented in figure 4.55. The intersection points of extended anode current line and extended cathode current line indicating the corrosion current for the material under consideration has been determined by feeding all the values into the software and has been mentioned in figure 4.55 and in table 4.20. The corrosion current for the 50% Nickel - 50% Titanium alloy subjected to low temperature annealing heat-treatment at 350°C has been found to be  $7.3 \times 10^{-3}$  amperes. Further, by substituting this value of corrosion current in the equation explained in the earlier section, the corrosion rate has been determined and has been presented in table 4.20. The electrochemical corrosion rate for the 50% Nickel - 50% Titanium alloy subjected to low temperature annealing heat-treatment at 350°C has been found to be 0.0394 mm/year.

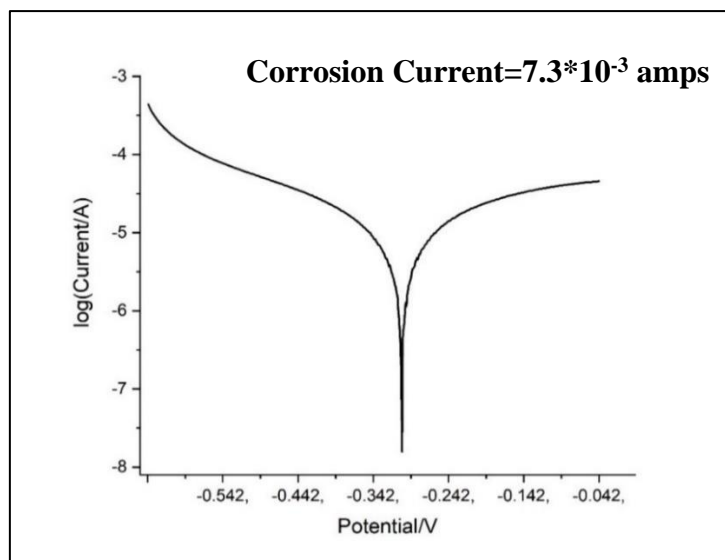


Figure 4.55 TAEFL plot for 50% Nickel - 50% Titanium alloy subjected to low temperature annealing temperature of 350°C in a corrosive medium of Hank's solution

Table 4.20 Corrosion Current and Electrochemical corrosion rate for 50% Nickel - 50% Titanium alloy subjected to low temperature annealing heat-treatment at 350°C

Sl. No.	Low temperature annealing heat treatment condition		Corrosion Current (I) Amps	Electrochemical Corrosion Rate (CR) mm/year
	Temperature °C	Duration Hours		
(1)	(2)	(3)	(4)	(5)
1	350	1	$7.3 \times 10^{-3}$	0.0394

The TAEFL plot i.e. semi log plot of current on log scale vs potential on plain scale for 50% Nickel - 50% Titanium alloy subjected to low temperature annealing temperature of 400°C in a corrosive medium of pH value 7.5 has been presented in figure 4.56.

The intersection points of extended anode current line and extended cathode current line indicating the corrosion current for the material under consideration has been determined by feeding all the values into the software and has been mentioned in figure 4.56 and in table 4.21.



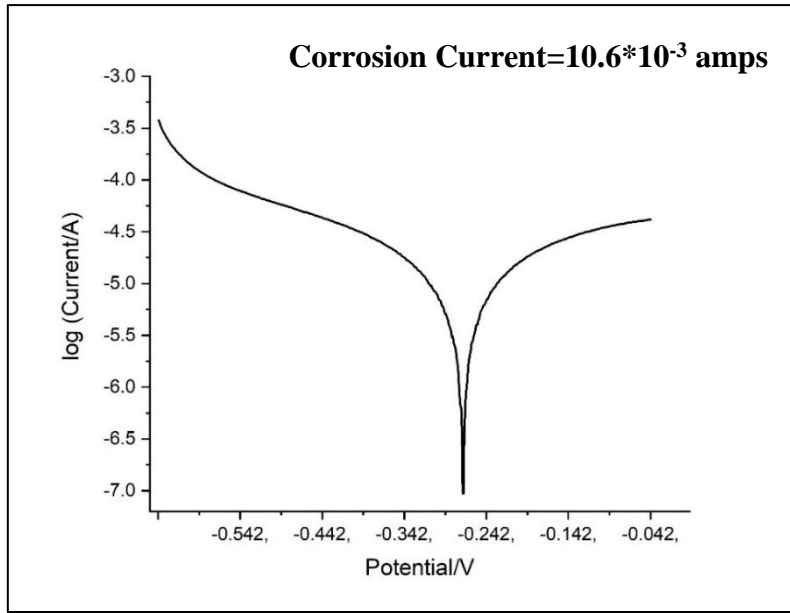


Figure 4.56 TAEFL plot for 50% Nickel - 50% Titanium alloy subjected to low temperature annealing temperature of 400°C in a corrosive medium of Hank's solution

Table 4.21 Corrosion Current and Electrochemical corrosion rate for 50% Nickel - 50% Titanium alloy subjected to low temperature annealing heat-treatment at 400°C

Sl. No.	Low temperature annealing heat treatment condition		Corrosion Current (I) Amps	Electrochemical Corrosion Rate (CR) mm/year
	Temperature °C	Duration Hours		
(1)	(2)	(3)	(4)	(5)
1	400	1	$10.6 \times 10^{-3}$	0.0573

The corrosion current for the 50% Nickel - 50% Titanium alloy subjected to low temperature annealing heat-treatment at 400°C has been found to be  $10.6 \times 10^{-3}$  amperes. Further, by substituting this value of corrosion current in the equation explained in the earlier section, the corrosion rate has been determined and has been presented in table 4.21. The electrochemical corrosion rate for the 50% Nickel - 50% Titanium alloy subjected to low temperature annealing heat-treatment at 400°C has been found to be 0.0573 mm/year.

The TAEFL plot i.e. semi log plot of current on log scale vs potential on plain scale for 50% Nickel - 50% Titanium alloy subjected to low temperature annealing temperature of 450°C in a corrosive medium of pH value 7.5 has been presented in figure 4.57.

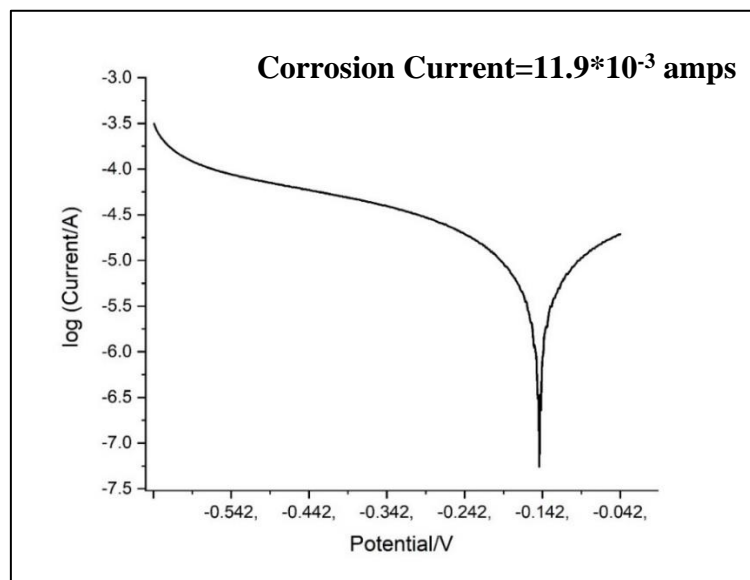


Figure 4.57 TAEFL plot for 50% Nickel - 50% Titanium alloy subjected to low temperature annealing temperature of 450°C in a corrosive medium of Hank's solution

The intersection points of extended anode current line and extended cathode current line indicating the corrosion current for the material under consideration has been determined by feeding all the values into the software and has been mentioned in figure 4.57 and in table 4.22.

Table 4.22 Corrosion Current and Electrochemical corrosion rate for 50% Nickel - 50% Titanium alloy subjected to low temperature annealing heat-treatment at 450°C

Sl. No.	Low temperature annealing heat treatment condition		Corrosion Current (I) Amps	Electrochemical Corrosion Rate (CR) mm/year
	Temperature °C	Duration Hours		
(1)	(2)	(3)	(4)	(5)
1	450	1	11.9*10 <sup>-3</sup>	0.0644

The corrosion current for the 50% Nickel - 50% Titanium alloy subjected to low temperature annealing heat-treatment at 450°C has been found to be 11.9\*10<sup>-3</sup> amperes. Further, by substituting this value of corrosion current in the equation explained in the

earlier section, the corrosion rate has been determined and has been presented in table 4.22. The electrochemical corrosion rate for the 50% Nickel - 50% Titanium alloy subjected to low temperature annealing heat-treatment at 450°C has been found to be 0.0644 mm/year. The corrosion current and electrochemical corrosion rate obtained for 50% Nickel - 50% Titanium alloy subjected to low temperature annealing treatment at different temperatures have been consolidated and presented in table 4.23 for the sake of comparison. It can be observed from table 4.23 that the corrosion current is lowest for the 50% Nickel - 50% Titanium alloy subjected to low temperature annealing treatment at 350°C. Further, it can be observed that electrochemical corrosion rate is lowest for 50% Nickel - 50% Titanium alloy subjected to low temperature annealing treatment at 350°C.

Table 4.23 Electrochemical corrosion rate for 50% Nickel - 50% Titanium alloy subjected to low temperature annealing heat-treatment at different temperatures

Sl. No.	Low temperature annealing heat treatment condition		Corrosion Current (I), Amps	Electrochemical Corrosion Rate (CR) mm/year
	Temperature °C	Duration Hours		
(1)	(2)	(3)	(4)	(5)
1	300	1	$8.74 \times 10^{-3}$	0.0471
2	350	1	$7.3 \times 10^{-3}$	0.0394
3	400	1	$10.6 \times 10^{-3}$	0.0573
4	450	1	$11.9 \times 10^{-3}$	0.0644

It appears from the literature survey that there is published information available on the influence of heat-treatment on the corrosion rate of the Nickel - Titanium alloys. Mealha et al. (2016) conducted thermal treatments on the Nickel - Titanium alloy. The alloys that were heat-treated were compared in terms of their corrosion resistance with the untreated alloys. It was mentioned that conducting heat-treatments at 350°C temperature in N<sub>2</sub>-controlled environment brought in a vast improvement in the corrosion resistance of the material followed by Nickel reduction at the surface. This confirms with our research work where 50% Nickel - 50% Titanium alloy subjected to

a heat-treatment of 350°C exhibits superior corrosion resistance. Some literature (Kharia Salman Hassan et al. 2015) has reported variation of corrosion rate with the hardness of an Aluminium alloy. They have reported that as the hardness of the material has increased, there has been a decrease in the corrosion rate.

In table 4.24 has been presented the hardness and corrosion rate of 50% Nickel - 50% Titanium alloy subjected to low temperature annealing treatment at different temperatures for the sake of discussion.

Table 4.24 Hardness and Electrochemical corrosion rate for 50% Nickel - 50% Titanium alloy subjected to low temperature annealing heat-treatment at different temperatures

Sl. No.	Low temperature annealing heat treatment condition		Hardness VHN	Electrochemical Corrosion Rate (CR) mm/year
	Temperature °C	Duration Hours		
(1)	(2)	(3)	(4)	(5)
1	300	1	438	0.0471
2	350	1	482	0.0394
3	400	1	427	0.0573
4	450	1	365	0.0644

From this table, it can be observed that as the hardness of the material has increased, there has been a decrease in the corrosion rate. Thus, the trend of results observed in this investigation has been found to be similar to the trend of results observed by the earlier investigators.

#### **4.8 Comparison of As-Received and Low Temperature Annealing Heat-Treated 50% Nickel - 50% Titanium Alloys**

In this section, the various properties of as-received and low temperature annealing heat-treated 50% Nickel - 50% Titanium alloy has been systematically compared. For the purpose of comparison, for a particular property, within the scope of the investigation, optimum value of low temperature annealing heat-treatment determined in the previous section of this investigation has been considered. The results are presented and discussed.

#### **4.8.1 Comparison of transmission electron micrographs of as-received and low temperature annealing heat-treated 50% Nickel - 50% Titanium alloys**

The Transmission electron microscopy micrographs of Ni-Ti alloy of the as-received sample has been presented in figure 4.1 in the previous section.

The presence of martensite which appears as a needle-like region can be observed. In addition, a shaded region indicating presence of dislocation network may also be observed. Similarly, the Transmission electron microscopy micrographs of the NiTi alloy subjected to low temperature annealing heat treatment at 350°C has been presented in figure 4.15 in the previous section. The microstructure indicates the presence of martensite, dislocation networks and formation of NiTi alloy grains.

When the NiTi alloy subjected to low temperature annealing treatment at 350°C has been compared with that of the as-received condition, it appears that the extent of dislocation network has relatively reduced and the grain size of NiTi alloy has relatively increased. However, literature (Kurnia Hastuti et al. 2016) mentioned that the presence of martensitic variants existed in the NiTi alloy samples annealed at temperatures below 500°C. This finding confirms with our results.

#### **4.8.2 Comparison of EDS of as-received and low temperature annealing heat-treated 50% Nickel - 50% Titanium alloys**

Comparison of EDAX of the 50% Nickel - 50% Titanium alloy in the as-received condition with the EDAX of low temperature annealing heat-treated 50% Nickel - 50% Titanium alloy at optimum temperature of 350°C for duration of 1 hour indicates that there is no change in the chemical composition of the alloy when subjected to heat-treatment.

#### **4.8.3 Comparison of X-Ray Diffractogram of as-received and low temperature annealing heat-treated 50% Nickel - 50% Titanium alloys**

The X-ray diffractogram of the as-received Ni-Ti alloy has been presented in figure 4.58.

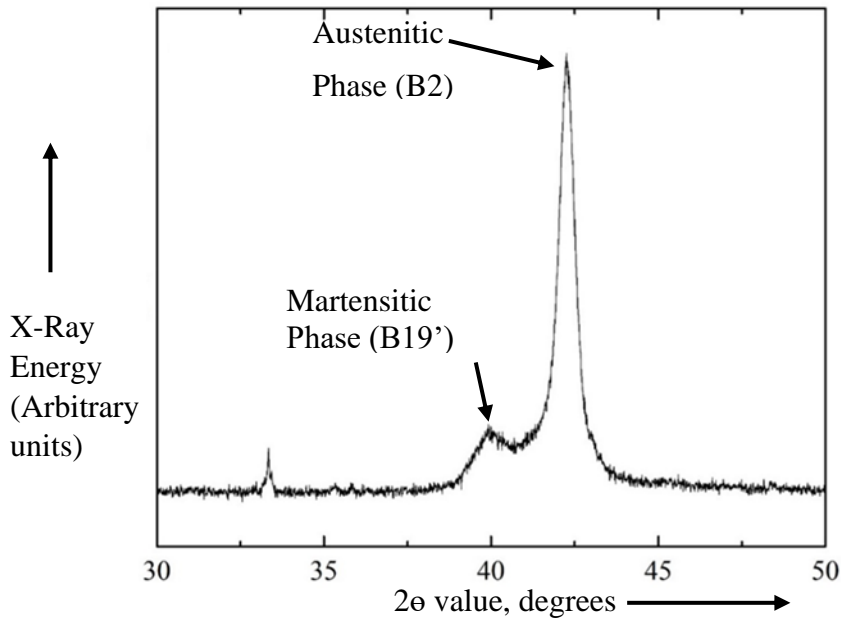


Figure 4.58 X Ray Diffraction of as-received 50% Nickel - 50% Titanium alloy

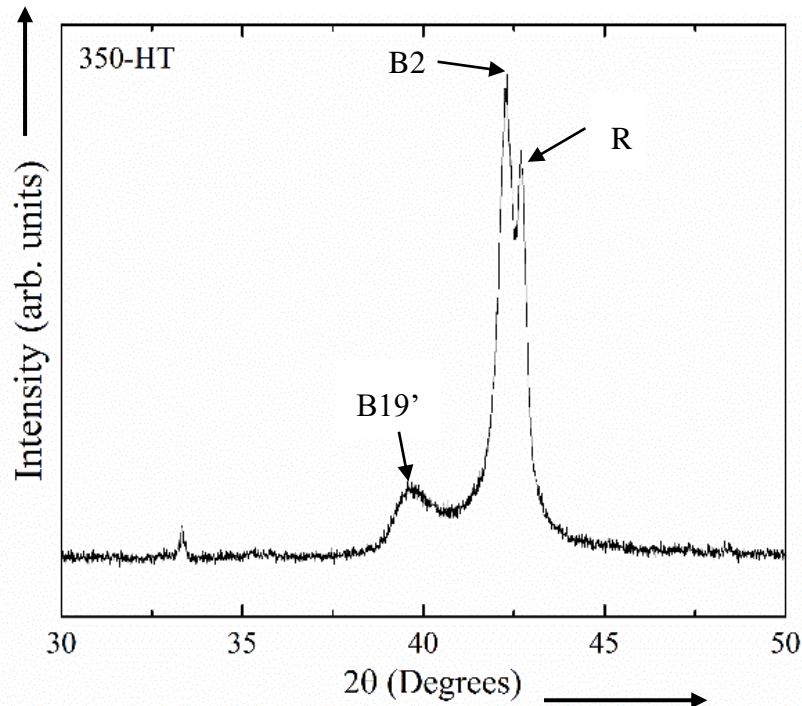


Figure 4.58 X-Ray Diffractogram of 50% Nickel - 50% Titanium alloy subjected to low temperature annealing heat treatment at 350°C

The martensitic phase has appeared at  $2\theta$  value of  $39.24^\circ$  and the austenitic phase was found to appear at a  $2\theta$  value of  $42.1^\circ$ . Further, the energy intensity value of martensitic phase has been observed to be lesser than the energy intensity values of austenitic phase.

The X-ray diffractogram of the 50% Nickel – 50% Titanium alloy subjected to a heat-treatment of 350°C has been presented in figure 4.59. Apart from the presence of the Austenitic and Martensitic phase, an additional phase named R-phase is present in the specimen. It can also be observed that the martensitic phase has appeared at a  $2\theta$  value of 39.24°. Whereas, the austenitic phase was found to appear at a  $2\theta$  value of 42.4° and the Rhombohedral phase (R-phase) is seen to appear at a  $2\theta$  value of 43.1°. Further, the energy intensity value of martensitic phase has been observed to be lesser than the energy intensity values of austenitic phase. The energy intensity value of Rhombohedral phase has been observed to be in between the energy intensity value of martensitic phase and the austenitic phase. Comparing the X-Ray diffractograms of the as-received sample and the sample heat-treated at 350°C, there appears to be no major difference in the  $2\theta$  angle of appearance of the peaks except that an additional R-Phase is seen to appear. Also, (Uchil et al. 2007) reports that in Titanium-rich NiTi alloys, heat-treatment has brought no major changes.

#### **4.8.4 Comparison of differential scanning calorimetry results of as-received and low temperature annealing heat-treated 50% Nickel - 50% Titanium alloys**

The result of DSC test for as-received Nickel - Titanium alloy obtained in terms of heating and cooling curves has been presented in figure 4.60. It is clear from figure 4.60 that there are no significant peaks observed in the heating as well as the cooling curves of as-received material indicating that there are no distinct phase transformations of either Austenite-Martensite or Martensite-Austenite present in the material. The absence of peaks in the material observed in this investigation may be the result of multi-step 40% cold-working process performed on the material as reported by supplier Baoji Sunhope Titanium Industries Ltd. The process of cold-working performed on the material may have resulted in huge dislocation network in the grain structure inhibiting temperature-induced-martensitic transformation from taking place. The result of DSC test for Nickel Titanium alloy heat-treated at 350°C obtained in terms of heating and cooling curves has been presented in figure 4.61.

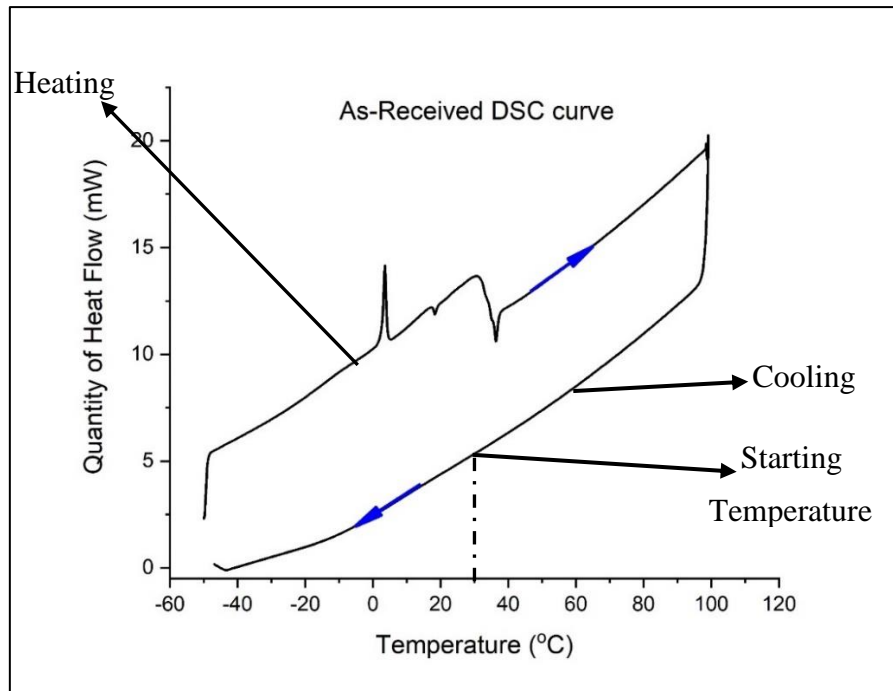


Figure 4.60 Differential Scanning Calorimetry curve of as-received 50% Nickel - 50% Titanium alloy

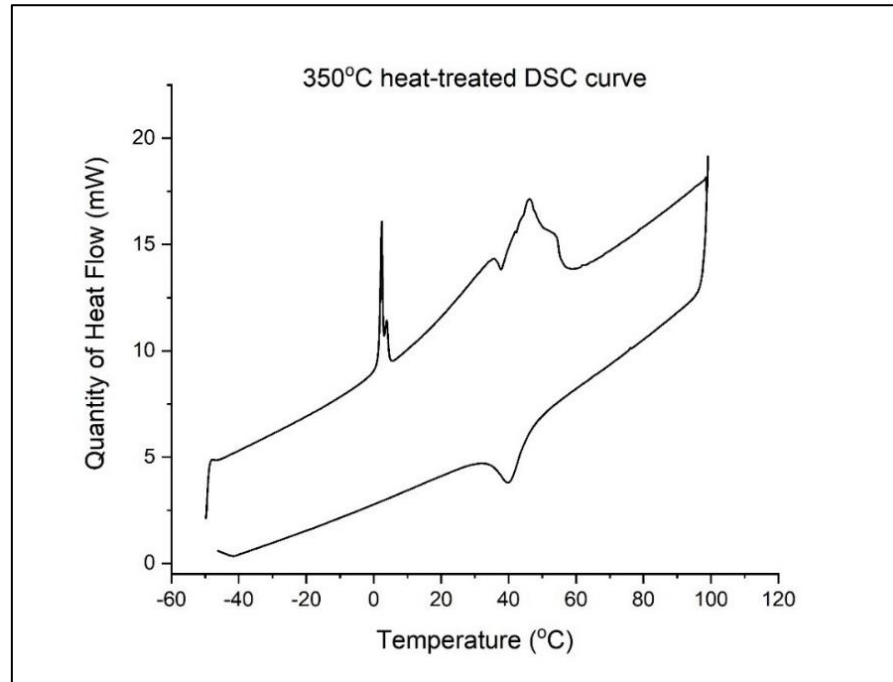


Figure 4.61 DSC Thermogram of 50% Nickel - 50% Titanium alloy subjected to low temperature annealing heat treatment at 350°C



It can be observed from figure 4.61 that when Nickel - Titanium alloy is subjected to low temperature annealing heat-treatment at 350°C, the specimens show a single-stage transformation from austenite phase to martensite phase in the cooling cycle and a two-stage transformation from martensite phase to rhombohedral phase and rhombohedral phase to austenite phase in the heating cycle. The transformation temperatures for start and finish of Martensite phase i.e.,  $M_s$  and  $M_f$  has been found to be 44°C and 33°C, respectively as presented in table 4.7. Similarly, the transformational temperatures for start and finish of Rhombohedral phase i.e.,  $R_s$  and  $R_f$  has been found to be 17°C and 37°C. This Rhombohedral phase transformation has been followed by transformation into Austenite phase. The transformational temperatures for start and finish of Austenite phase i.e.  $A_s$  and  $A_f$  has been found to be 38°C and 53°C. This observation indicates that at room temperature Martensite phase, Austenite phase and Rhombohedral phase are present in the alloy. The Rhombohedral phase, being an intermediate phase between austenite and martensite is not too desirable for shape memory effect or superelastic behaviour since this seems to exhibit a very small shape memory effect and superelasticity, within a narrow temperature range and a specific composition. The properties could be made to get affected by the suppression of martensitic transformation in the NiTi alloy such that the transformation strain could be amplified showing a shape memory and superelastic behaviour of about 1%. Such an effect of R-phase is not significantly observed in the present study. The literature (Wang et al. 2014) (Palloma Viera et al. 2014) confirms that upon heat-treating the NiTi alloy samples at predetermined temperatures of 350°C, the R-phase was found to appear at room temperature along with the Austenitic phase. In addition, the literature (Palloma Viera et al. 2014) indicated that upon increase of the annealing temperature to as high as 600°C, the R-phase was seen to disappear yielding a single-phase transformation in the alloy.

#### **4.8.5 Comparison of ultimate tensile strength of as-received and low temperature annealing heat-treated 50% nickel - 50% titanium alloys**

The ultimate tensile strength of as-received 50% Nickel - 50% Titanium alloy and the ultimate tensile strength of low temperature annealing heat-treated 50% Nickel - 50% Titanium alloy at optimum temperature of 350°C for duration of 1 hour has been tabulated in table 4.25. In column 4 of this table, the improvement in ultimate tensile

strength due to low temperature annealing heat-treatment has been computed in terms of percentage increase in the ultimate tensile strength with respect to the ultimate tensile strength in the as-received condition.

Table 4.25 Comparison of Ultimate tensile Strength (UTS) of as-received and low temperature annealing heat-treated 50% Nickel - 50% Titanium alloy

Sl. No.	Ultimate Tensile Strength, MPa		Improvement in Ultimate Tensile Strength w.r.t. as-received condition due to heat-treatment  $\frac{Col(3)-Col(2)}{Col(2)} * 100$ in (%)
	As-received condition	Optimum Low temperature annealing heat-treated condition*	
(1)	(2)	(3)	(4)
1	966	1395	44.40

\*From previous section, optimum condition was found to be heat-treating at 350°C for one hour

From table 4.25, it can be observed that the ultimate tensile strength of low temperature annealing 50% Nickel - 50% Titanium alloy is more than the ultimate tensile strength of as-received 50% Nickel - 50% titanium alloy. From column 4 of table 4.25, the extent of improvement in ultimate tensile strength of 50% Nickel and 50% Titanium alloy has been found to be 44.40% as compared to ultimate tensile strength of as-received 50% Nickel - 50% Titanium alloys. Studies on NiTi alloy conducted as per literature (Zupanc et al. 2018) mention that the low temperature annealing heat-treatment was found to improve the superelastic properties of the NiTi alloy. The work as per literature appears to be in connection to the work carried out in this investigation. In addition, literature (Praveen Sathiyamoorthi et al. 2018) mentioned that the alloy specimens subjected to a high temperature annealing treatment showed a remarkable improvement in ultimate tensile strength along with strain to failure. This confirms with the experimental work carried out with respect to 50% Nickel – 50% Titanium alloys.

#### 4.8.6 Comparison of Hardness of as-received and low temperature annealing heat-treated 50% Nickel - 50% Titanium alloys

The Vickers Hardness of as-received 50% Nickel - 50% Titanium alloy and the Vickers Hardness of low temperature annealing heat-treated 50% Nickel - 50% Titanium alloy at optimum temperature of 350°C for duration of 1 hour has been tabulated in table 4.26.

Table 4.26 Comparison of Vickers Hardness of as-received and low temperature annealing heat-treated 50% Nickel - 50% Titanium alloy

Sl. No.	Vickers Hardness, Kg/mm <sup>2</sup>		Improvement in Vickers Hardness w.r.t. as-received condition due to heat-treatment $\frac{Col(3)-Col(2)}{Col(2)} * 100$ in (%)
	As-received condition	Optimum Low temperature annealing heat-treated condition*	
(1)	(2)	(3)	(4)
1	421	482	14.5

\*From previous section, optimum condition was found to be heat-treating at 350°C for one hour

In column 4 of table 4.26, the improvement in hardness due to low temperature annealing heat-treatment has been computed in terms of percentage increase with respect to the hardness in as-received condition. From table 4.26, it can be observed that the hardness of low temperature annealing 50% Nickel - 50% Titanium alloy is more than the hardness of as-received 50% Nickel - 50% Titanium alloy. From column 4 of table 4.26, the extent of improvement in hardness of 50% Nickel - 50% Titanium alloy has been found to be of the order of 14.5% as compared to hardness of as-received 50% Nickel - 50% Titanium alloy. The literature (Mohamed et al. 2009) suggests that the hardness improves upto 350°C condition and appears to reduce from the 400°C to 450°C condition. This confirms to the investigation carried out for the 50% Nickel - 50% Titanium alloy sample.

#### 4.8.7 Comparison of abrasive wear characteristics of as-received and low temperature annealing heat-treated 50% Nickel - 50% Titanium alloys

The abrasive wear characteristics of as-received 50% Nickel - 50% Titanium alloy and the abrasive wear characteristics of low temperature annealing heat-treated 50% Nickel

- 50% Titanium alloy at optimum temperature of 350°C for duration of 1 hour has been tabulated in table 4.27.

Table 4.27 Comparison of Abrasive Wear characteristics of as-received and low temperature annealing heat-treated 50% Nickel - 50% Titanium alloy

Sl. No.	Load (P) N	Abrasive Wear, Mass Loss, mg		Improvement in Wear Resistance w.r.t. as-received condition due to heat-treatment $\frac{Col(3)-Col(4)}{Col(3)} * 100$ in (%)
		As-received condition	Optimum Low temperature annealing heat-treated condition*	
(1)	(2)	(3)	(4)	(5)
1	5	5.8	3.04	47.58
2	15	6.8	3.8	44.11
3	25	7.4	4.5	39.18
4	35	7.8	4.9	37.17
5	45	8.2	5	39.02

In column 5 of table 4.27, the improvement in wear resistance due to low temperature annealing heat-treatment has been computed in terms of percentage reduction in mass loss with respect to mass loss in as-received condition. The comparison of wear characteristics has been presented graphically in figure 4.62.

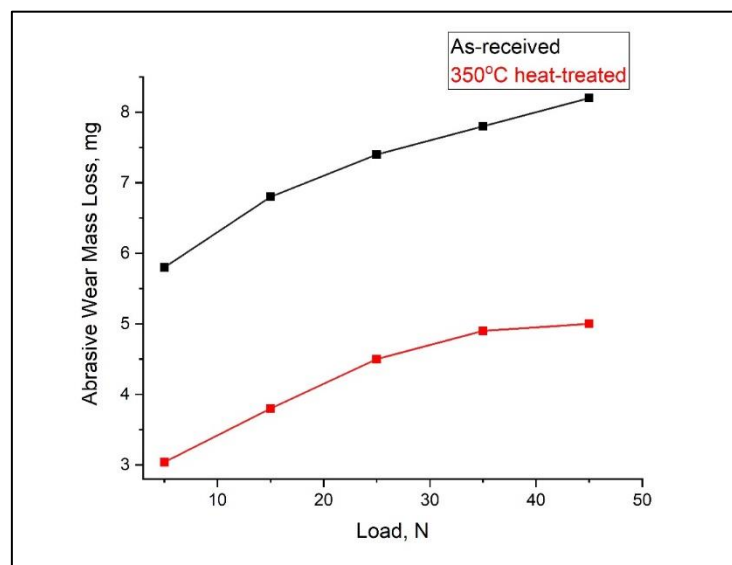


Figure 4.59 Comparison of Abrasive Wear characteristics of as-received and low temperature annealing heat-treated 50% Nickel - 50% Titanium alloy

From table 4.27 and figure 4.62, it can be observed that the mass loss of low temperature annealing 50% Nickel - 50% Titanium alloy is less than the mass loss of as-received 50% Nickel - 50% Titanium alloy. This trend has been found true at all the axial loads investigated within the scope of this investigation. From column 5 of table 4.27, the extent of improvement in wear resistance of 50% Nickel - 50% Titanium alloy has been found to be in the range of 37.17% - 47.58% as compared to wear resistance of as-received 50% Nickel - 50% Titanium alloys. (Abubakar et al. 2013) mentioned that there is a significant improvement in the wear resistance of the NiTi coating done on the 316N Stainless Steel material at higher annealing temperatures compared to the as-received condition. It was observed by (Palloma Vieira et al. 2015) that the NiTi alloy material annealed at temperatures of 350°C, 450°C, 500°C and 600°C, the material annealed at 350°C exhibited much less wear, of the order of 30% less than the as-received NiTi alloy material. This confirms with the experimental work on abrasive wear carried out with respect to 50%Nickel – 50%Titanium alloy.

#### **4.8.8 Comparison of Superelasticity Behaviour of as-received and low temperature annealing heat-treated 50% Nickel - 50% Titanium alloys**

The Superelasticity characteristics of as-received 50% Nickel - 50% Titanium alloy and the Superelasticity characteristics of low temperature annealing heat-treated 50% Nickel - 50% Titanium alloy at optimum temperature of 450°C for duration of 1 hour has been tabulated in table 4.28. In column 5 of table 4.28, the improvement in Superelasticity due to low temperature annealing heat-treatment has been computed in terms of percentage increase in the net energy dissipated in as-received condition. From table 4.28, it can be observed that the superelasticity percentage of low temperature annealing 50% Nickel - 50% Titanium alloy is more than the superelasticity of as-received 50% Nickel - 50% Titanium alloy. From column 5 of table 4.28, the extent of improvement in Superelasticity of 50% Nickel - 50% Titanium alloy heat-treated at 450°C has been found to be in the range of 54.5% to 95.2% as compared to superelasticity of as-received 50% Nickel - 50% Titanium alloys. The calculation of the net energy dissipated by the material is mentioned in the previous chapter. The superelasticity has been calculated by measuring the net energy dissipated by the as-

received NiTi alloy and also the alloy heat-treated at 450°C and tabulated accordingly in Table 4.28.

Table 4.28 Comparison of Superelasticity of as-received and low temperature annealing heat-treated 50% Nickel - 50% Titanium alloy

Sl. No.	Extent of straining	Superelasticity, MPa		Improvement in Superelasticity w.r.t. as-received condition due to heat-treatment $\frac{Col(4)-Col(3)}{Col(3)} * 100$ in (%)
		Net energy dissipated (J/cm <sup>3</sup> ) for As-received Condition	Net energy dissipated (J/cm <sup>3</sup> ) for Optimum Low temperature annealing heat-treated condition*	
(1)	(2)	(3)	(4)	(5)
1	2	6.20	12.1	95.2
2	6	14.2	25.2	77.5
3	8	13.1	20.25	54.5

\*From previous section, optimum condition was found to be heat-treating at 450°C for one hour

It is seen from table 4.28 that comparing the net energy dissipated at 6% predetermined strain of the as-received NiTi alloy and NiTi alloy annealed at 450°C, it is seen that there is a vast improvement in the energy dissipation by 77.5% in the 450°C heat-treated alloy as compared to the as-received NiTi alloy. The reason for comparison of only the 6% predetermined strains is the maximum superelastic performance seen for all the alloy samples at 6% predetermined strain.

As per literature (Abdy et al. 2014), it was studied that the stress-strain relationship was affected significantly upon an increase in the heat-treatment temperature. This finding is similar to the work carried out on the 50% Nickel - 50% Titanium alloy subjecting it to a low temperature annealing treatment. Also, (Paryab et al. 2019) suggested that the annealing carried out at temperature range of 350°C - 400°C yielded better superelasticity results compared to the as-received material. As per (Paryab et al. 2019) the superelastic property was expressed in terms of hardness and microstructure. It was found that the annealing carried out at 400°C yielded better hardness and also superelastic property as compared to specimens annealed at higher temperatures of 700

- 800°C. The reason according to the literature being the presence of precipitates such as  $\text{Ni}_4\text{Ti}_3$  coherent with the NiTi matrix causing good strength and hardness at lower annealing temperatures. These precipitates were seen to lose coherency with the matrix at higher annealing temperatures causing a drop in the superelastic properties. It was studied by (Xu Huang et al. 2001) that the superelasticity of the Nickel-Titanium alloy was affected upon an increase of the annealing temperature. As per (Xu Huang et al. 2001), the superelastic property has been discussed with respect to high plateau stress and low plateau strain when samples were annealed between 350 and 400°C. This has been further investigated with respect to the phases that are present in the material, being the austenitic phase and R-phase at lower annealing temperatures whereas the R-phase either coinciding or disappearing at temperatures higher than 600°C. The hysteresis curve proved to be the widest at annealing temperatures of 350 - 450°C ensuring high superelastic behavior of the alloy. In our present study, the superelastic property as per table 4.28 is the highest for the material annealed at 450°C, compared to the as-received material. The reason could be attributed to the tensile property of the NiTi alloy as discussed in section 4.5.1, wherein the alloy sample annealed at 450°C is seen to display the highest strength and toughness.

#### **4.8.9 Comparison of Corrosion Rate of as-received and low temperature annealing heat-treated 50% Nickel - 50% Titanium alloys**

The corrosion rate of as-received 50% Nickel - 50% Titanium alloy and the corrosion rate of low temperature annealing heat-treated 50% Nickel - 50% Titanium alloy at optimum temperature of 350°C for duration of 1 hour has been tabulated in table 4.29.

Table 4.29 Comparison of Corrosion Rate of as-received and low temperature annealing heat-treated 50% Nickel - 50% Titanium alloy

Sl. No.	Corrosion Rate, mm/year		Improvement in Corrosion Rate w.r.t. as-received condition due to heat-treatment $\frac{Col(3)-Col(2)}{Col(2)} * 100$ in (%)
	As-received condition	Optimum Low temperature annealing heat-treated condition*	
(1)	(2)	(3)	(4)
1	0.0613	0.0394	35.72

\*From previous section, optimum condition was found to be heat-treating at 350°C for one hour

In column 4 of table 4.29, the improvement in corrosion resistance due to low temperature annealing heat-treatment has been computed in terms of percentage reduction in corrosion rate with respect to corrosion rate in as-received condition. From table 4.29, it can be observed that the corrosion rate of low temperature annealing 50% Nickel - 50% Titanium alloy is less than the corrosion rate of as-received 50% Nickel - 50% Titanium alloy. From column 4 of table 4.29, the extent of improvement in the corrosion resistance of 50% Nickel - 50% Titanium alloy has been found to be 35.72% as compared to corrosion resistance of as-received 50% Nickel - 50% Titanium alloys. Literature (Dalibor et al. 2011) mentions that the corrosion resistance of the NiTi alloy annealed at temperatures of 400°C - 600°C was observed to go down. According to the literature (Dalibor et al. 2011) the heat-treatment temperatures increased beyond 400°C could be forming a defect oxide layer over the TiO<sub>2</sub> coating of the NiTi wire. This defect oxide layer worsens the protective effect leading to excessive corrosion of the material. Manju Chembath et al. (2014) conducted extensive corrosion studies on NiTi alloy and measured the Nickel release when immersed in Hank's solution. It was concluded from the study that the alloy immersed in Hank's solution released much less Nickel content into the solution in comparison with mechanically polished samples; thus, rendering a high corrosion resistance.



## **4.9 Summary**

The investigation has been carried out on as-received binary Nickel-Titanium alloy and Nickel-Titanium alloy samples heat-treated at four different temperatures and a time duration of one-hour. It is observed that heat-treatment has marginal effect on the microstructural, mechanical, tribological and corrosion properties since the nearly equi-atomic alloy is slightly rich on the Titanium-side.

However, the TEM structures show a marginal difference between the sub-microstructure of as-received and heat-treated samples in terms of marginal grain growth and reduction in the dislocation density of the heat-treated samples as compared to the as-received one. Similarly, the mechanical properties and the tribological properties have shown marginal improvements in the heat-treated samples of approximately 35% as compared to the as-received sample.

The low temperature annealing heat-treatment has brought about an improvement in the corrosion resistance of the material as compared to the as-received material.

## **CHAPTER 5**

### **CONCLUSIONS AND SCOPE FOR FUTURE WORK**

#### **5.1 Introduction**

In this chapter, the salient results of the systematic investigation carried out on the topic titled “Influence of Heat-Treatment on Structure and Properties of Nickel - Titanium Alloy” have been presented. The studies comprising of various aspects of NiTi alloy such as results of observation of microstructure under TEM, evaluation of mechanical properties, tribological characteristics and corrosion properties as discussed in the previous chapters, have been presented. The conclusions drawn from the previous chapter has been presented under three different sections; as-received NiTi alloy without heat-treatment; NiTi alloy subjected to low temperature heat-treatment and comparison of as-received NiTi alloy and heat-treated NiTi alloy.

#### **5.2 Studies on As-Received and Low temperature Heat-treated Nickel-Titanium Alloy**

##### **5.2.1 Microstructure observation under TEM**

- (i) The Transmission electron microscopy micrographs of Ni-Ti alloy of the as-received sample and diffraction pattern indicate the existence of Martensitic and Austenitic phase at room temperature.
- (ii) The TEM of the 50% Nickel - 50% Titanium alloy material subjected to low temperature annealing heat treatment at different temperatures indicated the presence of martensitic phase, dislocation network and formation of NiTi alloy grains. This observation had been found true at all annealing heat-treatment temperatures studied. However, variation in extent of dislocation density was found with increase in low annealing heat-treatment temperature. However, the martensitic phase had been found to be relatively more in the 350°C heat-treated sample.

### **5.2.2 EDS Analysis**

(iii) The chemical composition of the constituents present in the alloy assessed by EDAX analysis indicate that the Ni-Ti alloy used in this investigation is a 50:50 Ti-Ni alloy which is well within the tolerance limit for 50:50 TiNi alloy as per ASTM F1375 - 92(2012). The alloy is found to be slightly on the Titanium-rich side.

(iv) There has been no appreciable difference in the chemical composition of 50 % Nickel – 50 % Titanium alloy when subjected to low temperature annealing heat-treatment at different temperatures for one-hour duration.

### **5.2.3 X-Ray diffraction studies**

(v) The X-ray diffractogram of the as-received Ni-Ti alloy indicate that  $2\theta$  range for the appearance of peaks corresponding to Ni and Ti elements in Nickel-Titanium alloy used in this investigation is in the range of  $30^\circ$ - $50^\circ$ , wherein the Austenitic phase has appeared at a  $2\theta$  angle of  $42.1^\circ$  and martensitic phase has appeared at a  $2\theta$  angle of  $39.24^\circ$ .

(vi) The X-ray diffractogram of the 50% Nickel – 50% Titanium alloy subjected to low temperature annealing heat-treatment at different temperatures indicated the presence of both Austenitic phase and Martensitic phase. This has been found true at all low temperature annealing heat-treatment temperatures investigated for one-hour duration. However, the X-ray diffractogram of the 50% Nickel – 50% Titanium alloy subjected to low temperature annealing heat-treatment at  $350^\circ\text{C}$  and  $400^\circ\text{C}$  indicated the presence of an additional Rhombohedral phase. The extent of Rhombohedral phase has been found to be relatively more in the  $350^\circ\text{C}$  annealed sample as compared to that of at  $400^\circ\text{C}$  sample.

### **5.2.4 Differential scanning calorimetry**

(vii) The DSC test for as-received Nickel-Titanium alloy obtained in terms of heating and cooling curves indicate that there are no significant peaks noticed in the heating as well as the cooling curves of as-received material meaning that there are no distinct phases of either Austenite or Martensite present in the material.

(viii) The DSC study of 50% Nickel - 50% Titanium alloy subjected to low temperature annealing heat-treatment at different temperatures and a time duration of one-hour show a single-stage transformation from austenitic phase to martensitic phase in the cooling

cycle. This has been found true at all low annealing heat-treatment temperatures investigated for one-hour duration.

(ix) The DSC study of 50% Nickel – 50% Titanium alloy subjected to low temperature annealing treatment at 350°C, 400°C and 450°C show a two-stage transformation from martensitic phase to rhombohedral phase and rhombohedral phase to austenitic phase during heating cycle. However, the DSC study of 50% Nickel - 50% Titanium alloy subjected to low temperature annealing heat-treatment at 300°C shows a single-stage transformation from martensite phase to austenite phase during heating cycle.

### **5.2.5 Mechanical Properties**

#### **(a) Ultimate Tensile Strength (UTS)**

(x) The stress-strain diagram for the as-received Nickel-Titanium alloy indicates four distinct regions in the variation of stress with strain. The first region shows the elastic deformation of the austenitic phase. The second region is the region where transformation from austenite to martensite is observed. The third region represents starting and ending of elastic deformation of martensite. The fourth region represents further progression of plastic deformation of martensite.

(xi) The Lower Plateau Strength (LPS) or in other words the transformation of said austenite phase to martensite phase for NiTi alloy in this investigation has commenced at 7% of strain value which is less than 8% of superelastic strain value limit reported by the earlier investigators meaning that the material studied in this investigation appears to be super-elastic in nature. Further, the UTS value for the alloy has been found to be 966 MPa. Observation of fractograph of Nickel-Titanium alloy used in this investigation indicates the presence of dimples in the scanning electron micrograph, which in turn indicates that the nature of fracture is ductile in nature.

(xii) The stress-strain diagram for the Nickel-Titanium alloy subjected to low temperature annealing heat-treatment at different temperatures for a time duration of one-hour indicates four distinct regions in the variation of stress with strain. The first region shows the elastic deformation of the austenitic phase. The second region is the region where transformation from austenite to martensite is observed. The third region represents starting and ending of elastic deformation of martensite. The fourth region

represents further progression of plastic deformation of martensite. This trend has been found true at all the temperatures investigated.

(xiii) The UTS of Nickel-Titanium alloy subjected to low temperature annealing heat-treatment at different temperatures varies from 1252 MPa to 1378 MPa depending upon the annealing temperature. Within the scope of different low temperature annealing heat-treatment durations studied, the duration of 60 minutes has been found to exhibit superior Ultimate Tensile Strength. This has been found true at all temperatures investigated. Within the scope of different low temperature annealing heat-treatment temperatures studied, a temperature of 350°C has been found to exhibit superior Ultimate Tensile Strength.

(xiv) The observation of fractograph of 50% Nickel - 50% Titanium alloy subjected to low temperature annealing heat-treatment at different temperatures under SEM indicated that the nature of fracture of the material has been transgranular fracture. This trend has been found true at all annealing temperatures investigated. Observation of fractured surface of 50% Nickel – 50% Titanium alloy subjected to low temperature annealing heat-treatment of 350°C indicates that there are fewer and larger grains. Further, the fractured surface has been found to be relatively smoother.

#### **(b) Hardness**

(xv) It has been found from the investigation that VPN value of NiTi as-received material has been 421 VPN.

(xvi) The VPN value of 50% Nickel – 50% Titanium alloy subjected to low temperature annealing heat-treatment at different temperatures for one-hour duration has been found to be in the range of 438 VPN to 482 VPN. The VPN value has been found to increase when the annealing heat-treatment temperature has been increased from 300 to 350°C. With further increase in the temperature of the annealing heat-treatment to 450°C, there has been a decrease in the VPN. However, the 50% Nickel – 50% Titanium alloy subjected to optimum low temperature annealing heat-treatment at 350°C for one-hour duration has been found to exhibit maximum hardness of 482 VPN.

### **5.2.6 Tribological characteristics**

(xvii) The abrasive wear test indicates that when the load is increased, the wear mass loss rate is relatively at a higher rate upto 15N and with further increase in the load, the mass loss rate is relatively at a slower rate.

(xviii) Plough marks have been observed in the worn surface of as-received NiTi alloy when observed under SEM, which may be due to wear by rotating Alumina wheel.

(xviii) The abrasive wear of 50% Nickel – 50% Titanium alloy subjected to low temperature annealing heat-treatment at different temperatures for one-hour duration expressed in terms of mass loss increases with increase in time. This trend has been found true at all axial loads studied. The mass loss rate has been found to be relatively at a higher rate upto 15N. With further increase in the load, the mass loss rate has been found to be relatively at a slower rate. This trend has been found true at all temperatures of annealing heat-treatment.

(xix) When worn surfaces of Nickel-Titanium alloy samples subjected to low temperature annealing heat-treatment at different temperatures have been observed under SEM, plough marks have been observed which may be due to wear caused by rubbing Alumina wheel. Same observation has been found in samples heat-treated at different temperatures in this study. The 50% Nickel – 50% Titanium alloy annealed at 350°C for one-hour duration has been found to exhibit superior tribological characteristics by undergoing least hardness and displaying shallow groove marks when observed under SEM.

### **5.2.7 Superelastic behavior**

(xx) The variation of strain for different levels of stress during loading and after release of load at different predetermined strain values indicate that the material even after loading upto stress level of 700 MPa does not break but returns back to the original stress value after release of the load indicating that the unloading curve had followed a hysteresis path compared to loading curve by returning back to the same point which means that the material is exhibiting superelastic behavior.

(xxi) The hysteresis curve had broadened showing a much-lowered stress in the unloading cycle at 8% predetermined strain level as compared to that of 2% and 6% predetermined strain levels.

(xxii) The variation of strain for different levels of stress for all heat-treated samples, heat-treated for a duration of one-hour during loading and after release of load at different predetermined strain values indicate that the samples even after loading upto stress level of 1100 MPa do not break but return back to the original stress value after release of the load indicating that the unloading curve had followed a hysteresis path compared to loading curve by returning back to the same point which means that the samples are exhibiting superelastic behavior. This trend has been found true for 50% Nickel – 50% Titanium alloy samples subjected to low temperature annealing heat-treatment at all the different temperatures investigated.

(xxiii) Among the different low temperature annealing heat-treatment temperatures studied, and among the different predetermined strain rates studied, the area enclosed within loading and unloading curves of stress vs strain diagram for 50% Nickel - 50% Titanium alloy is maximum for 6% predetermined strain rate at an annealing temperature of 450°C and one-hour duration. In other words, among the different predetermined strain rates studied, the superelastic behavior for 50% Nickel - 50% Titanium alloy is superior at 6% predetermined strain rate when subjected to low temperature annealing at 450°C.

### **5.2.8 Corrosion characteristics**

(xxiv) The electrochemical corrosion study carried out for as-received 50 % Nickel - 50 % Titanium alloy indicate that at the intersection points of extended anode current line and extended cathode current line, the corrosion current was found to be  $11.3 \times 10^{-3}$  amperes and further the electrochemical corrosion rate for the material was found to be 0.0613 mm/year.

(xxv) The electrochemical corrosion rate for 50% Nickel - 50% Titanium alloy subjected to low temperature annealing heat-treatment at different temperatures for a duration of one-hour has been found to vary from 0.0471 mm/year to 0.0644 mm/year.

(xxvi) Among the different low temperature annealing heat-treatment temperatures studied, the 50% Nickel – 50% Titanium alloy annealed at a temperature of 350°C for one-hour duration exhibits superior corrosion resistance with a minimum corrosion rate of 0.0394 mm/year.

### **5.3 Comparative Study of Nickel-Titanium Alloy Without Any Heat Treatment and Nickel-Titanium Alloy Subjected to Different Low Temperature Annealing Heat Treatments**

#### **5.3.1 Comparison of transmission electron micrographs of as-received and low temperature annealing heat-treated 50% Nickel - 50% Titanium alloys**

(i) The comparison of Transmission Electron Micrographs of as-received and low temperature annealing heat-treated 50% Nickel - 50% Titanium alloys indicates that in the as-received condition, there is presence of martensite which appears as a needle-like region and also a shaded region indicating presence of dislocation density. Whereas the 50% Nickel - 50% Titanium alloy subjected to optimum low temperature annealing heat-treatment at 350°C for one-hour duration indicates the presence of martensite, dislocation density and formation of NiTi alloy grains. The extent of dislocation density has relatively reduced and the grain size of NiTi alloy has relatively increased.

#### **5.3.2 Comparison of EDAX of as-received and low temperature annealing heat-treated 50% Nickel - 50% Titanium alloys**

(ii) Comparison of the EDAX results of the as-received and low temperature annealing heat-treated 50% Nickel - 50% Titanium alloys one-hour duration indicates that there is no significant difference observed in the composition of Nickel and Titanium. This has been found true at all annealing temperatures investigated.

#### **5.3.3 Comparison of X-Ray Diffractogram of as-received and low temperature annealing heat-treated 50% Nickel - 50% Titanium alloys**

(iii) The XRD of as-received NiTi alloy indicates that the martensitic phase has appeared at  $2\theta$  value of  $39.24^\circ$  and the austenitic phase is at a  $2\theta$  angle value of  $42.1^\circ$ . Further, the energy intensity value of martensitic phase has been observed to be lesser than the energy intensity values of austenitic phase. Whereas, the X-ray diffractogram of the 50% Nickel – 50% Titanium alloy subjected to optimum low temperature annealing heat-treatment of 350°C for one-hour duration indicates the presence of the Austenitic and Martensitic phase along with an additional R-phase. The martensitic phase has appeared at a  $2\theta$  value of  $39.24^\circ$ . Further, the austenitic phase is seen to



appear at a  $2\theta$  angle value of  $42.4^\circ$  and the Rhombohedral phase (R-phase) is at a  $2\theta$  angle value of  $43.1^\circ$ .

#### **5.3.4 Comparison of differential scanning calorimetry results of as-received and low temperature annealing heat-treated 50% Nickel - 50% Titanium alloys**

(iv) The DSC thermogram of the as-received NiTi alloy indicates that there are no significant peaks seen in the heating as well as the cooling curves meaning that there are no distinct phase transformations of either Austenite-Martensite or Martensite-Austenite present in the material. Whereas, the DSC thermogram of 50% Nickel - 50% Titanium alloy subjected to optimum low temperature annealing heat-treatment at  $350^\circ\text{C}$  for one-hour duration indicates that the material shows a single-stage transformation from austenite-martensite phase in the cooling cycle and a two-stage transformation from martensite-rhombohedral phase and rhombohedral-austenite phase in the heating cycle. The transformation temperatures for start and finish of Martensite phase i.e.  $M_s$  and  $M_f$  is  $44^\circ\text{C}$  and  $33^\circ\text{C}$ ; the start and finish temperatures for Austenite phase is  $38^\circ\text{C}$  and  $53^\circ\text{C}$  and the start and finish temperatures for the R-phase is  $17^\circ\text{C}$  and  $37^\circ\text{C}$ .

#### **5.3.5 Comparison of ultimate tensile strength of as-received and low temperature annealing heat-treated 50% Nickel - 50% Titanium alloys**

(v) The comparison of the ultimate tensile strength of as-received 50% Nickel - 50% Titanium alloy and the alloy sample subjected to an optimum low temperature annealing heat-treatment of  $350^\circ\text{C}$  for a duration of 1 hour indicates that there is an improvement in ultimate tensile strength of  $350^\circ\text{C}$  heat-treated sample by 44.40% as compared to ultimate tensile strength of as-received 50% Nickel - 50% Titanium alloy.

#### **5.3.6 Comparison of hardness of as-received and low temperature annealing heat-treated 50% Nickel - 50% Titanium alloys**

(vi) The comparison of hardness of 50% Nickel - 50% Titanium alloy subjected to optimum low temperature annealing heat-treatment at  $350^\circ\text{C}$  for one-hour duration with the hardness of as-received 50% Nickel - 50% Titanium alloy indicates that the hardness has increased by 14.5% as compared to hardness of as-received 50% Nickel - 50% Titanium alloy.

### **5.3.7 Comparison of abrasive wear characteristics of as-received and low temperature annealing heat-treated 50% Nickel - 50% Titanium alloys**

(vii) The comparison of the abrasive wear between the as-received 50% Nickel - 50% Titanium alloy and 50% Nickel - 50% Titanium alloy subjected to optimum low temperature annealing treatment at 350°C for one-hour duration indicates that the mass loss of low temperature annealed 50% Nickel - 50% Titanium alloy is lesser by 37.17% to 47.58% than the mass loss of as -received 50% Nickel - 50% Titanium alloy. This trend of reduction in the mass loss or in other words the improvement in wear resistance has been found true at all the axial loads investigated within the scope of this investigation.

### **5.3.8 Comparison of Superelasticity Behavior of as-received and low temperature annealing heat-treated 50% Nickel - 50% Titanium alloys**

(viii) The superelasticity percentage of low temperature annealing 50% Nickel - 50% Titanium alloy is more than the superelasticity of as-received 50% Nickel - 50% Titanium alloy. Whereas, the extent of improvement in Superelasticity of 50% Nickel - 50% Titanium alloy subjected to optimum low temperature annealing heat-treatment of 450°C for one-hour duration is in the range of 54.5% to 95.2 % as compared to superelasticity of as-received 50% Nickel - 50% Titanium alloy.

### **5.3.9 Comparison of Corrosion Characteristics of as-received and low temperature annealing heat-treated 50% Nickel - 50% Titanium alloys**

(ix) The corrosion rate of 50% Nickel - 50% Titanium alloy subjected to low temperature annealing heat-treatment at different temperatures is less than the corrosion rate of as-received 50% Nickel - 50% Titanium alloy. This trend has been found true for all the annealing temperatures investigated.

(x) The extent of improvement in the corrosion resistance of 50% Nickel - 50% Titanium alloy subjected to optimum low temperature annealing heat-treatment at 350°C for one-hour duration is 35.72% as compared to corrosion resistance of as-received 50% Nickel - 50% Titanium alloy.

## **5.4 Scope for Future Work**

The NiTi alloy has proven itself as an interesting material for a number of applications.

1. However, systematic studies have to be carried out in order to confirm the effect of annealing on the suitability of the material for aerospace and marine applications, wherein, knowledge of impact and fatigue behavior is essential.

2. Also, the variation in the duration of the heat-treatment needs to be carried out on the material in order to study its effect on the microstructure as well as impact and fatigue behavior so as to be tailored for aerospace and marine applications.

## REFERENCES

- A. R. Pelton, J. D. (2001). "Shape memory and superelastic technologies." *Proceeding of International Conference in Shape memory and superelastic technologies*, 361-374.
- Abdy, A, Sadiq, H & Al-Mahaidi, R. (2014). "Effect of heat treatment on the recovery stresses generated by super-elastic NiTi shape memory alloy wires." *23rd Australasian Conference on the Mechanics of Structures and Materials (ACMSM23)*, Byron Bay, NSW, NSW, 211-216.
- Abedini, M., Ghasemi, H. M., Nili Ahmadabadi, M., & Mahmudi, R. (2010). "Effect of phase transformation on the wear behavior of NiTi alloy." *Journal of engineering materials and technology*, 132(3), 031010.
- Abubakar, T., Rahman, M., & Stokes, J. (2013). "Effect of annealing treatment on the wear properties of Ni rich NiTi alloy coatings." *In Advanced Materials Research*, 686, 192-200.
- Abujudom, D. N. (1990). *Material Science Forum*, 565-570
- Adharapurapu, R. R. (2007). "Phase transformations in nickel-rich nickel-titanium alloys: influence of strain-rate, temperature, thermomechanical treatment and nickel composition on the shape memory and superelastic characteristics", PhD thesis, UC, San Diego.
- Aliasgarian, R., Ghasemi, H. M., & Abedini, M. (2011). "Tribological Behavior of Heat-Treated Ni-rich NiTi Alloys." *Journal of tribology*, 133(3), 031602.
- Arciniegas, M., Casals, J., Manero, J. M., Pena, J., & Gil, F. J. (2008). "Study of hardness and wear behavior of NiTi shape memory alloys." *Journal of Alloys and Compounds*, 460(1-2), 213-219.
- Bhattacharya, K. (1992). "Self-accommodation in martensite." *Archive for Rational Mechanics and Analysis*, 120(3), 201-244.
- Bhattacharya, K. (2003). "Microstructure of martensite: why it forms and how it gives rise to the shape-memory effect." 2, Oxford University Press, New York, US.

Brooks, D. C. (Ed.). (1998). "Current review of minimally invasive surgery." Springer Science & Business Media.

Byrne, J. G. (1965). Recovery, recrystallization, and grain growth. 1965, 179 P. MACMILLAN CO., NEW YORK.

CAPOSI, M., Prodana, M., & IONIȚĂ, D. (2011). "Effect of temperature and pH on the metal release from TiNi." *Sci Bull*, 73, 27-36.

Chembath, M., Balaraju, J. N., & Sujata, M. (2014). "In Vitro corrosion studies of surface modified NiTi alloy for biomedical applications." *Advances in Biomaterials*, 2014.

Chen, J. T., Duerig, T. W., Pelton, A. R., & Stockel, D. (1995). "An apparatus to measure the shape memory properties of nitinol tubes for medical applications." *Journal de Physique IV*, 5(C8), C8-1247.

Chen, K. C. (2003). "NiTi-Magic or Phase Transformation." In *Proceedings of the ASEE Annual Conference & Exposition: Nashville, TN*.

Dalibor VOJTECH, J. K. (2011). "Study of Mechanical, Fatigue and Corrosion Properties of The Superelastic NiTi Alloy." *METAL 2011*, 1-7.

Delville, R., Kasinathan, S., Zhang, Z., Humbeeck, J. V., James, R. D., & Schryvers, D. (2010). "Transmission electron microscopy study of phase compatibility in low hysteresis shape memory alloys." *Philosophical magazine*, 90(1-4), 177-195.

Delville, R., Malard, B., Pilch, J., Sittner, P., & Schryvers, D. (2011). "Transmission electron microscopy investigation of dislocation slip during superelastic cycling of Ni-Ti wires." *International Journal of Plasticity*, 27(2), 282-297.

Drexel, M., Selvaduray, G., & Pelton, A. (2007). "The effects of cold work and heat treatment on the properties of nitinol wire." *ASME 2007 2nd Frontiers in Biomedical Devices Conference*, Irvine, California, USA, 89-90.

Duerig, T. W., & Wholey, M. (2002). "A comparison of balloon-and self-expanding stents." *Minimally invasive therapy & allied technologies*, 11(4), 173-178.

- Duerig, T. W., & Zadno, R. (1990). "An engineer's perspective of pseudoelasticity." *Engineering aspects of shape memory alloys*, Butterworth-Heinemann, London, 369-393.
- Duerig, T. W., Melton, K. N., & Stockel, D. (2013). "Engineering aspects of shape memory alloys." Butterworth-Heinemann.
- Duerig, T., Pelton, A., & Stockel, D. (1999). "An overview of nitinol medical applications." *Materials Science and Engineering: A*, 273, 149-160.
- Eaton-Evans, J., Dulieu-Barton, J. M., Little, E. G., & Brown, I. A. (2008). "Observations during mechanical testing of Nitinol." *Proceedings of the Institution of Mechanical Engineers, Part C: Journal of Mechanical Engineering Science*, 222(2), 97-105.
- Eggeler, G., Khalil-Allafi, J., Gollerthan, S., Somsen, C., Schmahl, W., & Sheptyakov, D. (2005). "On the effect of aging on martensitic transformations in Ni-rich NiTi shape memory alloys." *Smart materials and structures*, 14(5), S186.
- Fadlallah, S. A., El-Bagoury, N., El-Rab, S. M. G., Ahmed, R. A., & El-Ousamii, G. (2014). "An overview of NiTi shape memory alloy: corrosion resistance and antibacterial inhibition for dental application." *Journal of Alloys and Compounds*, 583, 455-464.
- Feeney, A., & Lucas, M. (2016). "Differential scanning calorimetry of superelastic Nitinol for tunable cymbal transducers." *Journal of Intelligent Material Systems and Structures*, 27(10), 1376-1387.
- Fei, G. A. O., & Hua-Ming, W. A. N. G. (2007). "Abrasive wear property of laser melting/deposited Ti<sub>2</sub>Ni/TiNi intermetallic alloy." *Transactions of Nonferrous Metals Society of China*, 17(6), 1358-1362.
- Fercec, J., Jenko, D., Buchmeister, B., Rojko, F., Budič, B., Kosec, B., & Rudolf, R. (2014). "Microstructure of NiTi orthodontic wires observations using transmission electron microscopy." *Metalurgija*, 53(4), 469-472.

- Flamini, D. O., & Saidman, S. B. (2014). "Corrosion behavior of Nitinol alloy coated with alkylsilanes and polypyrrole." *Materials Science and Engineering: C*, 44, 317-325.
- Frank, T. G., Xu, W., & Cuschieri, A. (2000). "Instruments based on shape-memory alloy properties for minimal access surgery, interventional radiology and flexible endoscopy." *Minimally Invasive Therapy & Allied Technologies*, 9(2), 89-98.
- Frick, C. P., Ortega, A. M., Tyber, J., Maksound, A. E. M., Maier, H. J., Liu, Y., & Gall, K. (2005). "Thermal processing of polycrystalline NiTi shape memory alloys." *Materials Science and Engineering: A*, 405(1-2), 34-49.
- G. Mealha, T. M. (2016). "Enhancement of NiTi alloys biocompatibility and corrosion resistance by thermal treatments." Master's Thesis, TECHNICO LISBOA.
- G. N. V. d. S. Mealha. (2016). "Enhancement of NiTi Alloys Biocompatibility." ISEL, Portugal.
- Gall, K., Sehitoglu, H., Chumlyakov, Y. I., Kireeva, I. V., & Maier, H. J. (1999). "The influence of aging on critical transformation stress levels and martensite start temperatures in NiTi: part I—aged microstructure and micro-mechanical modelling." *J. Eng. Mater. Technol*, 121(1), 19-27.
- Gallardo Fuentes, J. M., Gümpel, P., & Strittmatter, J. (2002). "Phase change behavior of nitinol shape memory alloys." *Advanced engineering materials*, 4(7), 437-452.
- George, G. K., Sanjeev, K., & Sekar, M. (2011). "An in vitro evaluation of the effect of deep dry cryotreatment on the cutting efficiency of three rotary nickel titanium instruments." *Journal of conservative dentistry: JCD*, 14(2), 169.
- Goodhew, P. (2011). "General introduction to transmission electron microscopy (TEM)." *Aberration-Corrected Analytical Transmission Electron Microscopy*, 1-19.
- Gusev, K. S. (2019). "Effect of heat-treatment on the mechanical behavior and fracture of TiNi alloy." *Physical Mesomechanics*, 22(3), 224-229.

- Hansen, A. W., Fuhr, L. T., Antonini, L. M., Villarinho, D. J., Marino, C. E. B., & Malfatti, C. D. F. (2015). "The electrochemical behavior of the NiTi alloy in different simulated body fluids." *Materials Research*, 18(1), 184-190.
- Hassan, K. S., Alwan, A. S., & Abbas, S. A. (2015). "Corrosion Behavior of Al alloys 6061-T6 Shot Peening in Different Aqueous Solution." *International Journal of Engineering and Innovative Technology (IJEIT)*, 4.
- Hastuti, K., Hamzah, E., & Hashim, J. (2016). "Effect of annealing on the microstructures and deformation behavior of Ti–50.7 at. % Ni shape memory alloy." *Proceedings of the Institution of Mechanical Engineers, Part L: Journal of Materials: Design and Applications*, 230(2), 436-445.
- Honarvar, M., Konh, B., Podder, T. K., Dicker, A. P., Yu, Y., & Hutapea, P. (2015). "X-ray diffraction investigations of shape memory NiTi wire." *Journal of Materials Engineering and Performance*, 24(8), 3038-3048.
- Huang, J. Y., Zhu, Y. T., Liao, X. Z., Beyerlein, I. J., Bourke, M. A., & Mitchell, T. E. (2003). "Microstructure of cryogenic treated M2 tool steel." *Materials Science and Engineering: A*, 339(1-2), 241-244.
- Huang, X., & Liu, Y. (2001). "Effect of annealing on the transformation behavior and superelasticity of NiTi shape memory alloy." *Scripta Materialia*, 45(2), 153-160.
- Iijima, M., Brantley, W. A., Kawashima, I., Ohno, H., Guo, W., Yonekura, Y., & Mizoguchi, I. (2004). "Micro-X-ray diffraction observation of nickel–titanium orthodontic wires in simulated oral environment." *Biomaterials*, 25(1), 171-176.
- J A Shaw, C. B. (2008). "Tips and tricks for characterizing shape memory alloy wire: Part I - Differential Scanning Calorimetry and Basic Phenomenon." *Experimental Characterization of Active Materials Series*, 32(5), 55-62.
- Karaman\*, I., Kulkarni, A. V., & Luo, Z. P. (2005). "Transformation behavior and unusual twinning in a NiTi shape memory alloy ausformed using equal channel angular extrusion." *Philosophical Magazine*, 85(16), 1729-1745.



- Kim, J. W., Griggs, J. A., Regan, J. D., Ellis, R. A., & Cai, Z. (2005). "Effect of cryogenic treatment on nickel-titanium endodontic instruments." *International endodontic journal*, 38(6), 364-371.
- Kus, K., & Breczko, T. (2010). "DSC-investigations of the effect of annealing temperature on the phase transformation behavior in Ni-Ti shape memory alloy." *Materials Physics and Mechanics*, 9(1), 75-83.
- Lagoudas, D. C., Rediniotis, O. K., & Khan, M. M. (2000). "Applications of shape memory alloys to bioengineering and biomedical technology." In *Scattering Theory and Biomedical Engineering Modelling and Applications*, 195-207.
- Lekston, Z., & Łągiewka, E. (2007). "X-ray diffraction studies of NiTi shape memory alloys." *Archives of Materials Science and Engineering*, 28(11), 665-672.
- Li, Y., Yang, C., Zhao, H., & Qu, S. (2004). Lili. "New developments of Ti-based alloys for biomedical applications." *Materials*, 1709-1800.
- Liu, M., Zhang, X. M., Li, Y. Y., Chen, J. Z., & Tu, M. J. (2002). "High-resolution transmission electron microscope (HRTEM) study of the transformation interface and substructure in NiTiHf40 melt-spun ribbons." *Journal of alloys and compounds*, 334(1-2), 147-153.
- Lucas, A. F. (2015). "Differential scanning calorimetry of superelastic Nitinol for tunable cymbal transducers." *Journal of Intelligent Material Systems and structures*, 1376 - 1387.
- M. Drexel, G. S. (2007). "The Effects of Cold Work and Heat Treatment on the Properties of Nitinol Wire." *ASME 2007 2nd Frontiers in Biomedical Devices Conference*, Irvine, California, USA, 114-119.
- M. G. M. A. R. Aliasgarian H. (2011). "Tribological Behavior of Heat-treated Ni-rich NiTi alloys." *Journal of Tribology*, 1-6.

- Ma, X. G., & Komvopoulos, K. (2005). "In situ transmission electron microscopy and nanoindentation studies of phase transformation and pseudoelasticity of shape-memory titanium-nickel films." *Journal of materials research*, 20(7), 1808-1813.
- Machado, L. G., & Savi, M. A. (2003). "Medical applications of shape memory alloys." *Brazilian journal of medical and biological research*, 36(6), 683-691.
- Miller, D. A., & Lagoudas, D. C. (2001). "Influence of cold work and heat treatment on the shape memory effect and plastic strain development of NiTi." *Materials Science and Engineering: A*, 308(1-2), 161-175.
- Milosev, I., & Kapun, B. (2012). "The corrosion resistance of Nitinol alloy in simulated physiological solutions: Part 1: The effect of surface preparation." *Materials Science and Engineering: C*, 32(5), 1087-1096.
- Mitwally, M. E., & Farag, M. (2009). "Effect of cold work and annealing on the structure and characteristics of NiTi alloy." *Materials Science and Engineering: A*, 519(1-2), 155-166.
- Miura, F., Mogi, M., Ohura, Y., & Hamanaka, H. (1986). "The super-elastic property of the Japanese NiTi alloy wire for use in orthodontics." *American Journal of Orthodontics and Dentofacial Orthopedics*, 90(1), 1-10.
- Moghaddam, N. S., Saedi, S., Amerinatanzi, A., Hinojos, A., Ramazani, A., Kundin, J., ... & Elahinia, M. (2019). "Achieving superelasticity in additively manufactured NiTi in compression without post-process heat treatment." *Scientific reports*, 9(1), 1-11.
- Molinari, A., Pellizzari, M., Gialanella, S., Straffelini, G., & Stiasny, K. H. (2001). "Effect of deep cryogenic treatment on the mechanical properties of tool steels." *Journal of materials processing technology*, 118(1-3), 350-355.
- Muterlle, P. V., de Barros Casto, Í., & Herrera, P. (2015). "Study of Micro-Abrasive Wear Resistance of Heat Treated NiTi Alloys." In *Advanced Materials Research*, 1120, 1069-1077.

- Muterlle, P. V., Villamarin, E. B., Herrera, P., & da Silva, E. P. (2014). "Effect of Aging Treatment on Phase Transformation of a Pseudoelastic NiTi Alloy." *In Advanced Materials Research*, 936, 1216-1223.
- Ni, W. (2004). "Indentation and tribological behavior of nickel titanium alloys and study of instrumented spherical indentation." Doctoral dissertation, Michigan State University.
- Nishida, M., Wayman, C. M., & Honma, T. (1986). "Precipitation processes in near-equiatomic TiNi shape memory alloys." *Metallurgical Transactions A*, 17(9), 1505-1515.
- Nurveren, K., Akdoğan, A., & Huang, W. M. (2008). "Evolution of transformation characteristics with heating/cooling rate in NiTi shape memory alloys." *Journal of materials processing technology*, 196(1-3), 129-134.
- Otsuka, K. (1990). "Engineering aspects of Shape memory alloys." London: Butterworth-Heinemann Ltd.
- Paryab, M. (2019). "The Effect of Heat Treatment on the Microstructural and Superelastic Behavior of NiTi Alloy with 58.5 wt.% Ni." *Journal of Environmental Friendly Materials*, 3(1), 23-27.
- Paula, A. S., Mahesh, K. K., Dos Santos, C. M. L., Fernandes, F. B., & da Costa Viana, C. S. (2008). "Thermomechanical behavior of Ti-rich NiTi shape memory alloys." *Materials Science and Engineering: A*, 481- 482, 146-150.
- Pelton, A. R., DiCello, J., & Miyazaki, S. (2000). "Optimization of processing and properties of medical grade Nitinol wire." *Minimally Invasive Therapy & Allied Technologies*, 9(2), 107-118.
- Pelton, A. R., Russell, S. M., & DiCello, J. (2003). "The physical metallurgy of nitinol for medical applications." *Jom*, 55(5), 33-37.
- Pelton, T. W. (1994). "Ti-Ni Shape Memory Alloys." *In G. W. R. Boyer, Materials Properties Handbook: Titanium alloys*, 1035-1048. Ohio: ASM International.

- Pelton, T. W. (1994). "Ti-Ni Shape Memory Alloys." In G. W. R. Boyer, *Materials Properties Handbook: Titanium alloys*, 1035-1048. Ohio: ASM International.
- Pena, J., Solano, E., Mendoza, A., Casals, J., Planell, J. A., & Gil, F. J. (2005). "Effect of the M s transformation temperature on the wear behavior of NiTi shape memory alloys for articular prosthesis." *Bio-medical materials and engineering*, 15(4), 289-293.
- Pitteri, M., & Zanzotto, G. (2002). "Continuum models for phase transitions and twinning in crystals." *Chapman & Hall*, CRC Press, New York, Washington D C.
- Qian, L. M., Sun, Q. P., & Zhou, Z. R. (2005). "Fretting wear behavior of superelastic nickel titanium shape memory alloy." *Tribology Letters*, 18(4), 463-475.
- Qian, L., Sun, Q., & Zhou, Z. (2008). "The role of martensite reorientation in the fretting behavior of nickel titanium shape memory alloy." *Proceedings of the Institution of Mechanical Engineers, Part J: Journal of Engineering Tribology*, 222(7), 887-897.
- Reed, R. E., & Abbaschian, H. R. (1973). "Physical metallurgy principles." *PWS Engineering*, Boston, Massachusetts.
- Robertson, S. W., Pelton, A. R., & Ritchie, R. O. (2012). "Mechanical fatigue and fracture of Nitinol." *International Materials Reviews*, 57(1), 1-37.
- Rupert, T. J., Cai, W., & Schuh, C. A. (2013). "Abrasive wear response of nanocrystalline Ni–W alloys across the Hall–Petch breakdown." *Wear*, 298, 120-126.
- S, M. (1990). "Engineering Aspects of Shape Memory Alloys." In T. Duerig, *Engineering Aspects of Shape Memory Alloys*, London: Butterworth-Heinemann, 369-413.
- Saburi, T., & Wayman, C. M. (1979). "Crystallographic similarities in shape memory martensites." *Acta Metallurgica*, 27(6), 979-995.

- Sadiq, H., Wong, M. B., Al-Mahaidi, R., & Zhao, X. L. (2010). "The effects of heat treatment on the recovery stresses of shape memory alloys." *Smart Materials and Structures*, 19(3), 035021.
- Şahin, Y., & Öksüz, K. E. (2014). "Effects of Al<sub>2</sub>O<sub>3</sub> Nano powders on the Wear Behavior of NiTi Shape Memory Alloys." *JOM*, 66(1), 61-65.
- Sanchez-Arevalo, F. M., & Pulos, G. (2008). "Use of digital image correlation to determine the mechanical behavior of materials." *Materials characterization*, 59(11), 1572-1579.
- Santamarta, R., Arróyave, R., Pons, J., Evirgen, A., Karaman, I., Karaca, H. E., & Noebe, R. D. (2013). "TEM study of structural and microstructural characteristics of a precipitate phase in Ni-rich Ni–Ti–Hf and Ni–Ti–Zr shape memory alloys." *Acta Materialia*, 61(16), 6191-6206.
- Sathiyamoorthi, P., Bae, J. W., Asghari-Rad, P., Park, J. M., Kim, J. G., & Kim, H. S. (2018). "Effect of annealing on microstructure and tensile behavior of CoCrNi medium entropy alloy processed by high-pressure torsion." *Entropy*, 20(11), 849.
- Schryvers, D., Potapov, P., Santamarta, R., & Tirry, W. (2004). "Applications of advanced transmission electron microscopic techniques to Ni–Ti based shape memory materials." *Materials Science and Engineering: A*, 378(1-2), 11-15.
- SHARIFI, E. M., & Kermanpur, A. (2018). "Superelastic properties of nanocrystalline NiTi shape memory alloy produced by thermomechanical processing." *Transactions of Nonferrous Metals Society of China*, 28(3), 515-523.
- Sharifi, E. M., Karimzadeh, F., & Kermanpur, A. (2014). "The effect of cold rolling and annealing on microstructure and tensile properties of the nanostructured Ni<sub>50</sub>Ti<sub>50</sub> shape memory alloy." *Materials Science and Engineering: A*, 607, 33-37.
- Sherif, M. M., & Ozbulut, O. E. (2017). "Tensile and superelastic fatigue characterization of NiTi shape memory cables." *Smart Materials and Structures*, 27(1), 015007.

- Steiner, G., Peterlechner, M., Waitz, T., & Karnthaler, H. P. (2008). "TEM investigation of severely deformed NiTi and NiTiHf shape memory alloys." *In EMC 2008 14th European Microscopy Congress 1–5 September 2008, Aachen, Germany*, 489-490. Springer, Berlin, Heidelberg.
- Stockel, D. (1998). "Nitinol-A material with unusual properties." *Endovascular Update*, 1(1), 1-8.
- Tadayyon, G., Mazinani, M., Guo, Y., Zebarjad, S. M., Tofail, S. A., & Biggs, M. J. (2016). "Study of the microstructure evolution of heat treated Ti-rich NiTi shape memory alloy." *Materials Characterization*, 112, 11-19.
- Tamura, I., & Wayman, C. M. (1992). "Martensitic transformations and mechanical effects." *ASM International, Martensite (USA)*, 1992, 228-242.
- Tazarv, M., & Saiid Saiidi, M. (2015). "Reinforcing NiTi superelastic SMA for concrete structures." *Journal of Structural Engineering*, 141(8), 04014197.
- Thayer, T. A., Bagby, M. D., Moore, R. N., & DeAngelis, R. J. (1995). "X-ray diffraction of nitinol orthodontic arch wires." *American Journal of Orthodontics and Dentofacial Orthopedics*, 107(6), 604-612.
- Tong, Y. X., Liu, J. T., Feng, C. H. E. N., Liang, C. Q., Bing, T. I. A. N., Li, L. I., & Zheng, Y. F. (2014). "Effect of aging on martensitic transformation and superelasticity of TiNiCr shape memory alloy." *Transactions of Nonferrous Metals Society of China*, 24(8), 2598-2605.
- Trepanier, C., Venugopalan, R., & Pelton, A. R. (2000). "Corrosion resistance and biocompatibility of passivated NiTi." *In Shape memory implants*, 35-45. Springer, Berlin, Heidelberg.
- Treppmann, D., & Hornbogen, E. (1997). "On the influence of thermomechanical treatments on shape memory alloys." *Le Journal de Physique IV*, 7(C5), C5-211.
- Uchil, J. (2002). "Shape memory alloys—characterization techniques." *Pramana*, 58(5-6), 1131-1139.

- Uchil, J., Fernandes, F. B., & Mahesh, K. K. (2007). "X-ray diffraction study of the phase transformations in NiTi shape memory alloy." *Materials characterization*, 58(3), 243-248.
- Velmurugan, C., Senthilkumar, V., Dinesh, S., & Arulkirubakaran, D. (2018). "Review on phase transformation behavior of NiTi shape memory alloys." *Materials Today: Proceedings*, 5(6), 14597-14606.
- VOJTĚCH, D. (2010). "Influence of heat treatment of shape memory NiTi alloy on its mechanical properties." In *International Conference Metals*, 18-20.
- VOJTECH, D., KUBASEK, J., VODEROVA, M., ŠEDÁ, P., & MICHALCOVÁ, A. (2011). Study of Mechanical, Fatigue and Corrosion Properties of the Superelastic Ni-Ti Alloy. *Journal of METAL*, 18(5).
- Walid, N. (2017). "Review and classification of heat treatment procedures of NiTi instruments and its implication on files fatigue." *J Dental Sci*, 2(2), 1-19.
- Wang, X. B., Verlinden, B., & Van Humbeeck, J. (2014). "R-phase transformation in NiTi alloys." *Materials Science and Technology*, 30(13), 1517-1529.
- Xavier, C. C., Correa, D. R. N., Grandini, C. R., & Rocha, L. A. (2017). "Low temperature heat treatments on Ti-15Zr-xMo alloys." *Journal of Alloys and Compounds*, 727, 246-253.
- Xu, L., & Wang, R. (2010). "The effect of annealing and cold-drawing on the super-elasticity of the Ni-Ti shape memory alloy wire." *Modern Applied Science*, 4(12), 109.
- Yan, L., & Liu, Y. (2015). "Wear behavior of austenitic NiTi shape memory alloy." *Shape Memory and Superelasticity*, 1(1), 58-68.
- Yan, L., Liu, Y., & Liu, E. (2013). "Wear behavior of martensitic NiTi shape memory alloy under ball-on-disk sliding tests." *Tribology International*, 66, 219-224.
- Yan, W. (2006). "Theoretical investigation of wear-resistance mechanism of superelastic shape memory alloy NiTi." *Materials Science and Engineering: A*, 427(1-2), 348-355.

- Yoon, S. H., & Yeo, D. J. (2004). "Phase transformations of nitinol shape memory alloy by varying with annealing heat treatment conditions." *In Smart Materials III*, 5648, 208-215.
- Yu, W. (1990). "The Application of Thermal Analysis in the Study of Ni--Ti Shape Memory Alloys." *Thermal Analysis in Metallurgy*, 187-201.
- Zhang, F., Zheng, L., Wang, Y., & Zhang, H. (2019). "Effect of Ni content and Hf addition on the unlubricated wear performance of Ni-rich NiTi alloys." *Intermetallics*, 112, 106548.
- Zhiqiang, S., Di, Z., & Guobin, L. (2005). "Evaluation of dry sliding wear behavior of silicon particles reinforced aluminum matrix composites." *Materials & design*, 26(5), 454-458.
- Zupanc, J., Vahdat-Pajouh, N., & Schäfer, E. (2018). "New thermomechanically treated NiTi alloys—a review." *International endodontic journal*, 51(10), 1088-1103.



## LIST OF PUBLICATIONS AND CONFERENCES

The thesis outlines “Influence Of Heat-Treatment on Structure and Properties of Nickel - Titanium Alloy” is a result of the research carried at Department of Mechanical Engineering, National Institute of Technology Karnataka between July 2011 and May 2020. The research during this period has resulted in the following publications and conference proceedings.

<b>S No</b>	<b>Title of the Paper</b>	<b>Authors (In the Name Order as In the Paper, Underline the Research Scholar’s Name)</b>	<b>Name of The Journal/Conference, Vol., No., Pages</b>	<b>Month, Year of Publication</b>	<b>Category*</b>
<b>1.</b>	Effect of low temperature annealing on the properties of nano Ni-Ti Alloys	Sriram Mukunda M Vinyas, S Narendranath, Mervin A Herbert	Materials Research Express (SCIE), Volume 6, (2019) 105711	September 2019	<b>1</b>

<b>2.</b>	Effect of Low Temperature Annealing on the Wear Properties of Nitinol	Sriram Mukunda Narendra Nath. S, Mervin A. Herbert, P. G. Mukunda	IOP Conf. Series: Materials Science and Engineering	February 2016	<b>3</b>
<b>3</b>	Effect of Heat Treatment and Alloying on The Mechanical Properties of Nitinol	Sriram Mukunda Narendra Nath. S, Mervin A. Herbert, P G Mukunda	Trends in Mechanical Engineering (Time-2014) National Conference	January 2014	<b>3</b>
<b>4</b>	Effect of Heat Treatment and Alloying on The Properties of NiTiCu	Sriram Mukunda Delli Babu, Narendra Nath. S, Mervin A. Herbert	3rd International Conference on Recent Advances in Material Processing Technology (Rampt-13)	January 2013	<b>3</b>

\*Category:

1: Journal Paper, Full Paper Reviewed. 2: Journal Paper, Abstract Reviews. 3: Conference/Symposium Paper, Full Paper Reviewed. 4: Conference/Symposium Paper, Abstract Reviewed. 5: others (including papers win workshops, NITK research bulletins, short notes etc.)

**SRIRAM MUKUNDA**

Research Scholar

Name and Signature,  
with date

**Dr. Narendra Nath S**

Research Guide

Name and Signature,  
with date

**Dr. Mervin A. Herbert**

Research Guide

Name and Signature,  
with date

## BIO-DATA

**Name:** Sriram Mukunda

**Father's Name:** Dr. P G Mukunda

**Date of Birth:** 26-November-1981

**Nationality:** Indian

**Marital Status:** Single



### Address:

#### Permanent Address

S/o Dr. P G Mukunda,  
#9/1, 14<sup>th</sup> A. Cross,  
Malleswaram, Bangalore – 560003  
Landmark – Behind MES College

#### Present Address

S/o Dr. P G Mukunda,  
#9/1, 14<sup>th</sup> A. Cross,  
Malleswaram, Bangalore – 560003  
Landmark – Behind MES College

**Mobile No:** 9108034241, 8217854704

**E-Mail:** [sriram.mukunda@nmit.ac.in](mailto:sriram.mukunda@nmit.ac.in), [mukunda.sriram78@gmail.com](mailto:mukunda.sriram78@gmail.com)

### Educational Qualification:

Course	Institution	University	Batch	Percentage
PhD (Mechanical Engineering)	National Institute of Technology Karnataka, Surathkal	NITK	2020	7.5 (CGPA) Course Work
M Tech (Manufacturing Engineering)	National Institute of Technology Karnataka, Surathkal	NITK	2011	7.6 (CGPA)

M S (Automobile Engineering)	M S Ramaiah School of Advanced Studies	Coventry, UK	2005	8 (CGPA)
B E (Mechanical Engineering)	S J C Institute of Technology, Chickballapur	VTU	2003	65%

**Work Experience:**

S No.	Company	Department	Duration	Position
1	NITTE Meenakshi Institute of Technology, Bangalore - 560064	Mechanical Engineering	January 2015 to Present	Assistant Professor
2	Vidya Vardhaka College of Engineering, Mysuru - 570002	Mechanical Engineering	July 2014 – December 2014	Assistant Professor
3	NITTE Meenakshi Institute of Technology, Bangalore - 560064	Mechanical Engineering	February 2009 – July 2014	Assistant Professor

4	Wipro Technologies	Engineering Design Services	March 2008 – February 2009	Project Engineer
5	Altair Engineering	Product Design & Development	September 2005 – March 2008	Project Engineer

### Publication Details

Papers Published	Under Review	Conference	Workshops/ Symposium	Awards and Recognitions
1	1	3	12	

I declare that the above information is true and correct to the best of my knowledge.

**(SRIRAM MUKUNDA)**